AD NUMBER

AD822318

LIMITATION CHANGES

TO:

Approved for public release; distribution is unlimited.

FROM:

Distribution authorized to U.S. Gov't. agencies and their contractors; Critical Technology; NOV 1967. Other requests shall be referred to National Aeronautics and Space Administration, Manned Spaceflight Center, Attn: EP-2, Houston, TX. This document contains export-controlled technical data.

AUTHORITY

AEDC ltr, 27 Jun 1973

AEDC-TR-67-193

OPERATING CHARACTERISTICS OF THE APOLLO LM DESCENT ENGINE WITH HELIUM INGESTION AND PROPELLANT DEPLETION IN A SIMULATED SPACE ENVIRONMENT

K. L. Farrow, J. A. German, and T. M. Gernstein

ARO, Inc.

November 1967

ROCKET TEST FACILITY
ARNOLD ENGINEERING DEVELOPMENT CENTER
AIR FORCE SYSTEMS COMMAND
ARNOLD AIR FORCE STATION, TENNESSEE

NOTICES

When U. S. Government drawings specifications, or other data are used for any purpose other than a definitely related Government procurement operation, the Government thereby incurs no responsibility nor any obligation whatsoever, and the fact that the Government may have formulated, furnished, or in any way supplied the said drawings, specifications, or other data, is not to be regarded by implication or otherwise, or in any manner licensing the holder or any other person or corporation, or conveying any rights or permission to manufacture, use, or sell any patented invention that may in any way be related thereto.

Qualified users may obtain copies of this report from the Defense Documentation Center.

References to named commercial products in this report are not to be considered in any sense as an endorsement of the product by the United States Air Force or the Government.

OPERATING CHARACTERISTICS OF THE APOLLO LM DESCENT ENGINE WITH HELIUM INGESTION AND PROPELLANT DEPLETION IN A SIMULATED SPACE ENVIRONMENT

K. L. Farrow, J. A. German, and T. M. Gernstein
ARO, Inc.

FOREWORD

The tests reported herein were sponsored by the Manned Spacecraft Center (MSC), National Aeronautics and Space Administration (NASA), under System 921E/9158. Two Apollo Lunar Module Descent Engines (LMDE) manufactured by TRW Systems, Inc., were tested using a Grumman Aircraft Engineering Company (GAEC) manufactured, heavy-duty, LMDE cavity (HD-4 rig) in Propulsion Engine Test Cell (J-2A) of the Rocket Test Facility (RTF).

The results of the tests presented were obtained by ARO, Inc. (a subsidiary of Sverdrup & Parcel and Associates, Inc.), contract operator of the Arnold Engineering Development Center (AEDC), Air Force Systems Command (AFSC), Arnold Air Force Station, Tennessee, under Contract AF40(600)-1200. The tests were conducted between April 23 and June 7, 1967, under ARO Project Number RL1618, and the manuscript was submitted for publication on August 21, 1967.

Information in this report is embargoed under the Department of State International Traffic in Arms Regulations. This report may be released to foreign governments by departments or agencies of the U. S. Government subject to approval of the National Aeronautics and Space Administration, Manned Spaceflight Center (ESP-2), Houston, Texas. Private individuals or firms require a Department of State export license.

This technical report has been reviewed and is approved.

Joseph R. Henry
Lt Col, USAF
AF Representative, RTF
Directorate of Test

Leonard T. Glaser
Colonel, USAF
Director of Test

ABSTRACT

An Apollo Lunar Module Descent Engine (LMDE) was tested under a simulated thermal radiation and pressure space environment in Propulsion Engine Test Cell (J-2A) to investigate (1) engine ignition characteristics at 10-percent throttle, while ingesting various trapped volumes of helium (the flight vehicle propellant tank pressurant), and (2) engine operating and shutdown characteristics while injecting various flow rates of helium into the propellant feed lines. Fifteen firings were conducted during two test periods. The first test period consisted of seven firings; four were checkout and baseline performance tests, and three were helium ingestion/propellant depletion tests. Eight firings were conducted during the second test period; seven were helium ingestion/propellant depletion tests. Helium volumes equivalent to over 9 ft of propellant feed line were ingested during the starts, and helium flow rates equivalent to more than 40 percent of the total volumetric flow of each propellant were injected into the feed lines during engine operation with insignificant engine damage. Except for the two largest helium volumes in the oxidizer system, ignition delay was decreased by helium ingestion. Chamber pressure was degraded by as much as 17 percent while injecting helium into the feed lines during steady-state operation, but the corresponding degradation of characteristic velocity was only approximately 2 percent.

CONTENTS

APPENDIXES

I. ILLUSTRATIONS

Figure

NOMENCLATURE

A	Area, ft^2
c*	Characteristic velocity, ft/sec
F	Thrust, average, lb_f
g	Dimensional constant, 32.174 lb_m-ft/lb_f-sec^2
I_{sp}	Specific impulse, lb_f-sec/lb_m

MR	Mixture ratio, $(\dot{w}_{ox}/\dot{w}_f)$
P	Pressure, psia
R	Gas constant, $ft\text{-}lb_f/lb_m\text{-}°R$
T	Temperature, °F
t	Time, sec
V	Volume, ft^3
$\dot{V}$	Volumetric flow rate, ft^3/sec
$\dot{W}$	Mass flow rate, lb_m/sec

SUBSCRIPTS

1	Pre-run
2	Post-run
a	Test cell
c	Closing
ch	Thrust chamber
d	Differential or depletion
e	Exit
exp	Nozzle exit plane
f	Fuel
He	Helium
i	Initial
M	Measured
n	Nominal
o	Opening
ox	Oxidizer
p	Propellant, oxidizer and fuel
se	Nozzle exit plane seal
ss	Steady state
t	Throat
t_o	Total
v	Vacuum

SECTION I
INTRODUCTION

During the Apollo earth-moon transit, the Lunar Module (LM), shown in Fig. 1 (Appendix I), will be operating in a weightless environment with no net accelerations; consequently, the interface between the gaseous helium (GHe), used as the propellant tank pressurant, and the propellants will not be clearly defined. The possibility of these constituents combining in a mixture of liquid and gas exists if the planned ullage maneuvers are not sufficient to settle the propellants. Combustion of this mixture could be detrimental to engine performance, or possibly cause a system malfunction as a result of "rough" burning. Similarly, in the event that propellant usage exceeds the scheduled amount during the descent phase causing the propellant tanks to reach a low level or completely deplete, slugs of GHe would enter the Lunar Module Descent Engine (LMDE) disrupting normal combustion. The success of an abort (using the Ascent Engine) during this critical period could depend largely on the reaction of the Descent Engine to a propellant depletion situation.

To investigate engine operating characteristics under these abnormal conditions, various quantities of GHe were allowed to displace propellants at the engine propellant shut-off valves prior to firing. In addition, various flow rates of GHe were injected into the supply lines during steady-state operation and during shutdown.

Two test projects using the LMDE have been conducted in the Propulsion Engine Test Cell (J-2A). The first program was conducted under ARO Project Number RL1433 between August 13 and December 2, 1965, and was reported in Ref. 1. Thermal studies and duty cycle firings were included. The second program, conducted between July 24, 1966, and June 7, 1967, under ARO Project Number RL1618, consisted of five test periods, the first three of which were reported in Ref. 2. Normal start and shutdown characteristics over a matrix of thrust levels and propellant temperatures were investigated. The results of the remaining two test periods (AD and AE) are contained in this report. The objectives of these last two test periods were to determine the following, with the LMDE and HD-4 rig exposed to a simulated space environment:

1. Engine start characteristics at 10-percent throttle setting with various sizes of helium volumes displacing propellants at the engine shutoff valves.
2. Engine operating and shutdown characteristics at 30- and 94-percent throttle with varying flow rates of helium injected into the propellants before and during the shutdown transients.

3. Engine shutdown characteristics at 30-percent throttle with complete propellant depletion.

Test periods AD and AE consisted of 15 firings, five of which were at ambient temperatures and served as engine flow control system balance checks and provided baseline data. The remaining ten were helium ingestion/propellant depletion tests conducted with the test cell at cryogenic conditions and at ignition altitudes in excess of 250,000 ft (Ref. 2).

To simulate the thermal environment, the engine was mounted inside a heavy-duty structure, designated the HD-4 rig, which simulated the LMDE cavity on the LM vehicle. To simulate the space vacuum, the engine and HD-4 rig were then installed in the J-2A test cell, a liquid-nitrogen (LN_2)-cooled test cell equipped with mechanical and cryogenic vacuum pumping systems and a variable output thermal radiation system.

A summary, in graphical form, of LMDE testing in Propulsion Engine Test Cell (J-2A) is included in Table I (Appendix II).

SECTION II
APPARATUS

2.1 TEST ARTICLE

The test article consisted of the LMDE and the HD-4 Propulsion Test Rig. The LMDE (Fig. 2) is manufactured by TRW Systems, a subsidiary of Thompson-Ramo-Woolridge, Inc. It is designed for throttled operation from 10 to 60 percent of rated thrust in addition to rated thrust operation. The overall length of the LMDE is approximately 85 in., and it weighs approximately 350 lb including the engine gimbal assembly, which allows 6 deg of gimbal from the neutral position. The engine produces a rated thrust of 10,500 lb at a total propellant flow rate of 34.0 lb_m/sec at a design mixture ratio of 1.6. The hypergolic propellants are inhibited nitrogen tetroxide (N_2O_4) as the oxidizer (NASA Spec. MSC-PPD-2A) and equal gravimetric parts of hydrazine (N_2H_4), and unsymmetrical dimethylhydrazine $[N_2H_2(CH_3)_2]$ as the fuel (MIL-P-27402). Rated chamber pressure is 107.3 psia. Engine accessories consist of propellant flow control valves, propellant shutoff valves, and throttle actuator. Engine nominal design characteristics are shown in Table II.

The HD-4 rig (Fig. 3) is a heavyweight support structure for the LMDE. It was manufactured by GAEC for use as a test fixture for the environmental tests at AEDC. The rig duplicates the engine cavity of the LM Descent Stage center compartment.

Test hardware identification by part drawing numbers and serial numbers is shown in Tables III and IV. The individual components of the test article are described below.

2.1.1 Ablative Chamber

The thrust chamber is ablatively cooled to an expansion ratio of 16:1 and weighs approximately 130 lb in the unfired condition. The ablative chamber consists of four sections:

1. Face plate
2. Turbulence ring
3. Throat
4. Divergent section

All are enclosed in a continuous titanium shell and are jacketed by a stainless steel foil/glass wool composite thermal blanket (Fig. 4). Sections 1, 2, and 4 are made of Fiberite MX2525®, a randomly oriented material composed of 0.50-in. squares of chopped silica cloth impregnated with phenolic resin. The throat is made of Fiberite MX2600®, a silica-phenolic tape, oriented at 60 deg to the centerline to minimize erosion. All four sections are wrapped externally with Fiberite MX2600 tape. All ablative components of the chamber are bonded to the titanium shell with Sylgard 182®.

2.1.2 Nozzle Extension

A crushable, radiation-cooled, columbium nozzle extension is normally bolted to the thrust chamber at the 16:1 expansion ratio position and provides controlled expansion of the combustion products to a ratio of 47.4:1. However, during this test series, the engine was equipped with a heavy-duty 0.030-in. wall thickness columbium nozzle extension. The extension exit flange was installed especially for this test program and was used for attachment of a flexible rubber diffuser inlet seal for compatibility with the operation of the J-2A test cell. An Inconel X750® seal with a "K" cross section was used to prevent leakage between the thrust chamber and nozzle extension flange. The bolt holes in both the chamber and extension upstream flange were slotted, and the bolt torque values were limited to allow for differential thermal expansion.

2.1.3 Gimbal Ring Assembly

The gimbal ring assembly consists of a rectangular aluminum beam frame and four aluminum trunnion subassemblies. Two of the trunnions are bolted to the engine through two Z-rings on the titanium chamber case, and the other two are bolted to the vehicle thrust mount struts. The thrust load is taken in shear across the bolts that fasten the trunnions directly to the chamber; the Z-rings do not transmit any thrust load. The trunnion bearings are single steel balls in a two-layer Teflon®-lined steel race.

2.1.4 Thrust Control Assembly

The thrust control assembly (Figs. 5 and 6) includes the propellant shutoff valves, throttle actuator, flow-control valves, and injector.

2.1.4.1 Shutoff Valves

The propellant shutoff valves are two-position, fuel-actuated, mechanically linked, series-parallel ball valves. The fuel and oxidizer valves each consist of four independent ball valves in series-parallel arrangement. The parallel arrangement provides redundancy for valve opening, and the series arrangement provides closing redundancy. Each fuel valve ball is mechanically linked to a corresponding ball in the oxidizer valve. In the normally closed position, the actuation fuel is shut off by the action of the spring-loaded plunger on the caged ball within the solenoid-operated pilot valve, and the actuator piston pressures are vented overboard. In the open position, the spring-loaded plungers are retracted by the solenoids, simultaneously sealing the overboard vents and permitting fuel to flow to the actuator pistons.

The prevalve is a two-way, solenoid-operated valve located in the shutoff valve actuation line (Fig. 6). It is activated to the open position when the engine electrical circuits are armed. The prevalve is normally closed, functioning as a safety device to prevent propellant from being discharged overboard should the solenoid-operated pilot valve for the shutoff valve fail to seat properly in the closed position.

2.1.4.2 Throttle Actuator

The throttle control is an electromechanical, linear servoactuator which positions the fuel and oxidizer pintles of the flow control valve in response to an electrical command input signal. The unit is powered by three d-c motors connected to a common output shaft. The three motors drive the rotating member of an output jackscrew which simultaneously adjusts the mechanical linkage connecting the flow control valve pintles and the injector metering sleeve for the desired throttle position.

2.1.4.3 Flow Control Valve

The functions of the flow control valve are to provide mixture ratio control over the full range of operation and to maintain a linear throttle position versus thrust relationship for the engine. The flow control valve consists of a pair of mechanically linked, variable area venturi valves. The valve pintles are contoured to vary the fuel and oxidizer flow rates linearly with pintle displacement over the engine thrust range.

At maximum thrust, the major portion of the controlling pressure drop (GAEC/TRW interface pressure minus chamber pressure) occurs in the injector manifold and orifices, and the engine operates as a calibrated fixed-thrust pressure-fed engine. As thrust decreases, the pressure drop across the flow control valves increases by an amount equal to the decrease in chamber pressure and the decrease in injector manifold pressure losses. At approximately 65 percent of rated thrust, cavitation occurs in the venturi throats, and propellant flow rates are controlled entirely by the flow control valve.

2.1.4.4 Injector

The injector (Fig. 7) is a variable-area, single-coaxial-element, impingement-type injector with a regeneratively cooled face plate and a fuel manifold assembly. The primary fuel is injected through an annular gap between the face plate and the metering sleeve. Oxidizer is injected radially into the chamber through radial slots located in the oxidizer feed tube and the metering sleeve (the only moving part in the injector). The areas of the fuel and oxidizer metering orifices are controlled by movement of the metering sleeve. The sleeve moves axially approximately 0.15 in. over the engine operating range. Fuel for film cooling is injected through 36 equally spaced fuel orifices on the face plate and is directed onto the chamber walls.

All metal parts in the injector are made from the high temperature alloys 17-4 PH® and Inconel 718®. The dynamic seals attached to the metering sleeve are two-ply nested bellows. The bearing between the element housing and the metering sleeve is a multiple-leaf-flexural bushing consisting of two concentric cylindrical tubes joined at each end by a series of thin circumferentially slotted disks. Relative axial movement between the tubes is permitted by flexing of the slotted disks.

2.1.5 HD-4 Propulsion Test Rig

The main frame assembly of the HD-4 rig (Fig. 3) was fabricated of welded steel beams and angles with a bolted-on heat shield support

assembly at the aft end. Both fixed and removable double-walled side panels were installed around the inside of the main frame assembly. An eight-piece LM base heat shield was mounted around the aft end of the rig, forming an eight-sided collar that surrounds the engine nozzle extension. The engine was equipped with a GAEC, one-piece, lightweight heat shield (Fig. 2) that fits around the radiation-cooled nozzle extension attachment flange and inside the periphery of the HD-4 rig heat shield. Provisions in the rig for mounting the engine include the engine truss mount, propellant supply lines, and gimbal actuators. For these tests, the gimbal actuators were removed, and rod assemblies were installed to hold the engine stationary.

2.1.6 Special Insulation

The upper half of the HD-4 rig blast deflector was removed, and a hole was cut in the +Z axis removable side panel to allow television and motion-picture camera access to the engine headend. Fifty layers of aluminized Mylar super insulation[1] were draped from the cameras to the HD-4 rig, tent fashion, to reduce radiation losses from the engine headend (Fig. 8).

2.2 INSTALLATION

2.2.1 Test Cell

The Propulsion Engine Test Cell (J-2A) (Fig. 9 and Refs. 4 and 5) is a near-space simulation, rocket engine test chamber, capable of attaining pressure altitudes in excess of 300,000 ft. The test cell consists of an LN_2-cooled, 18-ft-diam, 30-ft-long, stainless-steel, thermopanel liner installed within the 20-ft-diam basic test cell ducting. The linear interior and all major test cell components were painted flat black to increase the absorptivity for thermal radiation. Independent pumping systems provide the high vacuum.

The independent pumping systems consist of four mechanical vacuum pumps, two two-stage oil diffusion pumps, associated valves and ducting, and a cryogenic pumping system. The cryogenic pumping system consists of the LN_2-cooled liner and diffuser (-320°F) and 12 helium (He)-cooled 4- by 4-ft thermopanels (cryoplates) located symmetrically at the downstream end of the test cell liner (Fig. 9).

---

[1]Multiple layers of lightweight, reflective film used for reducing the transfer of radiant heat in a near vacuum.

2.2.2 Radiation Systems

The outside surface of the HD-4 rig was maintained at the desired temperature, while radiating to the test cell liner walls, by 12 rows of infrared heat lamps equally spaced around the liner. Each row normally contains 26 heat lamps on 6-in. centers. The five lamps in the downstream end of each row were removed for these tests so that the nozzle extension and downstream side of the LM base heat shield would receive no direct radiation. Four specially mounted variable output lamps located inside the HD-4 rig were directed at the engine headend to provide variable control of engine temperatures when required. Four additional lamps, mounted outside the HD-4 rig, were directed at the rig blast shield (upstream vertical panel) (Fig. 9) to control the blast shield temperature.

2.2.3 Thrust Measuring System

The HD-4 rig containing the engine was mounted on a thrust cradle. The thrust cradle was suspended from an LN_2-cooled support structure by four vertical and two horizontal double universal flexure assemblies. Axial movement of the thrust cradle was restrained by the LN_2-cooled thrust butt through a temperature-controlled load cell (Fig. 9).

2.2.4 Diffuser System

The exit plane of the exhaust nozzle extension was located at the LN_2-cooled diffuser inlet bulkhead. The outer diameter of a heated flexible silicon rubber seal was attached to the cooled bulkhead. The seal inner diameter was attached to the nozzle extension exit flange. The seal was used to minimize exhaust gas flow into the liner during and after an engine firing.

The exhaust diffuser consists of a 72-in.-diam by 20.5-ft-long, LN_2-cooled section; a 72-in.-diam by 18-ft-long water-cooled section; a hydraulically operated 72-in.-diam multiple Mylar disk changer or restart valve; and a hydraulically actuated exhaust diffuser valve. The multiple disk changer provides the test cell with a 24 rocket-firing capability during a single test period and consists of twenty-four 20-mil Mylar disks, 24 disk mounting rings, a traversing disk holder, a hydraulic actuation system, and a pyrotechnic system for rupturing the disks. One disk is positioned in the exhaust diffuser duct to seal the liner from the facility exhauster pressure during high vacuum operation (when the exhaust diffuser valve is open), and the remaining disks are located under the exhaust diffuser duct in the disk holder inside the test cell exhaust ducting (20-ft-diam). The Mylar disk in the diffuser duct is cut away at engine ignition by pyrotechnics ignited by an electrical signal from a rocket thrust chamber pressure transducer. After an

engine firing, the diffuser valve is closed, the 72-in.-diam exhaust diffuser duct is opened, the expended disk mounted ring is removed, and a new disk inserted. The duct is then closed, and procedures for the next firing are initiated. The disk changer is operated remotely from the J-2A control room.

The exhaust diffuser valve is installed to prevent atmospheric pressure from rupturing the inplace disk during periods when the facility exhaust system (Ref. 6) is not required. Also, the valve is closed immediately after a firing to prevent an excessive pressure rise in the liner. During engine firings, the rocket exhaust gases serve as the driving fluid by which the supersonic diffuser, in series with the facility exhaust system, maintains the pressure altitude at the nozzle exit plane of the engine (approximately 130,000 ft for throttle settings above approximately 27 percent).

2.2.5 Propellant System

The propellant system (Fig. 10) consisted of a GN_2 pressurizing system; 1500-gal supply tanks; one 40- and one 25-μ absolute filter in each supply line; flow measuring sections, each with two turbine-type flowmeters; temperature conditioning systems; recirculation circuits; high-pressure warning and relief systems; and associated valves, pumps, and piping.

Three recirculation circuits were used in each propellant system. The primary circuit allowed propellant recirculation from the supply tanks to the 25-μ absolute filters; the return line was 1 in. in diameter. The two secondary circuits allowed recirculation from the supply tanks to either the engine flow control valves or the engine shutoff valves. All facility service lines were fitted with either strainers or filters adjacent to the engine ranging from 5 to 300μ nominal.

The oxidizer and fuel propellant supply systems were designed such that the dynamic pressure losses through each would be approximately equal.

2.2.6 Helium Ingestion Propellant Depletion System

The capability was provided, through a helium ingestion/depletion system, to inject known quantities of GHe into the propellant feed lines to displace propellants and form a trapped volume against the engine shutoff valves and also to inject known flow rates of helium into the propellant feed lines during engine operation.

The helium ingestion/propellant depletion system (shown in Fig. 11) consisted of a 2100-psia source; two regulators in series; a three-way flow circuit fitted with remotely controlled valves and nozzles; an emergency relief system; check valves; filters; restricted volume (RV)[2] and instrumentation. Helium entered the propellant feed lines immediately upstream of the GAEC/TRW interface flange.

2.3 INSTRUMENTATION

Instrumentation systems were provided to obtain measurements of axial thrust; engine, test cell, and helium ingestion/propellant depletion system pressures and temperatures; propellant flow rates, pressures, and temperatures; and various engine accelerations, control voltages, currents, and actuator positions. All primary engine parameters were recorded redundantly on different recording systems.

2.3.1 Axial Thrust

Engine thrust was measured with one 10,000-lb, dual-column, strain-gage-type load cell. To permit operation in a cryogenic environment, the load cell contained thermostatically controlled heaters and an external heater remotely controlled from the control room. The outputs from the load cell were recorded in analog form on light-beam oscillograph and null-balance potentiometer and in frequency form on magnetic tape. A deadweight calibrator was provided for calibration of the thrust measuring system at altitude before and after each firing. The calibrator consisted of a flexure-mounted balanced beam to which calibrated weights were suspended in steps of 100 and 150 lb up to a total of 1150 lb. The calibrator beam provided a known mechanical advantage, and incremental axial loads up to approximately 11,500 lb were applied to the thrust cradle. The applied loads were measured with a secondary standard at sea level and were corrected for buoyancy loss of the weights at altitude and thrust butt deflection under thrust load.

---

[2]The Restricted Volume is defined as that section of propellant supply line downstream of the 2-in. facility valves to the engine shutoff valves including the short lengths composing the drain, recirculation, and helium injection lines which terminate in the supply lines (see Fig. 11a).

2.3.2 Pressure

Propellant system helium ingestion/propellant depletion system, and engine pressures (Figs. 10, 11, and 12) were measured with strain-gage-type transducers. The transducers used to measure propellant system line pressures, shutoff valve inlet pressures, helium ingestion/depletion system pressures, and injector manifold pressures were mounted near the source inside the test cell.

Thrust chamber pressure was measured by five transducers, four of which were strain-gage type connected to a manifold from a single tap located on the injector. Two of the four transducers were used for data, and two were used to provide a chamber pressure signal to activate the pyrotechnic system for rupturing the diffuser Mylar disk. The fifth was a TRW-supplied Model 615A Kistler® piezoelectric pressure transducer close coupled to the injector with a Model 504 Kistler charge amplifier for recording high frequency fluctuations during transients. The output was transmitted to an additional d-c amplifier to obtain dual-range (0 to 200 and 0 to 1000 psia) signals for recording in analog form on light-beam oscillograph and in frequency form on magnetic tape. The thrust chamber pressure data acquisition system was inplace certified by a direct comparison with a secondary standard. The Kistler transducer used a GHe purge, which was initiated at ignition fire switch -0.5 sec, for cooling and to improve the frequency response of the data.

Test cell pressure was measured with three variable-capacitance pressure transducers and five ionization gages. The ionization gage data were recorded in analog form on null-balance potentiometers, and the three transducer channels were recorded in frequency form on magnetic tape.

All transducers were laboratory calibrated with a secondary standard before installation in the test cell. Before, during, and at the end of each test period, the pressure transducers were calibrated by an electrical, four-step, resistance substitution calibration using precision resistances in the transducer circuits to simulate selected pressure levels. The ionization gages and capacitance-type transducers were laboratory calibrated using a secondary standard.

2.3.3 Engine, HD-4 Rig, Helium Ingestion/Propellant Depletion System, and Propellant Temperatures

Temperatures were measured on the test article with copper-constantan thermocouples at the locations shown in Fig. 12. Immersion thermocouples were used in each propellant system at selected

locations to measure propellant temperature. The electrical outputs from the thermocouples were recorded on magnetic tape by an analog-to-digital commutating data system and were converted to engineering units and tabulated by a digital computer. Propellant temperatures downstream of the flowmeters were measured by resistance temperature transducer probes, recorded in frequency form on magnetic tape, converted to engineering units, and tabulated by a digital computer. Selected temperature measurements from thermocouples and probes used to monitor the engine, test cell components, helium ingestion/depletion and propellant system temperatures were recorded on null-balance potentiometers (strip chart) located in the test cell control room.

2.3.4 Propellant Flow Rates

Two turbine-type flowmeters were installed in each propellant feed line to measure propellant flow rates (Fig. 10). The outputs of the flowmeters were recorded in frequency form on both a light-beam-type oscillograph and magnetic tape and in analog form on null-balance potentiometers. The flowmeter outputs were also converted to instantaneous digital and analog displays of mixture ratio in the control room. The flow measuring sections, consisting of the flowmeters, flow straighteners, and tubing, were bench calibrated before and after the test series, utilizing both water and propellants as the flowing media. The bench calibration data obtained using the propellants were used to reduce the flowmeter data for the engine performance calculations presented in this report. The flow measuring recording systems were calibrated before, during, and after each test period by applying a known frequency at the flowmeter electrical connector to simulate a selected flowmeter output.

A null-balance, two-axis plotter was located in the control room to give a direct indication of fuel and oxidizer flow and mixture ratio during the firing.

2.3.5 Vibration

Nine piezoelectric-type accelerometers (Figs. 12a and c) provided acceleration measurements along the three principal axes (X-X, Y-Y, Z-Z) of the test article. These accelerometers were mounted on the injector, gimbal ring, and truss assemblies. All accelerometers were spanned to 1000 g's except for those on the injector, which were spanned to 2000 g's; for test period AE, accelerometers A_{J_X} and A_{G_Z} were spanned to 7000 g's. The data were recorded on both magnetic tape and lightbeam oscillograph. The frequency response range was 0 to 5000 cps on the magnetic tape and 0 to 2000 cps on the light-beam oscillograph.

To preclude possible hardware damage during the helium depletion tests, a combustion stability monitor was installed with an acceleration input from the injector X-X axis accelerometer to shut down the engine. The unit was adjusted to shutdown the engine when a limit of 800 g's peak was exceeded during any 70-msec duration of the firing after T + 5 sec.

2.3.6 Visual Coverage

Three motion-picture cameras and three closed-circuit television cameras were used to provide permanent documentation of test article operation and continuous visual monitoring, respectively. The pre- and post-fire conditions of the test articles were documented by still photographs.

SECTION III
PROCEDURE

3.1 TESTING

Pre-test procedures included electrical and mechanical checks, pressure checks, and a final inspection of the test article. The propellant tanks were loaded, and samples were taken from each tank and analyzed to determine the specific gravity and that the applicable propellant specification requirements were met. The diffuser restart valve Mylar disk pyrotechnic circuits were installed, instrumentation calibrations were performed, and the test cell pumpdown was initiated followed by test cell chilldown as described in Refs. 3 and 4.

Prior to chilldown, the propellant lines were vented to the reduced test cell pressure. Propellant bleed-in was then accomplished by permitting pressurized propellants to flow to the engine through the evacuated propellant lines. The high points in the propellant system and the liquid pressure transducers outside the test cell were manually rebled to allow any entrained gas to escape. The bulk temperatures of the propellants in the tanks were maintained at approximately 40°F by use of the propellant temperature conditioning system and the recirculation system.

The HD-4 rig was maintained at approximately 40°F by using the test cell thermal radiation systems. The heat input to the HD-4 rig by the test cell thermal radiation system simulated the heat source of the flight vehicle propellant tanks which surround the engine compartment. The downstream side of the HD-4 rig base heat shield and engine nozzle

extension, which in the flight vehicle would view the heat sink of space, were allowed to radiate directly to the -320°F LN_2-cooled surfaces of the test cell aft heat shield and diffuser. Installation precautions were taken to ensure that no surfaces downstream of the base heat shield viewed direct radiation from the test cell thermal radiation system.

A leak check of the helium ingestion/depletion system and RV were conducted by pressurizing both to the maximum operating pressures and observing pressure decay and test cell pressure.

Prior to each engine firing, instrumentation altitude calibrations were performed, the facility exhausters (Ref. 6) were valved to evacuate the J-2A exhaust ducting, propellant recirculation was stopped, and the helium ingestion/propellant depletion system was prepared. All propellants were drained, purged, and aspirated from either the oxidizer or fuel RV as appropriate for the particular firing. The RV was then closed with a trapped pressure of 0.5 psia or less and the pressure monitored to ensure that all propellants had been removed and that no atmospheric leakage existed.[3] The RV was then pressurized with GHe to a predetermined level and again monitored for leakage and temperature stabilization. The appropriate 2-in. propellant supply line valve was opened allowing propellant, under pressure, to compress the GHe to a predetermined calculated volume. The ingestion/depletion system regulators were adjusted to supply the desired upstream pressure at the three-way flow control circuit. In addition, the propellant systems were pressurized, the exhaust diffuser valve was opened, and the LN_2 flow to the diffuser was increased. After these test preparations were performed, the engine firing was initiated. The diffuser Mylar disk pyrotechnic detonaengine firing was initiated. The diffuser Mylar disk pyrotechnic detonation system cut the disk from the diffuser to allow the rocket exhaust gases to be pumped away by the facility rotating exhausters, the helium volume was ingested, the engine was throttled, and the three-way helium flow circuit valves were opened and closed by the sequencer to inject GHe into the supply lines according to the profiles shown in Fig. 13. For the last two firings, during which total propellant tank depletion was simulated, the 2-in. valve in the appropriate propellant supply line was

---

[3]Any significant quantity of propellants remaining in the RV would raise the pressure to the vapor pressure of the respective propellants (oxidizer at 40°F = 6.5 psia, fuel at 40°F = 0.55 psia, Ref. 7).

closed simultaneously with the opening of the three-way flow control circuit helium valve.

After engine shutdown, the exhaust diffuser valve was closed, the next exhaust diffuser restart valve Mylar disk was positioned in the diffuser, and the LN_2 flow to the diffuser was reduced. The propellant tanks were vented to 40 psia, and the propellant temperature conditioning systems were reactivated.

At the completion of each test period, the thermal radiation system and propellant recirculation systems were utilized to maintain engine and propellant system temperatures near 40°F during the test cell warm-up, and ambient conditions were restored in the test cell as outlined in Ref. 4. The test cell was opened, and post-test procedures were performed on the test article and test cell.

A test summary is included in Table V.

3.2 DATA REDUCTION

The three major divisions of the data reduction effort proceeded chronologically from quick-look, to primary, to performance data.

3.2.1 Quick-Look Data

During the periods between the firings, temperatures of the HD-4 rig and engine were monitored at 30-min intervals or on demand. The data were presented in tabulated engineering units. The same commutating digital system used for recording the above was used during the firings to record selected temperatures, pressures, flows, and thrust which were used as inputs for a basic quick-look engine performance program. Data from strip charts and oscillograms were reduced manually between firings as corroborative information for the quick-look performance program.

The accelerometers and Kistler chamber pressure transducer signals, recorded on magnetic tape, were converted to oscillograms for wave analysis and determination of peak accelerations and pressures immediately after each firing.

3.2.2 Primary Data

Data recorded on magnetic tape, using the commutating digital and analog-to-frequency conversion systems, provided the highest accuracy

and greatest utility data and were considered the primary data. Generally, the commutating digital system was used to record temperatures and other slow-response parameters. The analog-to-frequency systems provided better response rates and were used to record pressures, thrust, and selected temperatures, voltages, and currents. Flowmeter data were recorded directly in pulse form. These data were presented in tabulated engineering units at the conclusion of each test period.

3.2.3 Performance Data

Primary data from the analog-to-frequency systems and manual inputs were used to calculate the classic rocket engine performance parameters of vacuum thrust (F_V), mixture ratio (MR), total flow ($\dot{W}_{t_O}$), vacuum specific impulse (I_{sp_V}), characteristic velocity (c*), and other parameters of interest. These data were tabulated in engineering units for 0.02- and 0.1-sec intervals.

3.2.3.1 Thrust

Thrust was redundantly recorded, and each of the data channels was converted to lb_f using scale factors obtained from the deadweight calibrations. The deadweight calibrator was certified at atmospheric temperatures and pressures before the test series using a secondary standard traceable to the National Bureau of Standards. Vacuum thrust (F_V) was calculated from

$$F_V = F_M + P_a A_e - A_{se}(P_{exp} - P_a) \tag{1}$$

where:

F_M = Measured thrust, lb_f

P_a = Test cell pressure, psia

P_{exp} = Diffuser pressure, psia

and the nozzle seal effective area (A_{se}) was determined by applying a known differential pressure across the nozzle exit area (A_e) and seal area and measuring the force (F_d) on the thrust measuring system with a 500-lb_f load cell. Then

$$A_{se} = \frac{F_d}{P_{exp} - P_a} - A_e \tag{2}$$

3.2.3.2 Thrust Chamber Pressure

Three channels of thrust chamber pressure, measured at the injector face, were recorded on magnetic tape; two of the channels (the Kistler chamber pressure data were presented in analog form only) were converted to engineering units using scale factors obtained from laboratory calibrations of the transducers. The average of the measured chamber pressure data (P_{ch}) was asjusted to an estimated total pressure at the nozzle throat (P_{cht}) by the relationship

$$P_{ch_t} = 0.975\, P_{ch} \tag{3}$$

where the factor 0.975 was supplied by the engine manufacturer.

3.2.3.3 Engine Performance Parameters

Vacuum specific impulse (I_{sp_v}), and characteristics velocity (c*) were calculated from the following equations:

$$I_{sp_v} = F_v/\dot{W}_{to} \tag{4}$$

$$c^* = \frac{P_{ch_t} A_t g}{\dot{W}_{to}} \tag{5}$$

where

$\dot{W}_{to}$ = Total propellant flow, lb_m/sec

g = Dimensional constant, 32.174 lb_m-ft/lbf-sec^2

A_t = Pre-fire throat area, $in.^2$

3.2.3.4 Helium Ingestion Volume Determination

The volumes were calculated from the following arrangement of the perfect gas equation of state:

$$V_2 = V_1 \frac{P_1}{P_2} \frac{T_2}{T_1} \tag{6}$$

where:

V_2 = Ingestion volume, ft^3

V_1 = Restricted volume (determined by water fill)
oxidizer = 0.379 ft^3
fuel = 0.363 ft^3

P_1 = Pre-charge helium pressure, psia

P_2 = Pre-fire interface pressure, psia

T_1 = Pre-charge helium temperature, °R

T_2 = Pre-fire interface temperature, °R

3.2.3.5 Helium Depletion Injection Rate Determination

Injection flow rate was determined from a calibration curve relating supply pressure to helium flow rate. The flow control circuits (Fig. 11) were calibrated by flowing helium at various pressures through each of the six flow control circuits, while measuring both upstream and downstream pressures and temperatures. Flow quantities during each calibration step were calculated from the pressure decay in a known volume using the perfect gas equation of state:

$$\dot{W}_{He} = \frac{V(P_1 - P_2)(144)}{RTt} \tag{7}$$

where

$\dot{W}_{He}$ = Mass flow rate of helium, lb_m/sec

V = Volume of supply bottle, ft^3

P_1 = Pre-run pressure, psia

P_2 = Post-run pressure, psia

R = Gas constant, 386.25 ft $lb_f/lb_m\,°R$

T = Temperature, °R

t = Duration of calibration run, sec

Helium temperatures were monitored in the supply bottle, upstream and downstream of the flow control orifices, and were found to vary by less than 5°R during the calibration steps. During calibration of the 0.015- and 0.030-in.-diam orifices and the first eight depletion firings, inlet pressures to the orifices were sufficiently high to ensure choked flow. During calibration of the 1-in.-diam flow circuits, choked orifice flow control was not utilized; therefore, back pressure was varied using either a manual throttling valve or the engine flow control valves. During the last two total depletion firings, helium injection pressures were adjusted to maintain interface pressure at the operating level with helium flow replacing propellant flow on the depletion side.

Propellant depletion helium flow rates as a percentage of the nominal (no injection) volumetric propellant flow rate (% $\dot{V}_{1_{He}}$) was calculated from:

$$\%\dot{V}_{1_{He}} = \frac{\dot{V}_{He}}{\dot{V}_n} \times 100 \tag{8}$$

where:

$\dot{V}_n$ = Nominal volumetric flow rate (oxidizer or fuel), ft^3/sec

$\dot{V}_{He}$ = Measured volumetric flow rate of helium, ft^3/sec

Propellant depletion helium flow rate as a percentage of the total volumetric flow rate on the depletion side ($\%\dot{V}_{2_{He}}$) was calculated from:

$$\%\dot{V}_{2_{He}} = \frac{\dot{V}_{He}}{\dot{V}_{He} + \dot{V}_{Md}} \times 100 \qquad (9)$$

where:

$\dot{V}_{Md}$ = Measured propellant flow rate during depletion (oxidizer or fuel), ft^3/sec

3.2.3.6 Operating Times

Shutoff valve initiation (t_i), opening (t_o), and closing (t_c) times were determined from data recorded on oscillograms as follows:

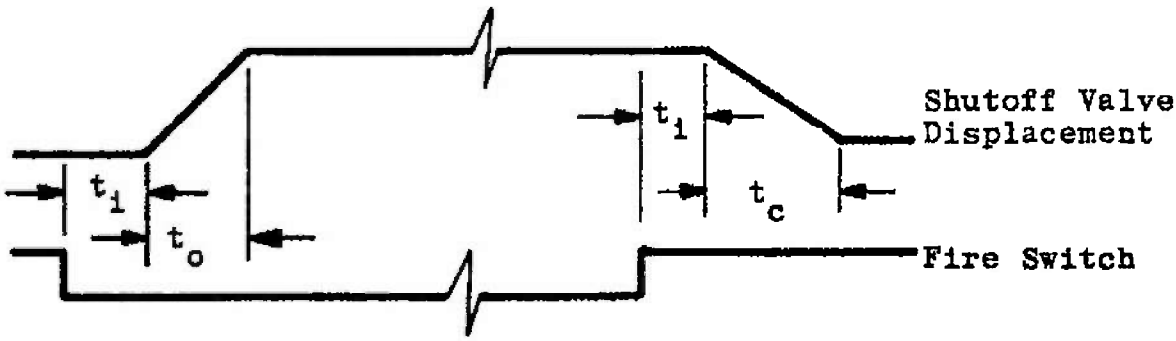

Initial chamber pressure rise (t_{ch}) and ignition delay times (I.D.) were also obtained from data recorded on oscillograms as follows:

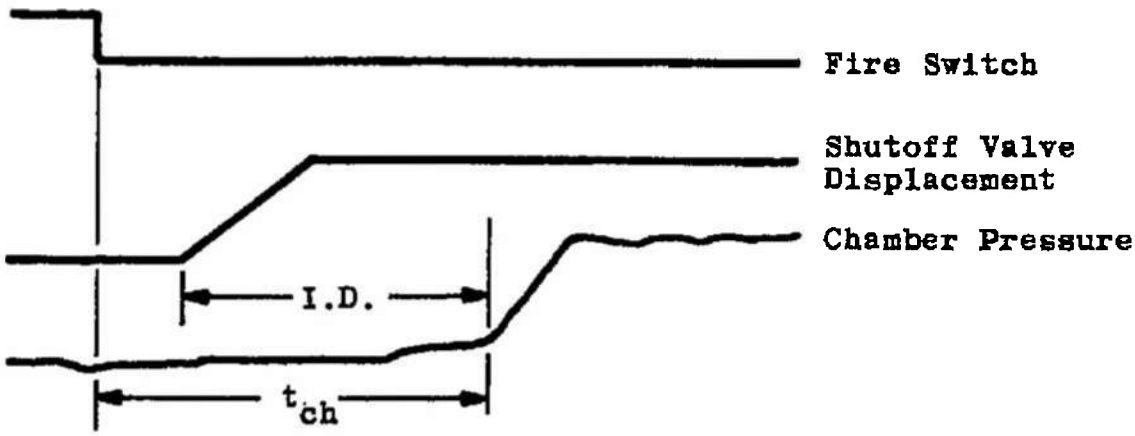

The ignition time (t_{ch}) was chosen as that time corresponding to the chamber pressure initial fast rise time with a persistent pressure greater than 1.0 psia as determined by data analysis and engineering judgement.

SECTION IV
RESULTS AND DISCUSSION

The displacement of propellants at the engine shutoff valves by propellant tank pressurant is a possible flight condition which could occur during the weightless translunar voyage. Initial ignition could result in subjecting the LMDE to a mixed flow of helium gas and propellants if the ullage maneuvers are not entirely successful in establishing a continuous liquid volume from the propellant tanks to the engine shutoff valves.

Each propellant supply system for the LMDE includes two tanks connected in parallel (Fig. 1). During the descent phase of the LM, the possibility exists that the horizontal maneuvers necessary in the selection of a suitable landing area will result in asymmetric propellant usage from the two tanks. This situation in addition to an extended descent burn, propellant vortexing, or sloshing could result in supplying the LMDE with a mixture of propellants and helium.

Fifteen firings were conducted during two test periods (AD and AE) to investigate the conditions just described. The specific objectives of these tests were to determine:

1. Engine start characteristics at 10-percent throttle with various sizes of helium volumes displacing propellants at the engine shutoff valves.
2. Engine operating and shutdown characteristics at 30- and 94-percent throttle with various quantities of helium injected into the propellants before and during the shutdown transient.
3. Engine shutdown characteristics at 30-percent throttle with complete propellant depletion.

4.1 HELIUM INGESTION

Preceding nine of the ten helium ingestion/propellant depletion firings, helium gas was allowed to displace propellants at the engine

shutoff valves. The helium ingestion volume, intentionally injected into the propellant lines for these tests, was varied in size from 0.019 to 0.221 ft^3 or from 0.8 to 9.5 ft of equivalent 2-in.-diam propellant feed line length. Four ingestion volumes, increasing in size with each successive firing, were ingested on the fuel side and five on the oxidizer side. All engine starts were conducted at 10-percent throttle. The temperatures of critical engine components, prior to each helium ingestion firing, were reduced to a level comparable with those expected at the end of the translunar voyage based on temperatures established during previous testing. Pre-fire temperatures on the injector and chamber are presented in Table VI for each helium ingestion firing. The helium ingestion volume sizes were determined as described in Section 3.2.3.4, and the sizes for each test are presented in Table V.

Interface pressures, injector pressures, chamber pressure, propellant flow rates, and propellant shutoff valve movement traces have been selected for presentation as variables which influence ignition. These variables are shown in Fig. 14 for a firing with no helium ingestion, to establish baseline behavior, and for a typical firing with ingestion on each of the oxidizer and fuel sides. For the fuel ingestion firing, there is evidence of some combustion prior to complete ingestion of the initial volume. The high frequency flowmeter indication is typical of the increased propellant flow rate at the flowmeter location during ingestion of the GHe at volumetric flow rates greater than the normal liquid flow rate. This phenomenon is discussed more fully in Section 4.1.5.1.

Each of the parameters shown in Fig. 14 is discussed relative to the helium ingestion volume in the following sections. Axial acceleration, selected as the best indicator of the severity of ignition, is discussed in Section 4.1.6.

4.1.1 Interface Pressure

The TRW/GAEC propellant interface pressures are shown in Figs. 15 and 16 for helium ingestion in the fuel and oxidizer propellant systems. The ingestion volumes were increased with each successive firing, and a general trend can be seen of overall higher pressure peaks and longer transients with increasing ingestion volume. Firing AD-32 was a notable exception and, based on the trend, appears to have had a smaller ingestion volume than firing AD-30 which was intended to be the smallest volume ingested on the fuel side. The peak interface pressures recorded on the fuel and oxidizer sides, respectively, were 316 and 402 psia during firings AD-31 and AE-36 as compared with an ideal steady-state value of 233 psia.

4.1.2 Injector Pressures

Injector manifold pressure histories are shown in Fig. 17. Correlation is evident with ingestion volumes, particularly for the oxidizer pressures. Both AD-28 and AE-37 are noningestion firings and provide a good baseline reference for comparing the ingestion profiles. Firing AD-32 continues to be suspect and does not conform to the trend of the other firings. The peak pressures recorded were 63 and 153 psia for fuel and oxidizer during firings AE-34 and AE-36, respectively. The time of ignition as determined from oscillograms (see Section 3.2.3.5) is shown on each of the injector pressure traces. There is no apparent correlation between ignition time and the shapes of the injector pressure traces. This would support a conclusion that the shapes of the curves are primarily the result of the dynamics of the ingestion process and are influenced little if any by the ignition pressure buildup in the combustion chamber.

4.1.3 Thrust Chamber Pressure

Chamber pressure histories during the helium volume ingestion with the ignitions identified are shown in Fig. 18. Examination of the pressure levels at 4.0 sec shows that the chamber pressure recovered more slowly from the ingestion of helium on the fuel side than on the oxidizer side. Examination of the pressure levels at a later time than shown in Fig. 18 revealed that chamber pressure stabilization occurred at approximately 7.5 sec on the fuel side and at 4 sec on the oxidizer side.

The time lapse between injector pressure rise and chamber pressure rise for all ingestion firings on the fuel side, except AD-32, was found to be between 600 and 800 msec. The same period for firing AD-32 was only 14 msec.

Ignition peaks during the starts for those firings with spikes large enough to be recorded are presented in Table VII as sensed by the high response Kistler transducer. The difference in the dynamic response of the Kistler and the facility transducer, and their respective data reduction systems from which the data presented in Fig. 18 were taken, account for the apparent inconsistency in the peaks as sensed by the two systems.

4.1.4 Shutoff Valve Operating Time

The actuation times for valve sets "A" and "B" are given in Table VIII and illustrated in Fig. 19 for set "B" only as a function of ingestion volume size. The fuel ingestion firings show a large (13 to 123 msec) variation.

This is caused by helium entering the shutoff valve pressurization line during the draining and aspirating process (see Section 3.1). The valve operates faster with gas or a gaseous mixture as the actuating medium. The actuation time for the oxidizer ingestion firings ranged from 87 to 106 msec. This compares favorably with the average normal actuation time of 103 msec.

4.1.5 Ignition Delay

For the purposes of this report, ignition delay is defined as the time interval between initial shutoff valve movement and the chamber pressure ignition rise (see Section 3.2.3.5). An ignition lag ratio was computed as the ratio of the actual ignition delay to the average non-ingestion ignition delay.[4]

The effect of the ingestion volume on ignition delay is shown in Fig. 20 which presents the ignition lag ratio as a function of ingestion volume. It can be seen that only two of the firings with oxidizer ingestion and none with fuel ingestion had a longer delay than the noningestion firings. This rather surprising result is discussed further in the following sections.

4.1.5.1 Fuel System Helium Ingestion

In general, it would be expected that the normal built-in oxidizer lead of the LMDE would increase as a result of a bubble in the fuel system, thereby increasing ignition delay. As can be seen in Fig. 20, such is not the case since the values of the ignition lag ratio are less than unity. It is concluded that this phenomenon was caused by the entrainment of fuel by the rapidly expanding helium and the subsequent injection of the two-phase mixture at a high velocity, and consequently high mixing energy level, into the chamber. The relatively low vapor pressure of the fuel could also contribute to residual propellant in the low points of the flow control and shutoff valves during the vacuum cleaning of the restricted volume and thereby provide additional fuel for entrainment. This phenomenon, in an extreme case where a very large quantity of fuel is entrained very soon after shutoff valve opening, is a possible explanation for the peculiar behavior during firing AD-32. Evidence of ignition occurring while the helium volume is being ingested can be seen in Fig. 14b as indicated by the continuous high frequency flowmeter response.

---

[4]The average ignition delays of six firings at 40 to 50°F propellant interface temperature with 10-percent throttle ignition were used.

4.1.5.2 Oxidizer System Helium Ingestion

As the ingestion volume in the oxidizer system increases in size, the normal oxidizer lead decreases. In Fig. 20, it may be seen that ignition delay increased with increasing ingestion volume, but that the delay experienced during the small volume firings was less than the average of the noningestion firings. Entrainment of propellant in the helium, as already discussed, is believed to be the cause of this apparent anomaly; however, residual oxidizer within the restricted volume contributing to this effect is less likely because of the higher vapor pressure of the oxidizer.[5] The only two firings during ingestion testing that exhibited longer ignition delays than those normally experienced during noningestion were firings AE-39 and -40 which had ingestion helium volumes in the oxidizer system equivalent to 6.7 and 9.5 ft of feed line, respectively. It is believed that these volumes were large enough to move the liquid/gas interface to a point in the propellant feed line sufficiently far from the engine to minimize the entrainment effect; this produces ignition delays greater than those experienced during noningestion firings. The severity and probability of a hardstart increases with increasing ignition delay.

4.1.6 Acceleration Data

Peak accelerations are presented in Table VII for the portions of each firing during which measurable data were recorded. The normal noningestion 10-percent rated throttle ignitions exhibited a smooth transient. During the fuel system ingestion firings, only AD-30 (smallest volume) exhibited a measurable ignition spike (745 g's peak along the thrust axis). Since no other fuel system ingestion firings resulted in an ignition spike, it is believed that the AD-30 ignition shock was a random occurrence and that ingestion in the fuel system had a low probability of producing an ignition shock.

The oxidizer system ingestion firings resulted in three firings with measurable ignition shocks: AE-35, -39, -40. The ignition shock during firing AE-35 (smallest volume) is considered a low probability random occurrence with 231 g's peak along the thrust axis. Firings AE-39 and -40 (largest volumes) exhibited ignition shocks of 813 and 960 g's peak along the thrust axis, respectively. However, the ignition

---

[5]See Section 3.1 for a discussion of the effectiveness of the draining and aspirating of the restricted volumes.

shocks are not considered severe when compared with the throttle transients with shocks of approximately 1600 g's (Table VII).

4.2 PROPELLANT DEPLETION

Ten firings simulating propellant depletion were accomplished during this test program (Table V). The first eight firings were partial depletion tests during which different helium volumetric flow rates (for each propellant system) were injected into the propellant lines. The helium volumetric flow rates ranged from approximately 6.6×10^{-3} to 4.5×10^{-2} ft^3/sec or from 8.0 to 45.0 percent (by volume) of the propellant plus helium flow rate (Table V)[6]. During the partial depletion firings, the engine was subjected to two helium injection periods, each at identical flow rates. Each helium injection period was preceded by steady-state engine operation. The first helium injection period normally occurred after 15 sec of the firing had elapsed and continued for 5 sec. After a 5-sec period of engine steady-state operation, the second helium injection cycle was initiated (Fig. 13). The duration of the second helium injection cycle was approximately 8 sec, after which time the engine was shutdown. Helium injection was continued during the shutdown transient to determine the effects of partial propellant depletion on engine shutdown. The final two firings of the test program were total depletion tests during which the propellant flow was terminated (by closing a 2-in. valve installed in the propellant line upstream of the flow control valve) and helium was simultaneously injected at a flow rate sufficient to choke the flow control valves at 30-percent throttle and to provide an upstream pressure approximately equal to run interface pressure. The helium volumetric flow rate during the total fuel depletion firing was approximately 0.655 and 1.34 ft^3/sec during the total oxidizer depletion firing.

4.2.1 Partial Propellant Depletion

As the volume of helium injected into the respective propellant systems was increased, the propellant flow rate, chamber pressure, and thrust decreased. The effect of partial depletion on the primary parameters of chamber pressure, propellant flow rates, and injector pressure for 30-percent (by volume) helium injection is presented in Figs. 21 and 22. The two to three Hz oscillations of oxidizer injector and chamber

---

[6]Two different methods of calculating the helium volumetric flow rate during the depletion firings are of interest and the methods of calculation are shown in Section 3.2.3.5.

pressures during injection were characteristic of firing AE-34 and all subsequent firings but were more pronounced during injection into the oxidizer system. The frequency remained essentially the same, but the amplitude increased with increasing injection flow rates becoming 20-psi peak-to-peak for chamber pressure during firing AE-38. The source of these pulsations could not be determined, but is known to have occurred downstream of the ingestion/depletion system three-way flow control circuit and was not experienced during GHe flow calibrations. Small amplitude (3- to 4-psi peak-to-peak) pulsations occurred during firings AE-35 and -36 at 94-percent throttle.

The parameters of propellant flow rate, chamber pressure, and mixture ratio were nondimensionalized and are presented as a function of percent helium injected in Figs. 23a, b, and c. The accompanying peak acceleration levels are presented in Table VII. The slopes of curves a and b indicate that the injection of helium into the oxidizer propellant system had a more significant effect on the primary engine parameters than helium injection into the fuel propellant system. When 40 percent of the volumetric flow rate was helium, there was approximately an 8-percent reduction in fuel flow rate and 12-percent reduction in oxidizer flow rate. These reductions were accompanied by a variation in propellant mixture ratio as shown in Fig. 23c. As the percent of helium injection was increased to 40 percent of the total flow on the fuel side, the mixture ratio increased 30 percent. As expected, the mixture ratio decreased as the helium was increased to 40 percent of the total flow on the oxidizer side. The decrease was approximately 20 percent. The chamber pressure and thrust experienced a 12.5- and 10.0-percent degradation, respectively, at 40-percent helium injection on the fuel side. A degradation of 17.5 and 15.0 percent in chamber pressure and thrust, respectively, was experienced at 40-percent helium injection into the oxidizer flow.

Although propellant flow rate, chamber pressure, and thrust decayed with the increasing volumetric helium injection, the characteristic velocity and specific impulse experienced little degradation with various amounts of helium injection. These parameters were nondimensionalized and are presented as functions of percent of helium depletion in Figs. 23d and e. Combustion efficiency is apparently only slightly affected (approximately two percent) by helium ingestion up to 40 percent of the total flow on a particular propellant side. A portion of this small degradation is undoubtedly the result of off-design mixture ratio operation resulting from the injection.

4.2.2 Total Propellant Depletion

The last two firings of the test program were conducted to obtain engine shutdown characteristics under conditions simulating total depletion of the fuel (firing AE-39) and oxidizer (firing AE-40). Histories of the depletion portion of the firings showing chamber pressure, propellant flow rates, and injector pressures are presented in Figs. 24 and 25. The helium injection pressure was set to deliver a helium flow rate sufficient to choke the flow control valves at 30-percent throttle and to maintain engine interface pressure approximately equal to nominal run pressure. At this helium flow rate, the pressure drop through the helium ingestion/propellant depletion system from the regulator to the engine interface was approximately 40 and 100 psid for fuel and oxidizer, respectively. On closure of the 2-in. facility shutoff valve and simultaneous opening of the helium valves, the initial high pressure helium forced the remaining propellant slug into the chamber at a higher than normal flow rate, which caused the increase in chamber pressure shown in Figs. 24 and 25. This situation would not occur in the flight vehicle during propellant depletion. The measured interface pressures sustained by helium flow during the latter portion of the depletion when the initial peaks have subsided were 205 and 190 psia for the fuel and oxidizer total depletions, respectively. Although total depletion on the oxidizer side appears to be more severe than on the fuel side, the acceleration data in Table VII do not support this conclusion. The apparent severity of the oxidizer depletion is attributed, in part, to the higher oxidizer injection pressure required to overcome friction losses as discussed above.

4.3 HARDWARE DURABILITY

The only apparent test article damage incurred during the tests described herein was the deformation of a screen on the engine head-end which serves as an oxidizer strainer at the injector inlet. The damage is shown in Fig. 26 and is probably the result of hydraulic hammer resulting from the ingestion tests. No further engine damage was revealed through data analysis or visual inspections; however, only cursory external inspections were made at Arnold Center after testing.

SECTION V
SUMMARY OF RESULTS

A series of 15 LMDE test firings was conducted under simulated space conditions in the cryogenic test cell J-2A. Nine ignition tests were conducted at 10-percent throttle with helium ingestion volumes ranging in size from 0.8 to 9.5 ft of equivalent 2-in.-diam piping, displacing propellants in the feed lines adjacent to the main engine shutoff valves.

Partial depletion of propellant was simulated during eight test firings at 30- and 94-percent throttle with helium volume flow up to 45 percent of the total flow on the depletion side. Two total depletion firings were conducted at 30-percent throttle with helium interrupting completely the propellant flow in first the fuel system and then the oxidizer system. The results of these tests are summarized as follows:

1. No significant hardware damage was incurred during the helium ingestion/propellant depletion tests. A deformed oxidizer injector strainer was the only damage experienced.
2. Propellant was entrained by the GHe during the ingestion period decreasing ignition delay for the fuel and oxidizer system ingestion firings except for the two largest oxidizer ingestion volumes. These were sufficiently large to minimize the entrainment effect and to create ignition delays greater than those experienced during noningestion firings.
3. Helium ingestion into the fuel system resulted in one firing out of four with an ignition shock of 745 g's believed to be a random occurrence.
4. Oxidizer system helium ingestion resulted in three firings out of five with ignition shocks as large as 960 g's; one was concluded to be a random occurrence, and the other two were the result of increased ignition delay induced by the GHe ingestion.
5. Thrust chamber pressure at 30-percent throttle decayed 12.5 and 17.5 percent with 40-percent helium volume injection on the fuel and oxidizer sides, respectively. Corresponding degradation of characteristic velocity was approximately two percent.
6. All pressures downstream of the TRW/GAEC interface exhibited a sinusoidal oscillation of unknown origin at 2 to 3 Hz during partial propellant depletion for five of the eight firings. The amplitude increased with increasing helium injection rate to a maximum of 20-psi peak-to-peak and was more pronounced during oxidizer depletion.
7. Shutoff valve actuation time was reduced during the fuel system ingestion firings by GHe trapped in the shutoff valve actuation pressure line during insertion of the helium into the restricted volume.

REFERENCES

1. Farrow, K. L., Matkins, E. H., and Gernstein, T. M. "A Performance Evaluation of the Integrated LM Descent Stage Throttlable Engine and Engine Compartment at Altitudes from 100,000- to 300,000-ft." AEDC-TR-66-122 (AD374883), August 1966.

2. Farrow, K. L., German, J. A., Gernstein, T. M., and Matkins, E. H. "Simulated Space Start Investigation of the Integrated Lunar Module Descent Stage Throttlable Engine and Engine Compartment." AEDC-TR-67-87 (AD381517), June 1967.

3. Minzer, R. A., Champion, K. S. W., and Pond, H. L. "The ARDC Model Atmosphere, 1959." AFCRC-TR-59-267, August 1959.

4. Ansley, S. P., Jr. "Cryogenics as Applied to the Design and Fabrication of a Space Simulation Test Cell." AEDC-TR-62-201 (AD293898), January 1963.

5. Reeves, J. R. "General Description and Performance of the Propulsion Engine Test Cell (J-2A)." AEDC-TDR-64-138 (AD444326), August 1964.

6. Test Facilities Handbook (6th Edition). "Rocket Test Facility, Vol. 2." Arnold Engineering Development Center, November 1966.

7. Goldford, A. and Haupt, C. "Theoretical Performance of Nitrogen Tetroxide-Aerozine-50 Propellant System." Grumman Aircraft Engineering Corporation, Report No. LED-271-2, August 20, 1963.

APPENDIXES

I. ILLUSTRATIONS
II. TABLES

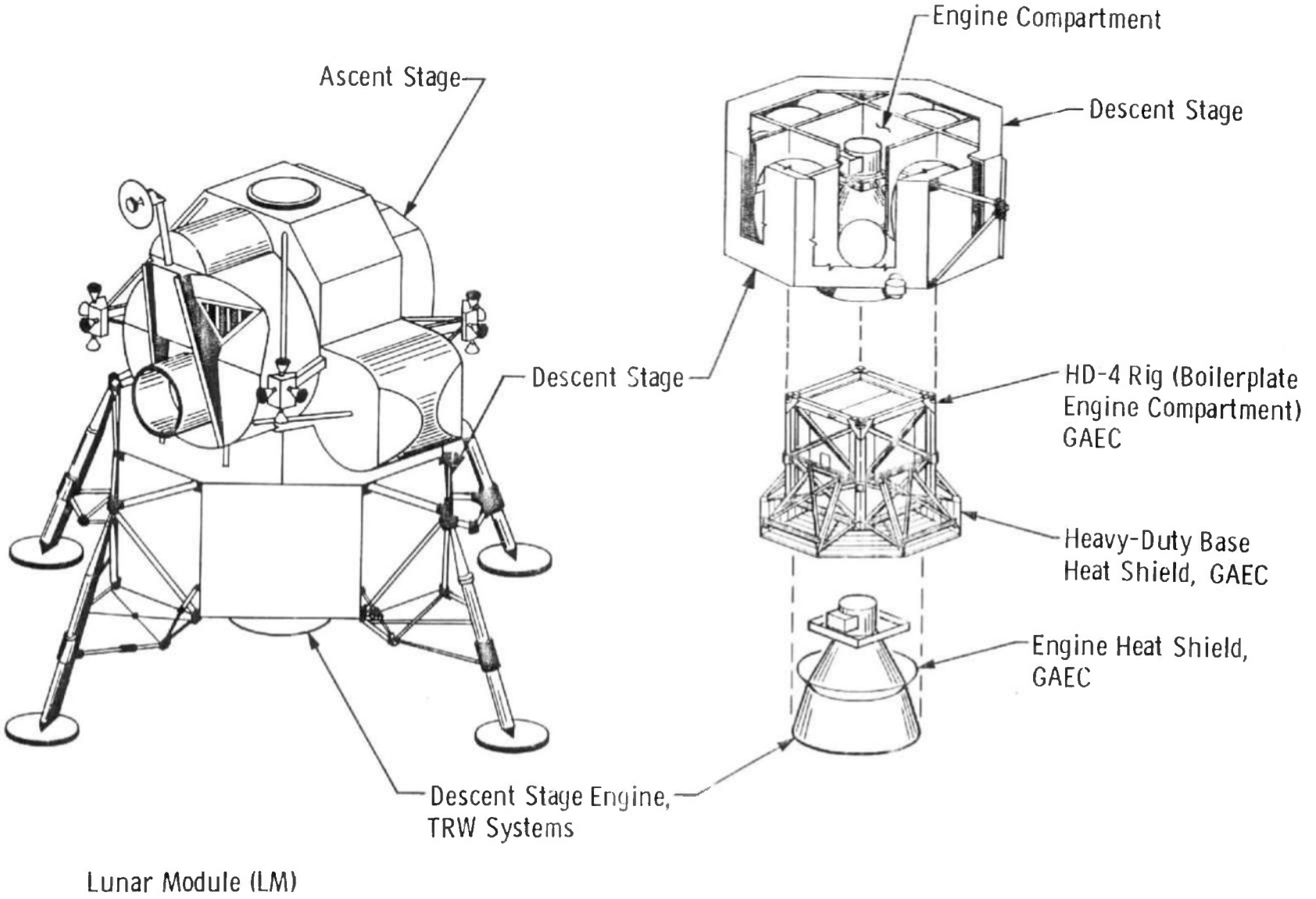

Fig. 1 Relationship of the Test Articles to the LM

AEDC-TR-67-193

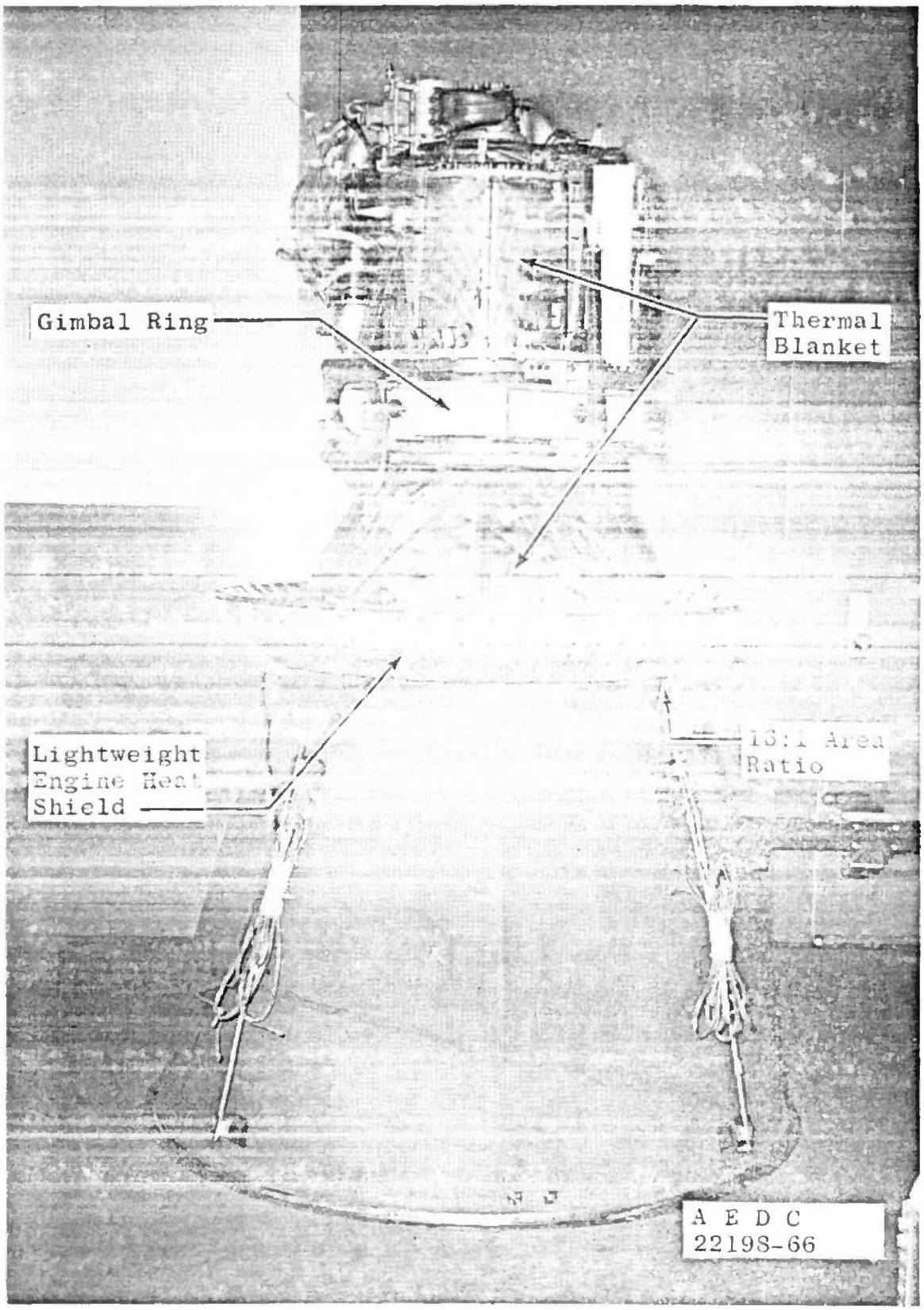

Fig. 2 Photograph of LMDE

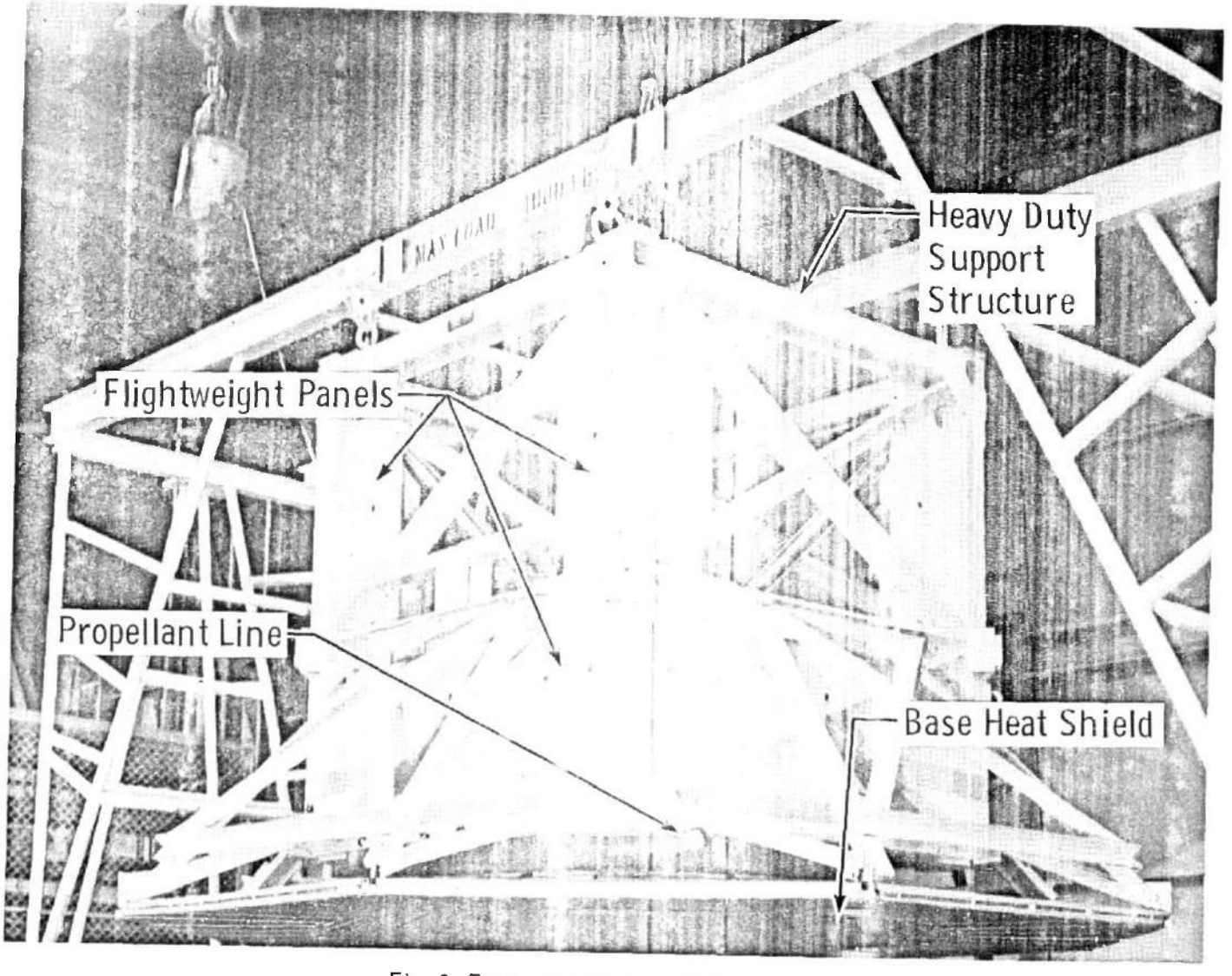

Fig. 3 Engine Compartment (HD–4 Rig)

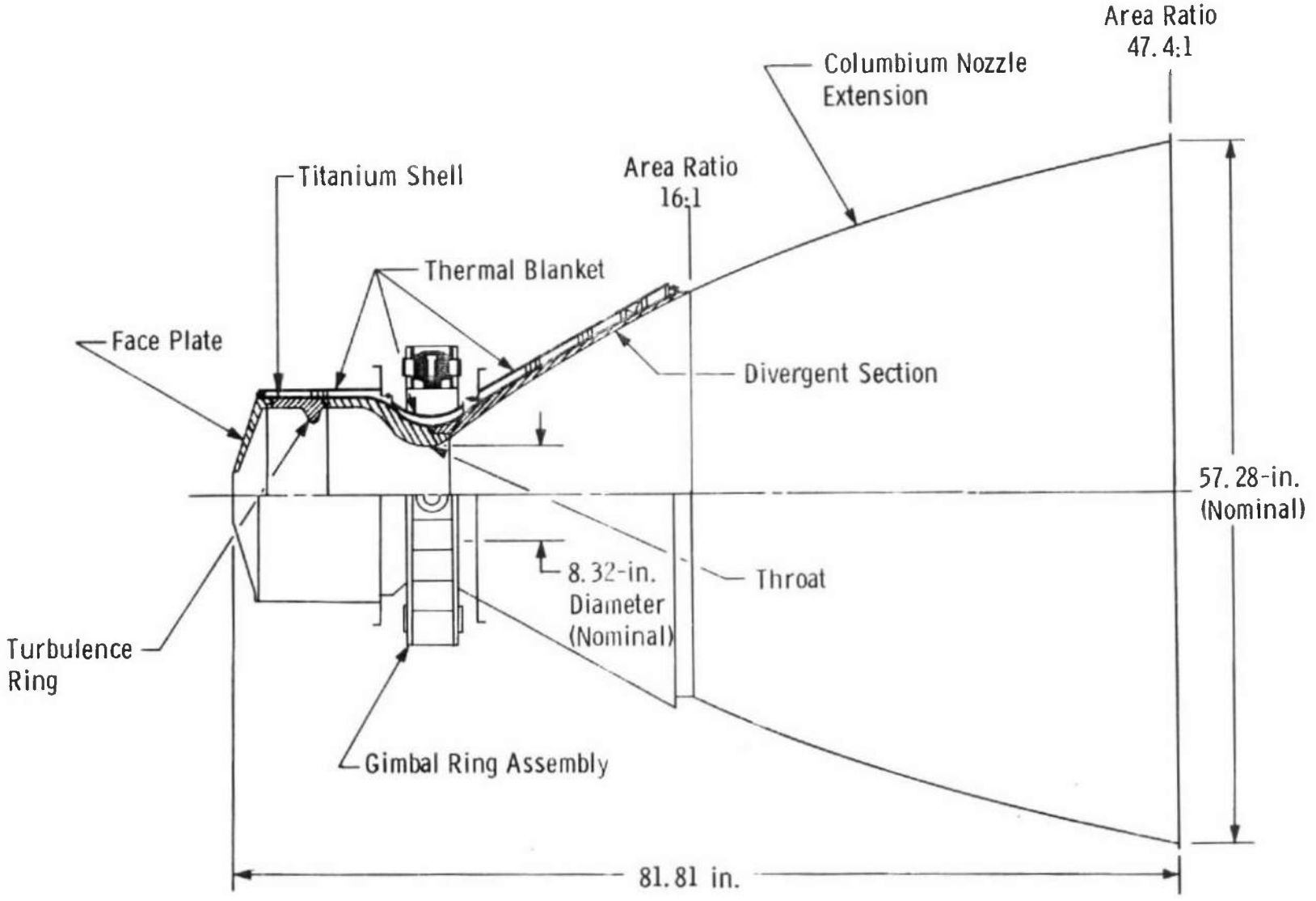

Fig. 4 Cross Section of the LMDE Chomber ond Nozzle Extension

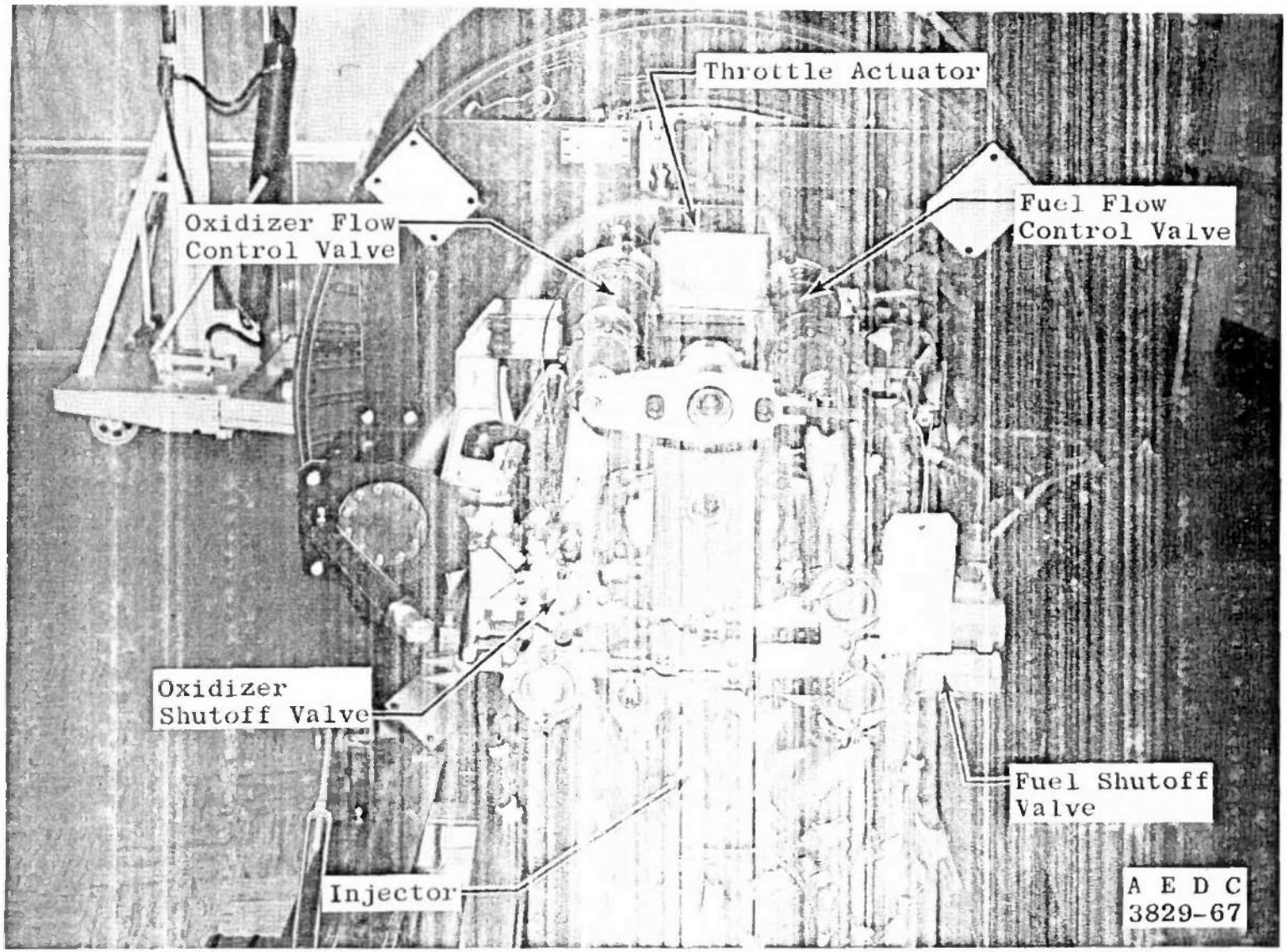

Fig. 5 Thrust Control Assembly

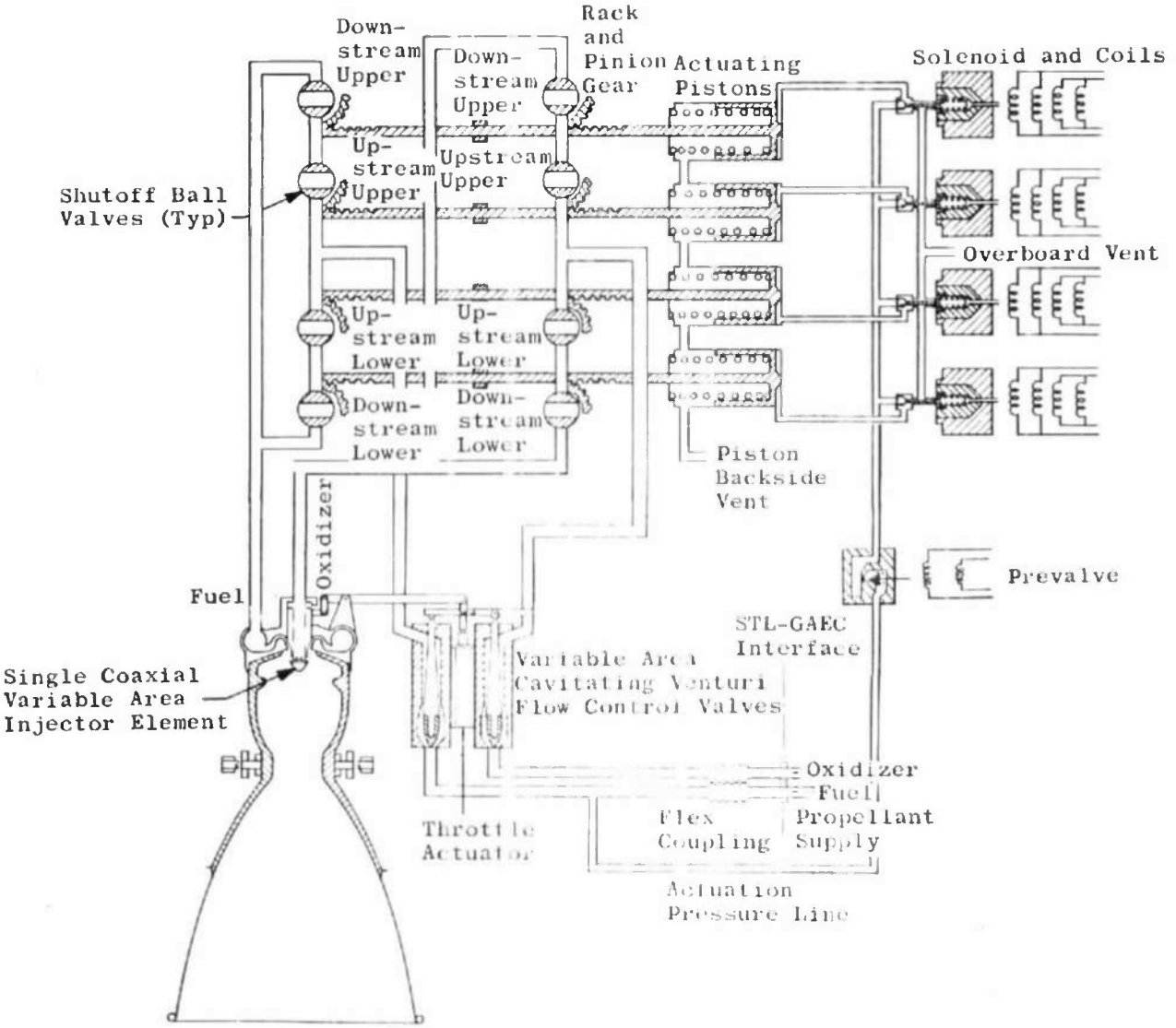

Fig. 6 Schematic of the Thrust Control System

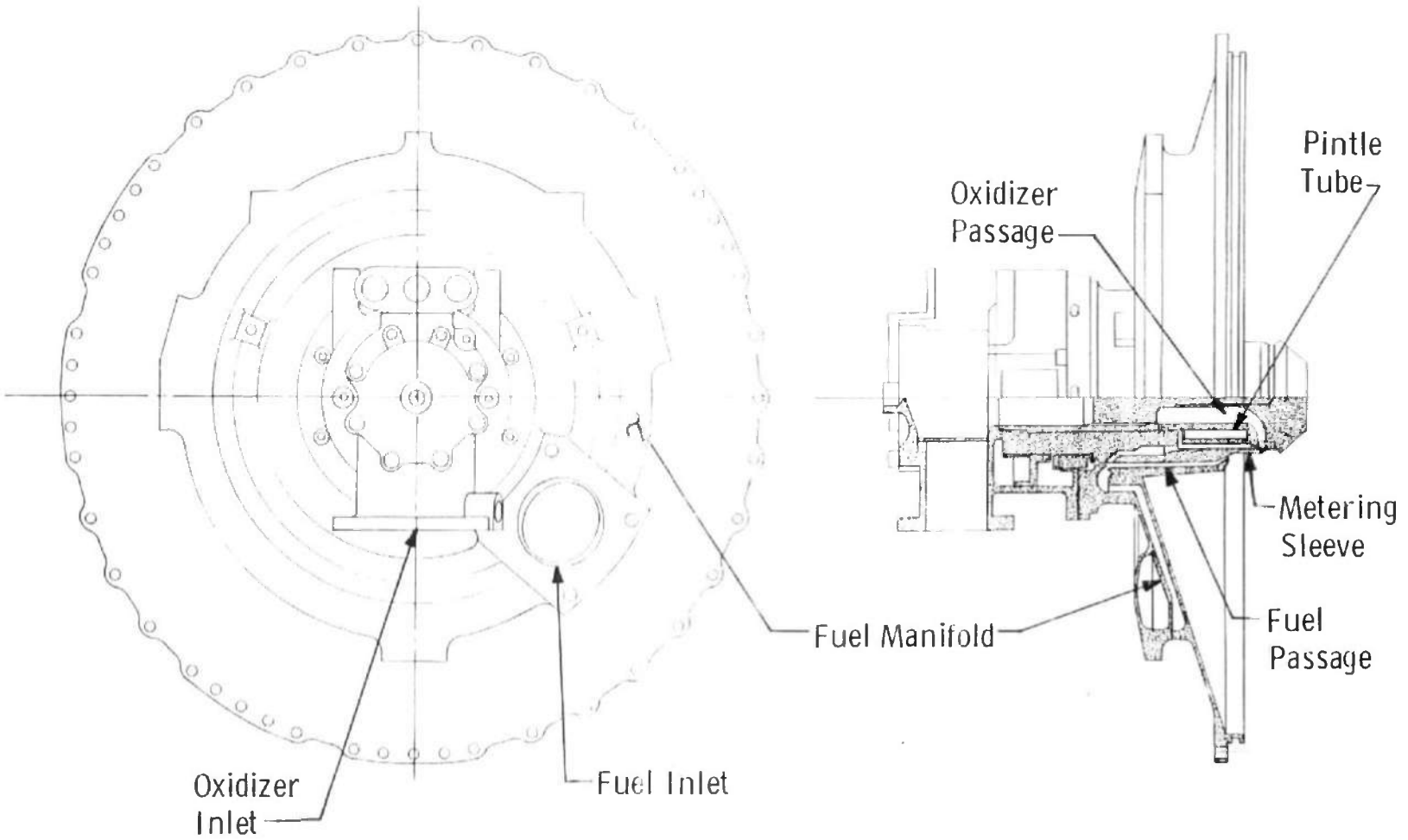

a. Assembly

Fig. 7 Propellant Injector

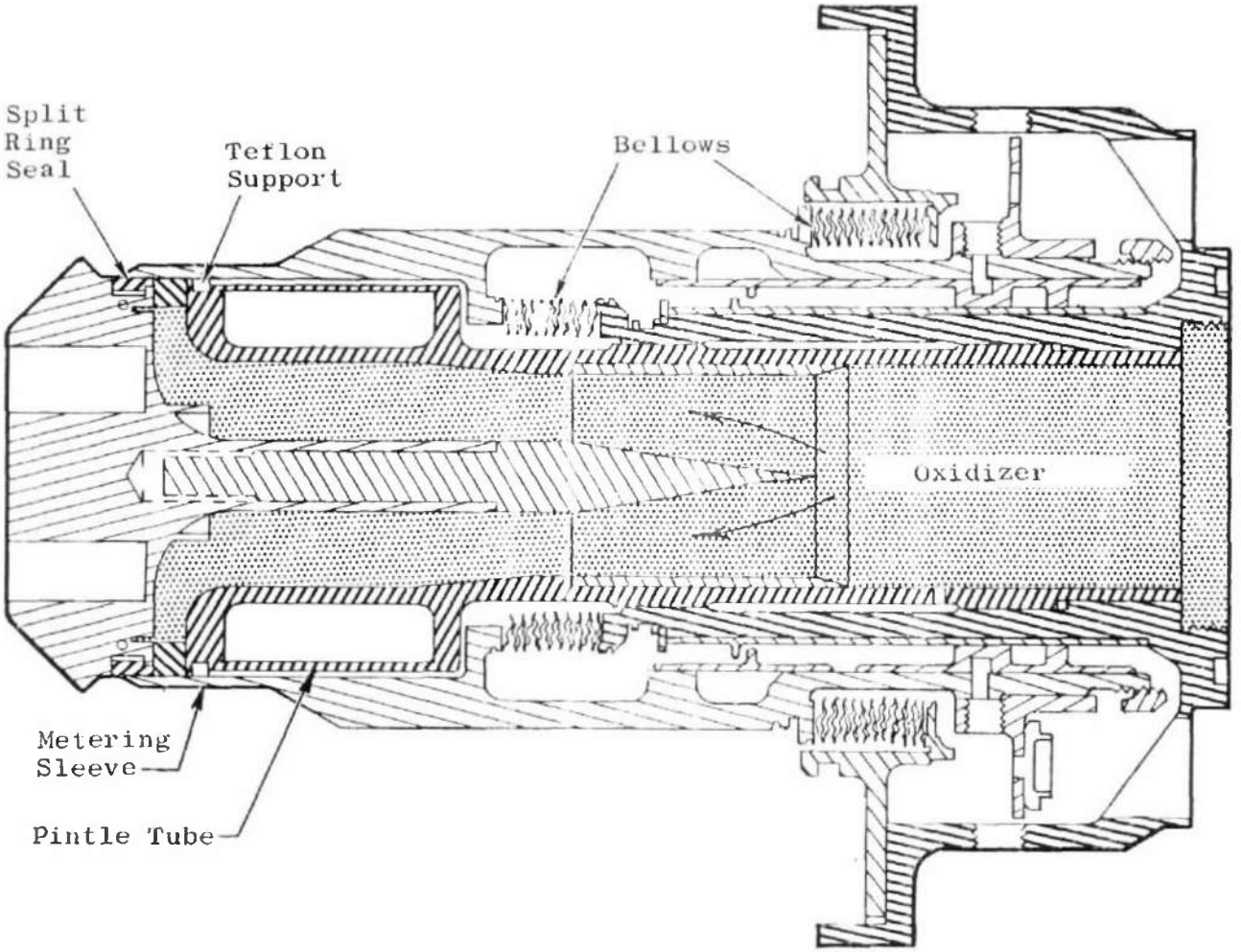

b. Pintle Schematic

Fig. 7 Concluded

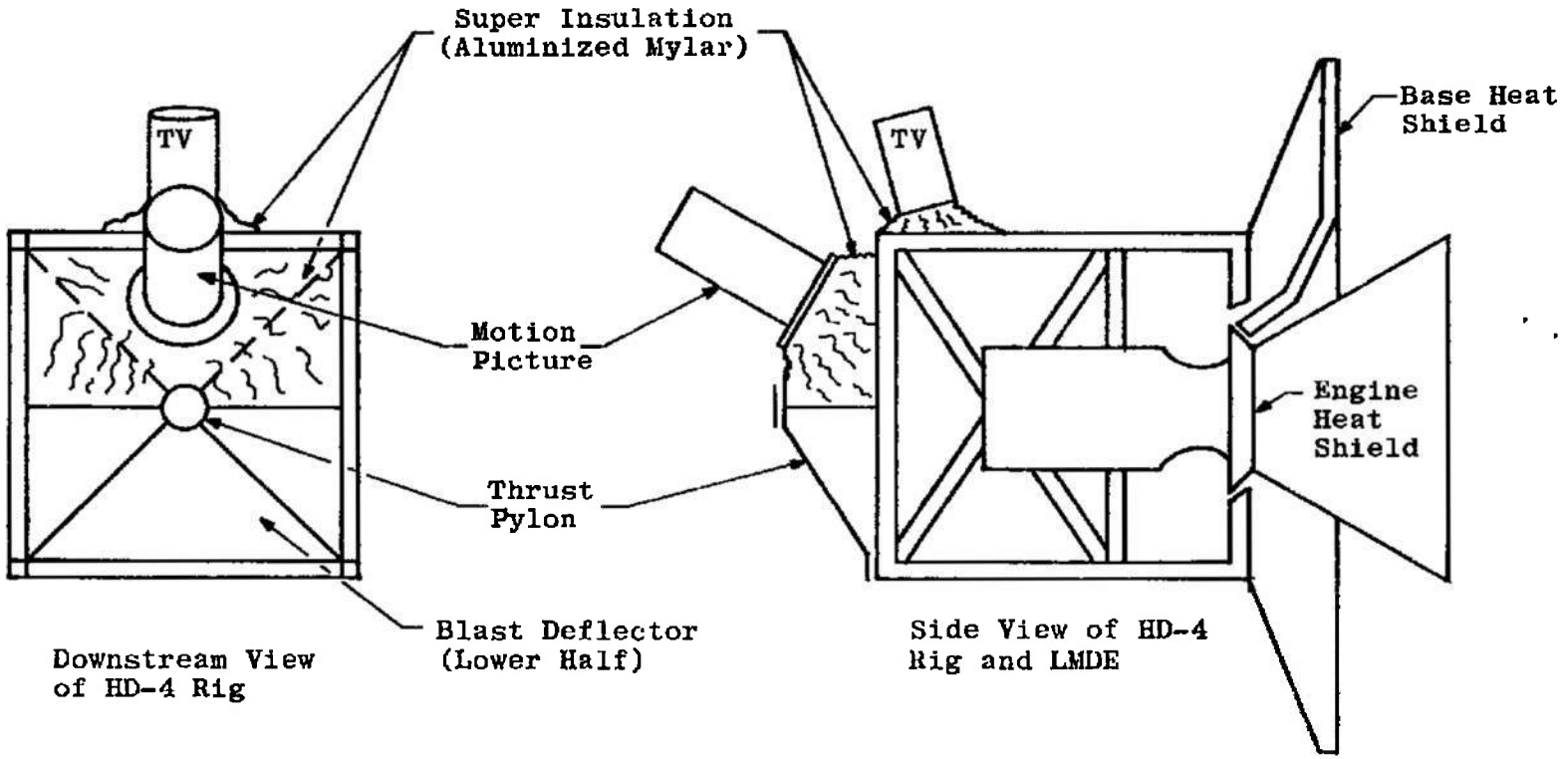

Fig. 8 Super Insulation Installation

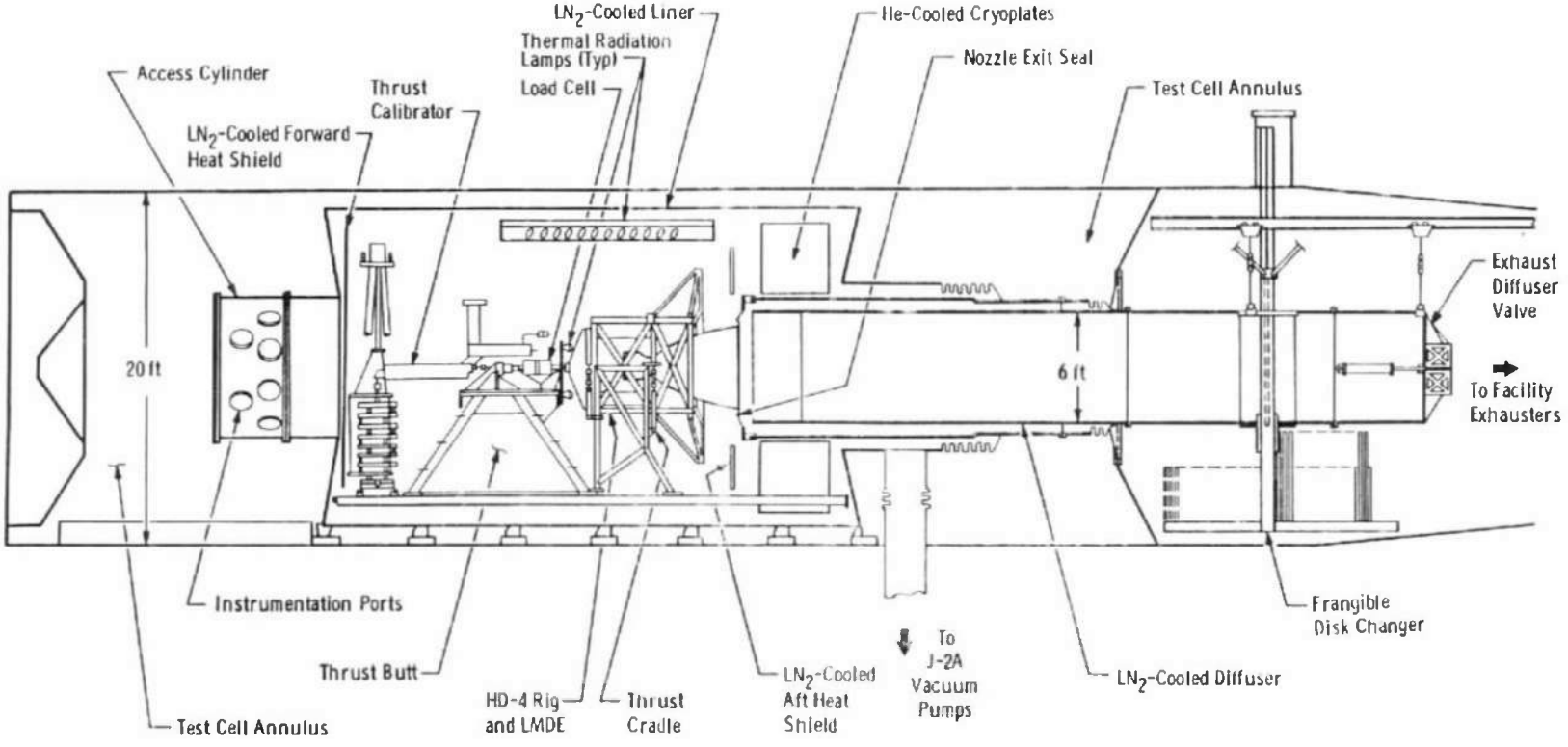

Fig. 9 Schematic of Test Article Installation in the J-2A Test Cell

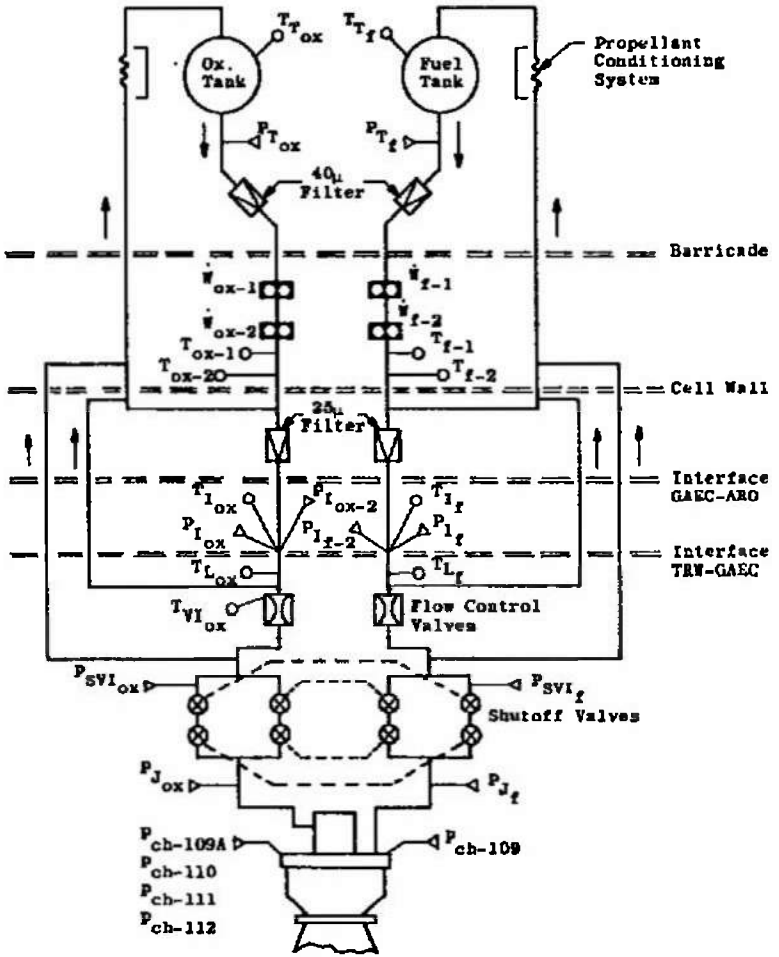

Nomenclature	Identification
	Pressures
$P_{T_{ox}}$	Oxidizer Tank
P_{T_f}	Fuel Tank
$P_{I_{ox}}$	Oxidizer Interface
$P_{I_{ox-2}}$	Oxidizer Interface No 2
P_{I_f}	Fuel Interface
$P_{I_{f-2}}$	Fuel Interface No. 2
$P_{SVI_{ox}}$	Oxidizer Shutoff Valve Inlet
P_{SVI_f}	Fuel Shutoff Valve Inlet
$P_{J_{ox}}$	Oxidizer Injector Inlet
P_{J_f}	Fuel Injector Inlet
P_{ch-109}	Chamber Pressure
$P_{ch-109A}$	↓
P_{ch-110}	↓
P_{ch-111}	↓
P_{ch-112}	↓
	Temperatures
$T_{T_{ox}}$	Oxidizer Tank
T_{T_f}	Fuel Tank
T_{ox-1}	Oxidizer (at Flowmeter)
T_{ox-2}	Oxidizer (at Flowmeter)
T_{f-1}	Fuel (at Flowmeter)
T_{f-2}	Fuel (at Flowmeter)
$T_{I_{ox}}$	Oxidizer Interface
T_{I_f}	Fuel Interface
$T_{VI_{ox}}$	Oxidizer Flow Control Valve Inlet
$T_{L_{ox}}$	Oxidizer Line
T_{L_f}	Fuel Line
	Flows
$\dot{W}_{ox-1}$	Oxidizer
$\dot{W}_{ox-2}$	Oxidizer
$\dot{W}_{f-1}$	Fuel
$\dot{W}_{f-2}$	Fuel

Fig. 10 Propellant System Schematic and Instrumentation Locations

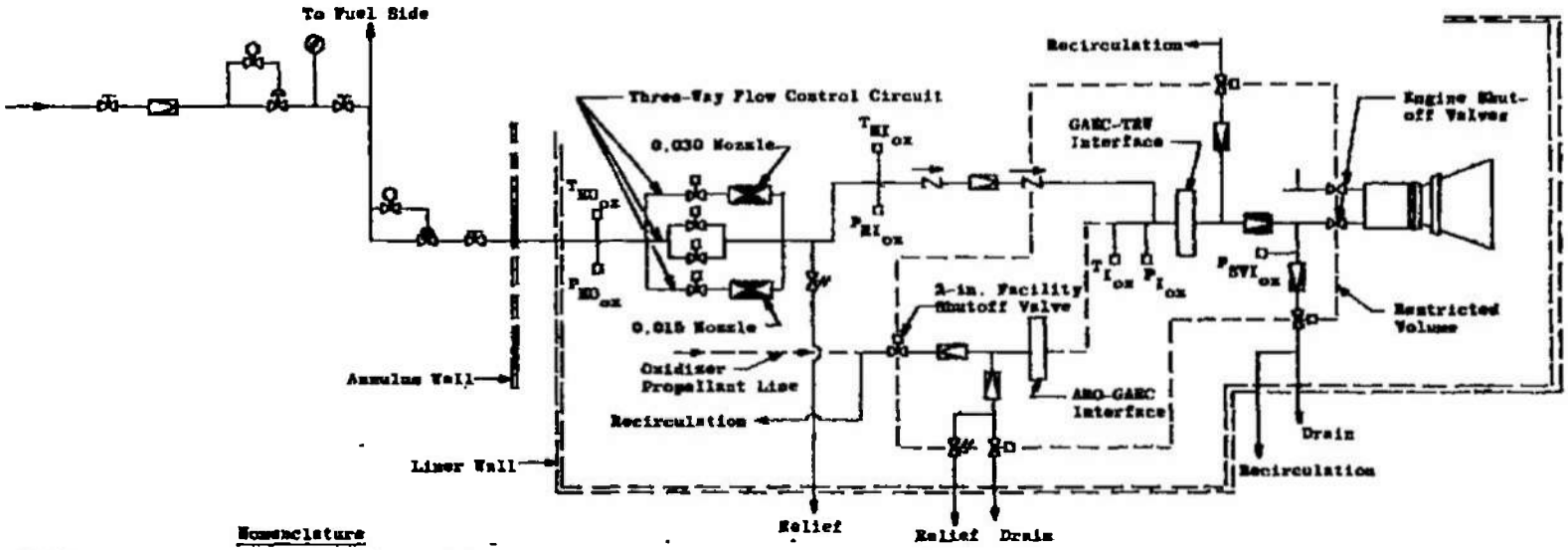

Nomenclature

Plumbing	Instrumentation	
Hand Valve	$P_{NO_{ox}}$	Nozzle Upstream Pressure
Remote Valve	$T_{NO_{ox}}$	Nozzle Upstream Temperature
Remote Loader	$P_{NI_{ox}}$	Injector Pressure
Regulator	$T_{NI_{ox}}$	Injector Temperature
Relief Valve	$T_{I_{ox}}$	Interface Temperature
Venturi	$P_{I_{ox}}$	Interface Pressure
Filter	$P_{SVI_{ox}}$	Shutoff Valve Inlet Pressure
Check Valve		
Pressure Gage		

Restricted Volumes

Oxidizer 0.379 ft^3

Fuel 0.383 ft^3

a. Schematic and Instrumentation Locations

Fig. 11 Propellant Helium Ingestion/Depletion System (Oxidizer Side, Typ)

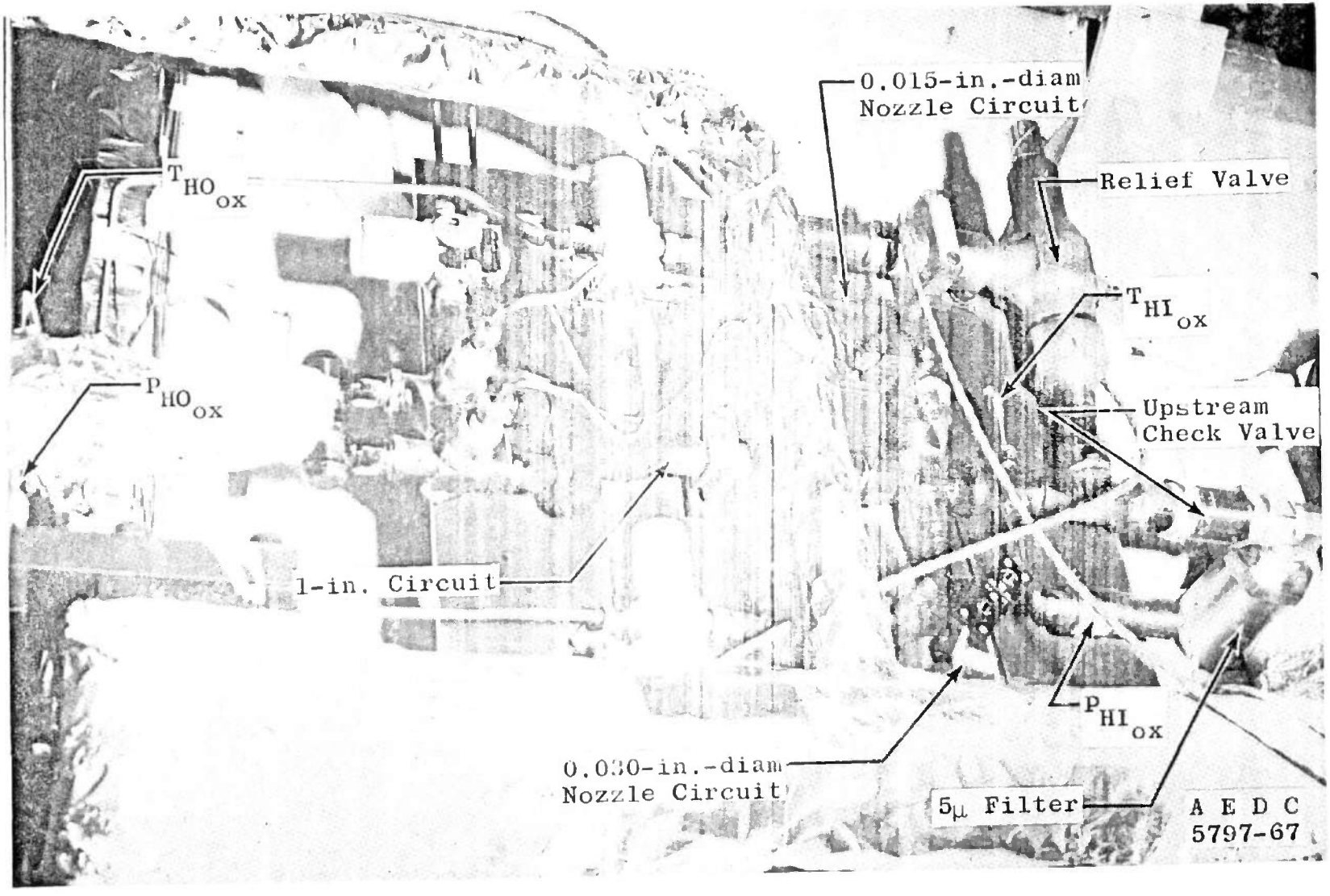

b. Valve Panel

Fig. 11 Continued

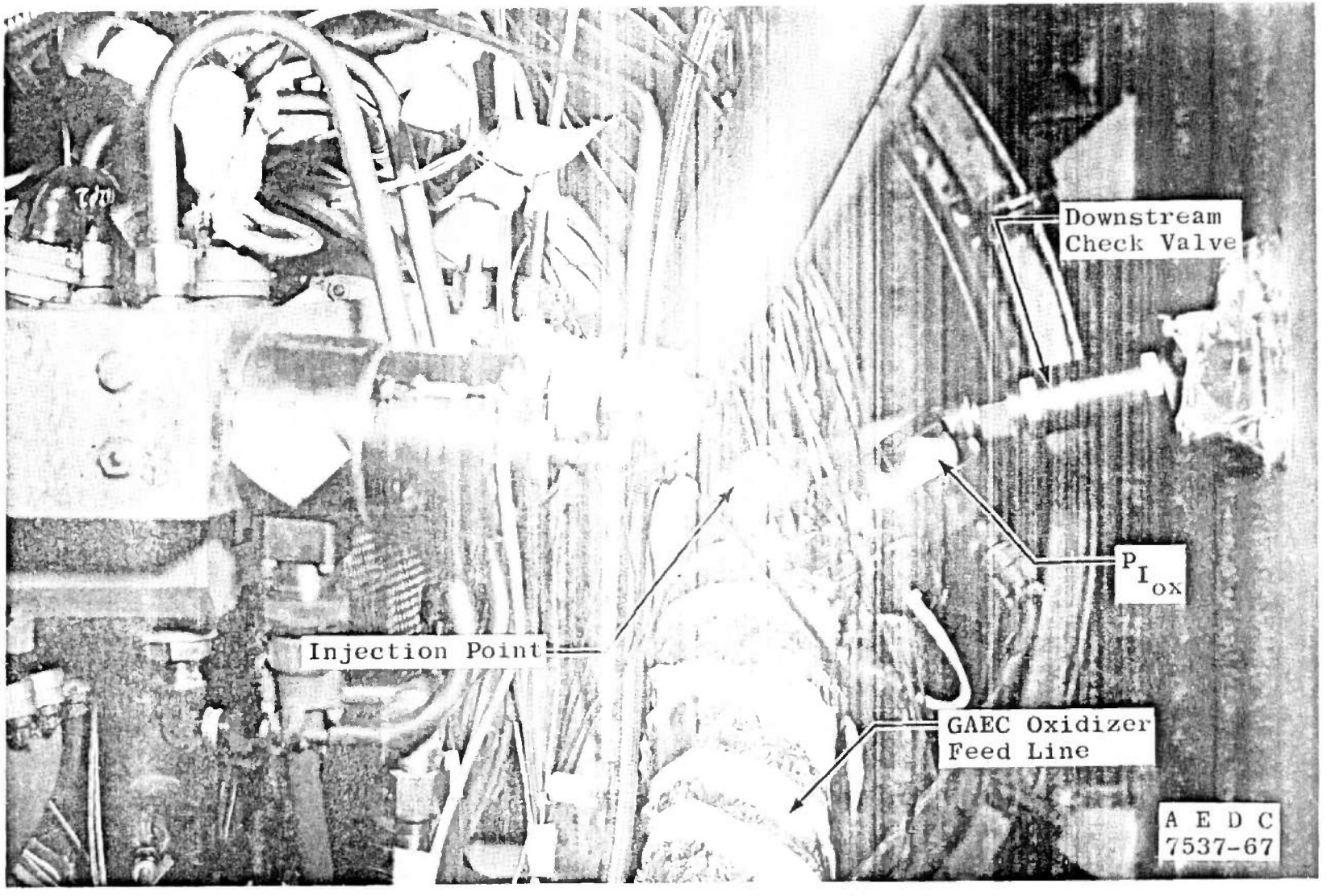

c. HD-4 Rig Interior

Fig. 11 Concluded

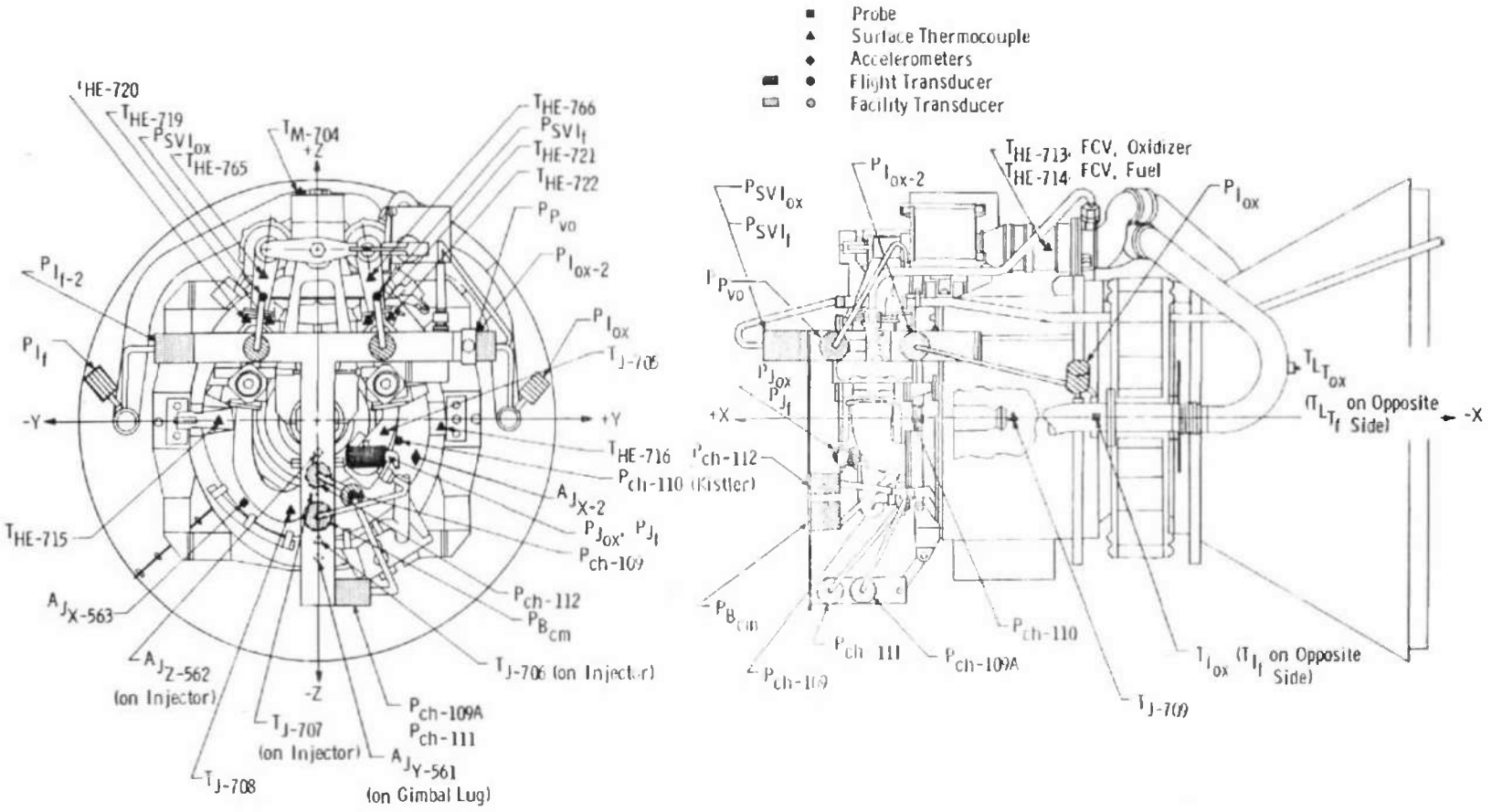

a. Headend

Fig. 12 Engine Instrumentation Locations

Nomenclature	Identification
	Pressures
$P_{I_{ox}}$	Oxidizer Interface
$P_{I_{ox-2}}$	Oxidizer Interface
P_{I_f}	Fuel Interface
$P_{I_{f-2}}$	Fuel Interface
$P_{SVI_{ox}}$	Oxidizer Shutoff Valve Inlet
P_{SVI_f}	Fuel Shutoff Valve Inlet
$P_{J_{ox}}$	Oxidizer Injector Inlet
P_{J_f}	Fuel Injector Inlet
$P_{P_{vo}}$	Pre-Valve Outlet
$P_{B_{cm}}$	Barrier Coolant Manifold
$P_{ch-109A}$	Chamber Pressure
P_{ch-109}	↓
P_{ch-110}	↓
P_{ch-111}	↓
P_{ch-112}	↓
	Temperatures
$T_{I_{ox}}$	Oxidizer Interface
T_{I_f}	Fuel Interface
$T_{VI_{ox}}$	Oxidizer Flow Control Valve
T_{M-704}	Throttle Actuator Housing
T_{J-705}	Injector
T_{J-706}	↓
T_{J-707}	↓
T_{J-708}	↓
T_{J-709}	↓
T_{HE-713}	Headend Assembly
T_{HE-714}	↓
T_{HE-719}	↓
T_{HE-720}	↓
T_{HE-721}	↓
T_{HE-722}	↓
T_{HE-765}	↓
T_{HE-766}	↓
	Accelerometers
$A_{J_{X-563}}$	Headend Assembly X-X Axis
$A_{J_{Y-561}}$	Headend Assembly Y-Y Axis
$A_{J_{Z-562}}$	Headend Assembly Z-Z Axis
$A_{J_{X-2}}$*	Headend Assembly

*Test Period AE Only

Fig. 12a Concluded

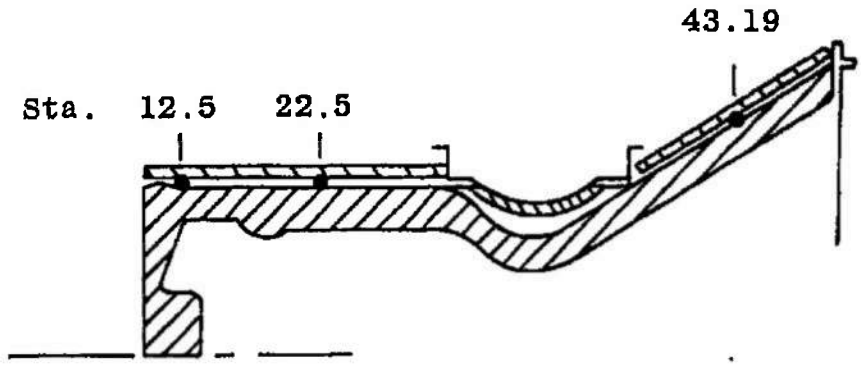

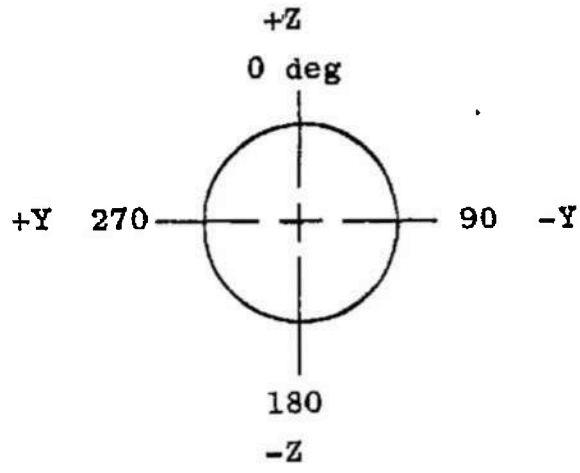

View Looking Upstream

Thermocouples	Station, in.	Angular Location, deg
T_{C-725}	12.5	0
-726	12.5	180
-731	22.5	0
-732	22.5	180
-741	43.19	0
-742	43.19	180

b. Combustion Chamber Titanium Case Exterior

Fig. 12 Continued

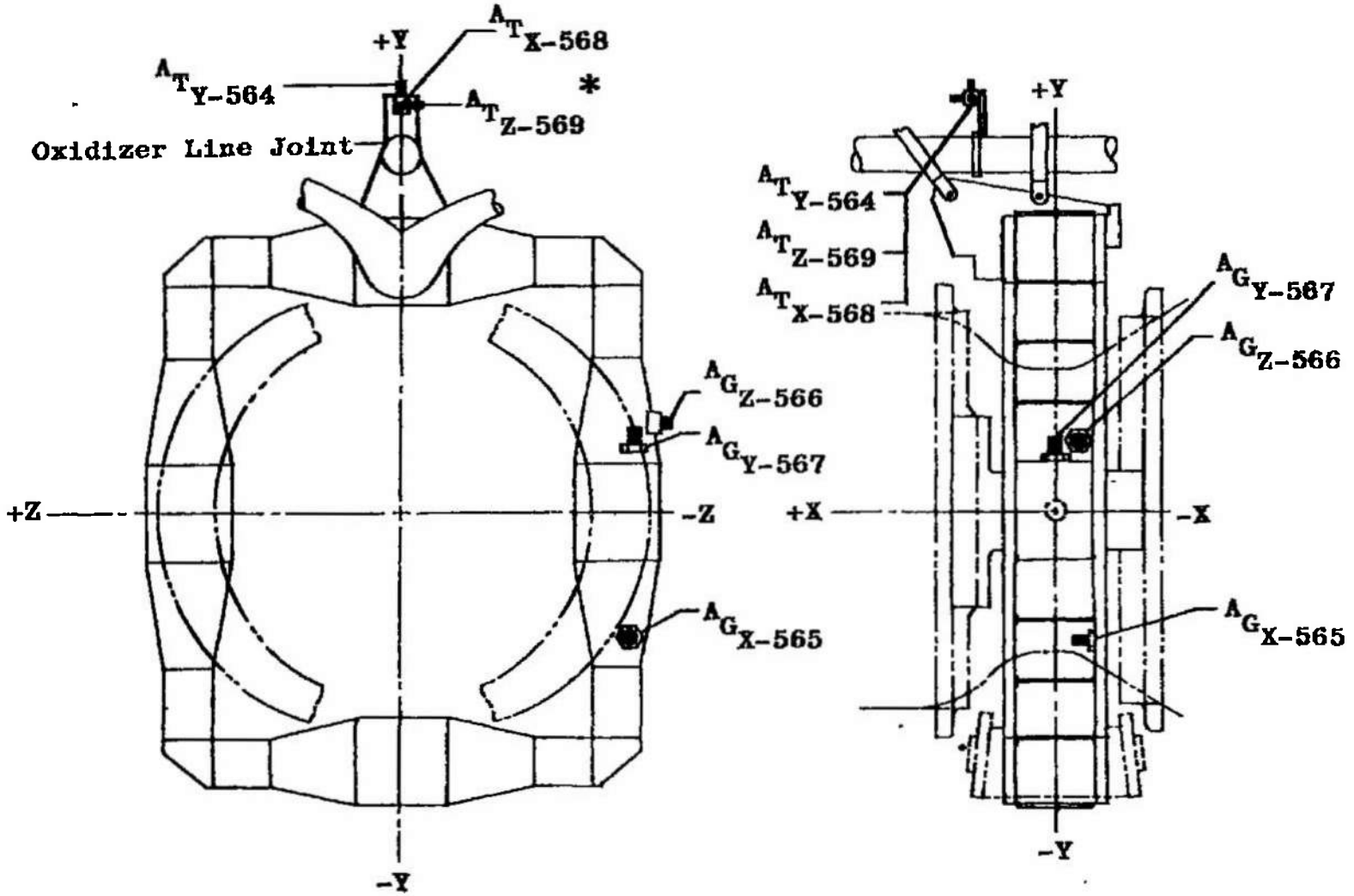

* Test Period AD Only

c. Gimbal Assembly

Fig. 12 Concluded

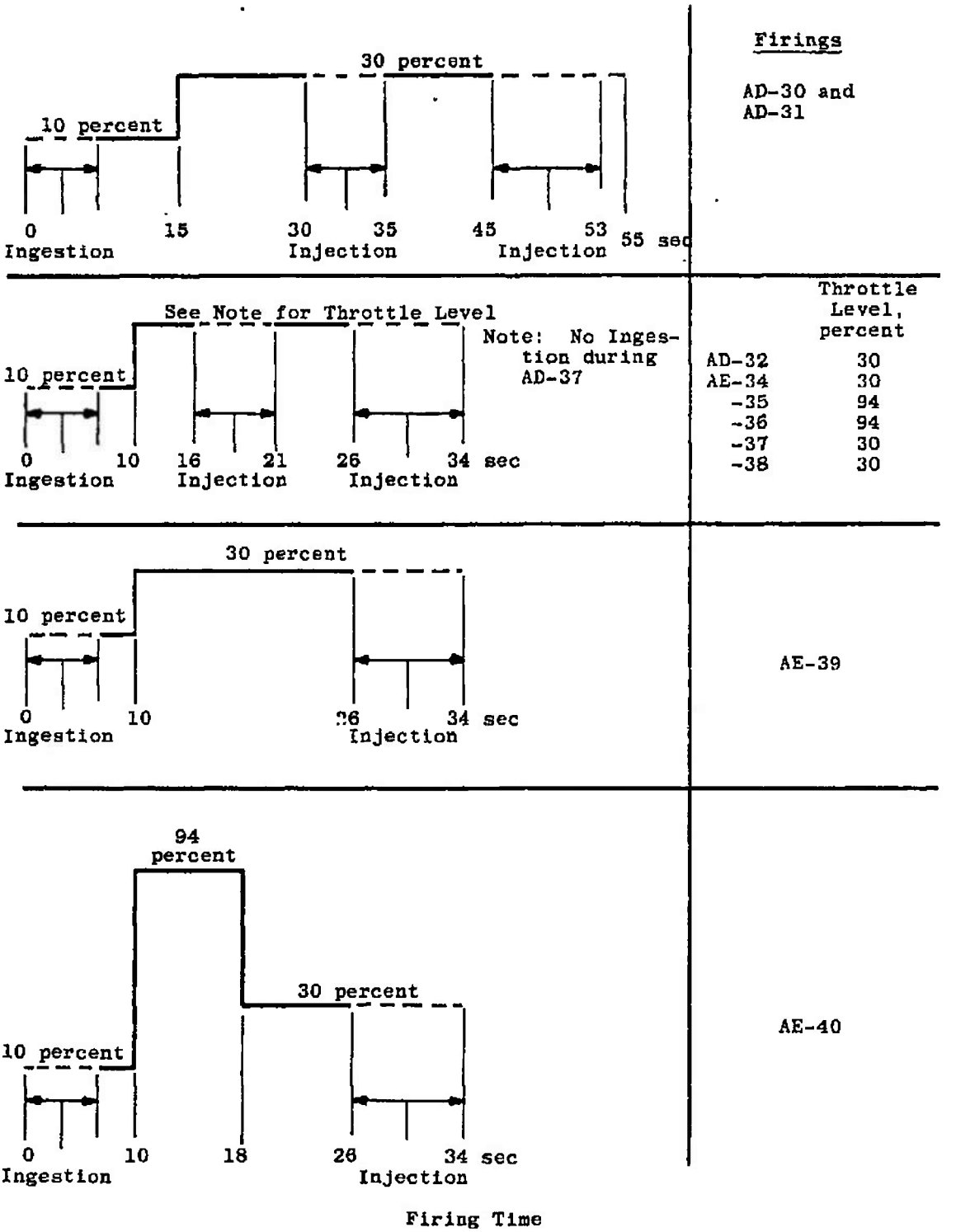

Fig. 13 Nominal Ingestion Profiles

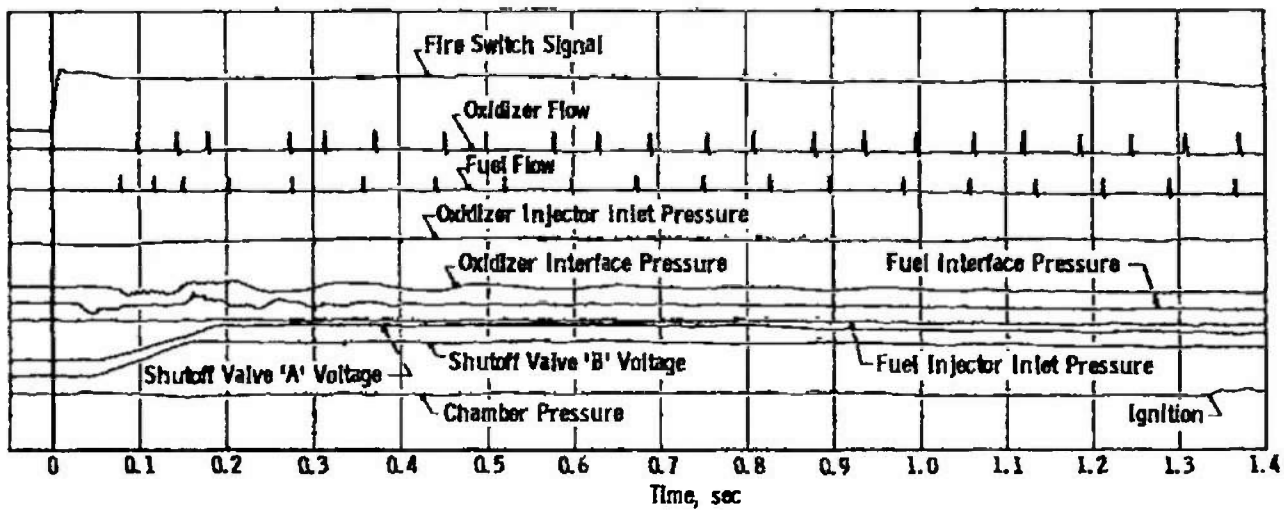

a. No Ingestion (Firing AD-28)

Fig. 14 Typical Ignition History

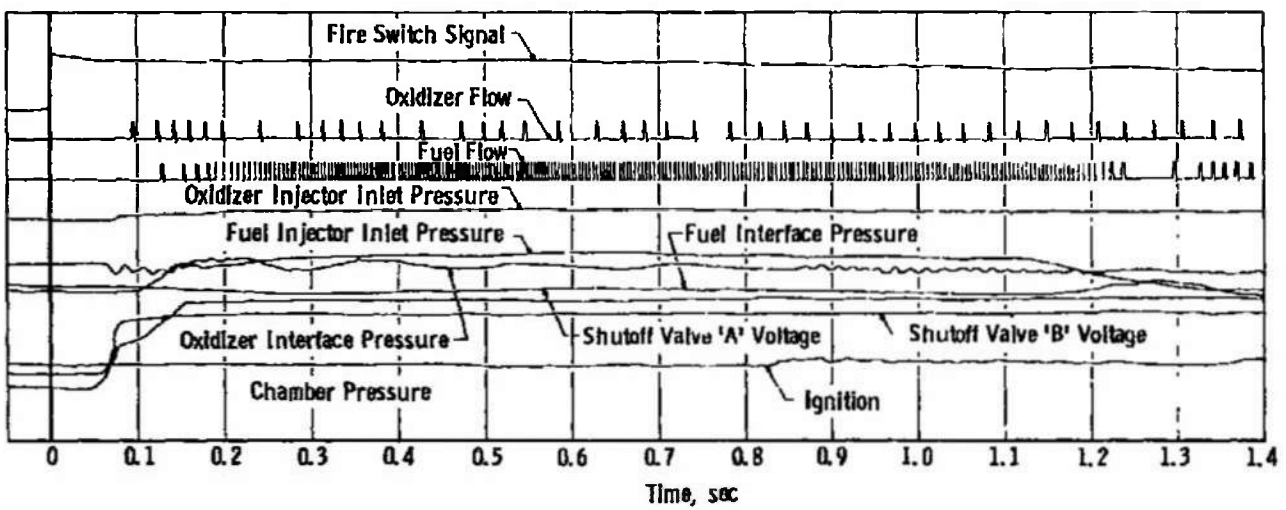

b. Fuel System Ingestion (Firing AE-34, Volume = 0.218 ft³)

Fig. 14 Continued

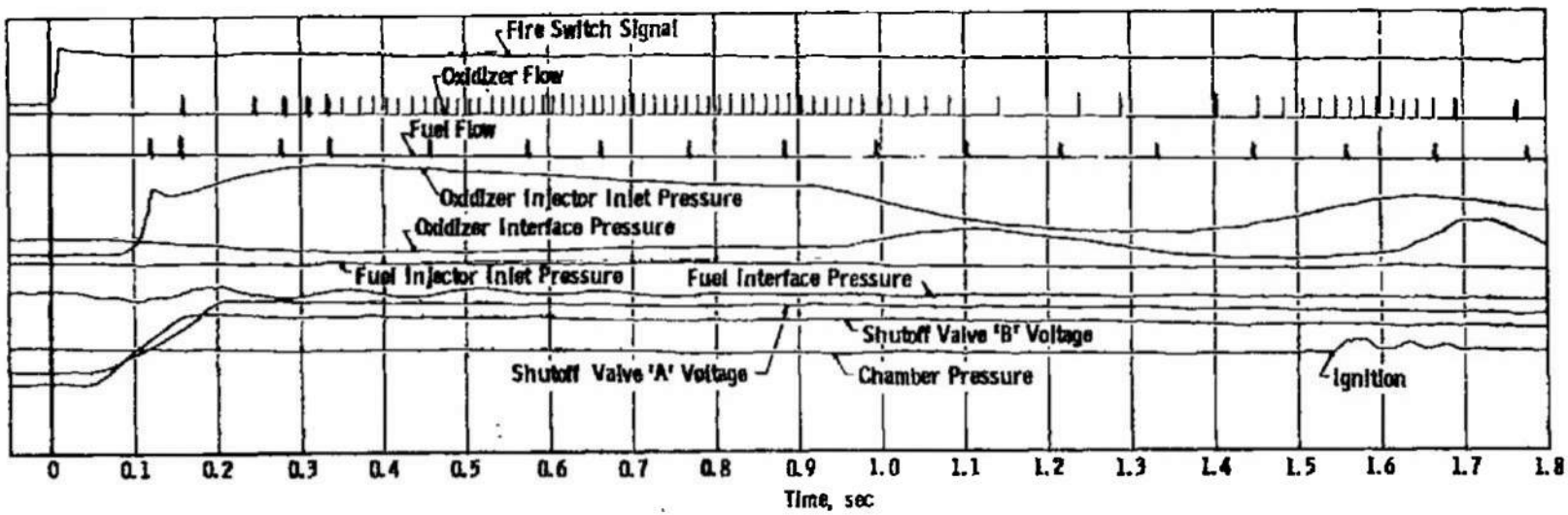

c. Oxidizer System Ingestion (Firing AE-40, Volume = 0.221 ft^3)

Fig. 14 Concluded

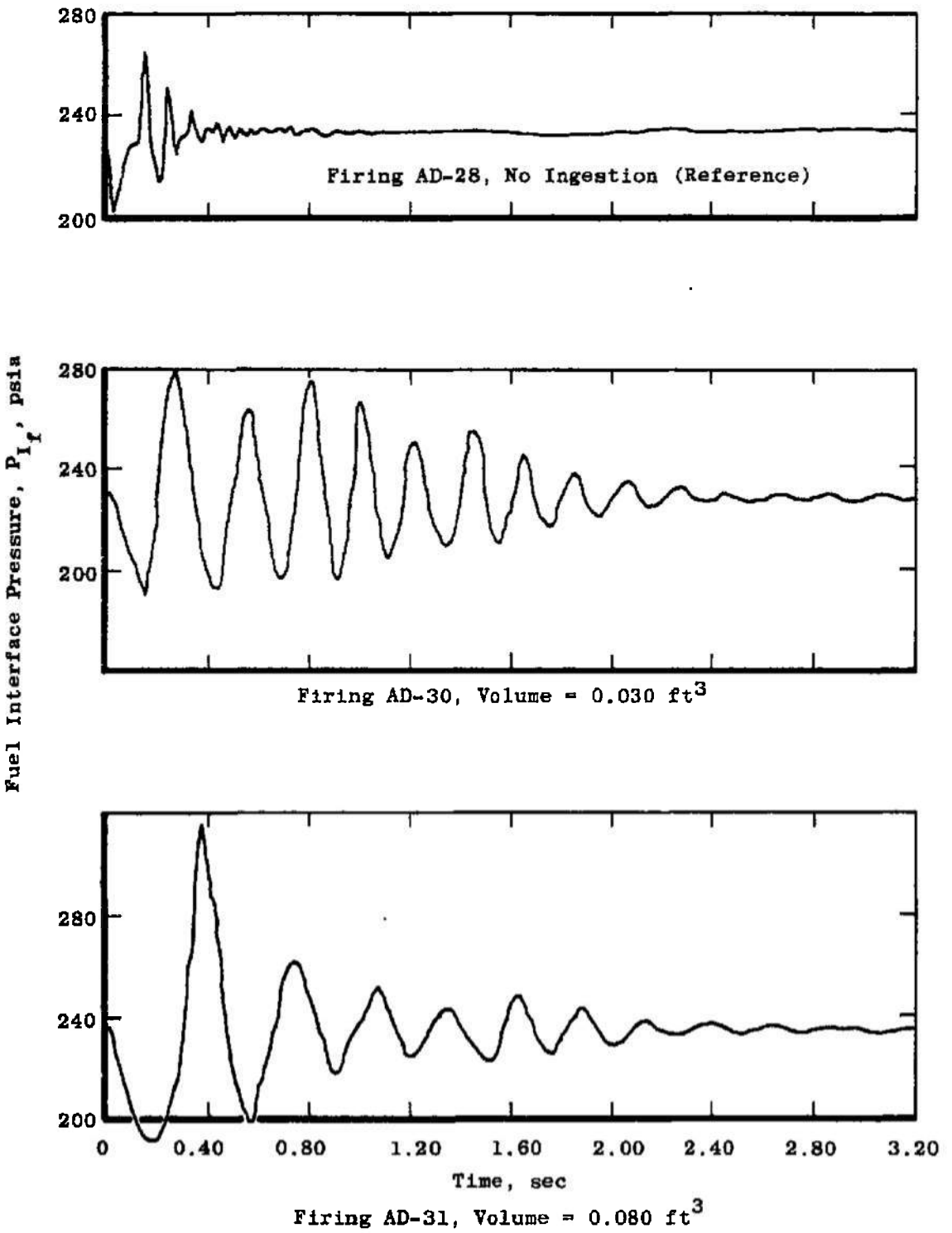

Fig. 15 Fuel Interface Pressure Ignition History

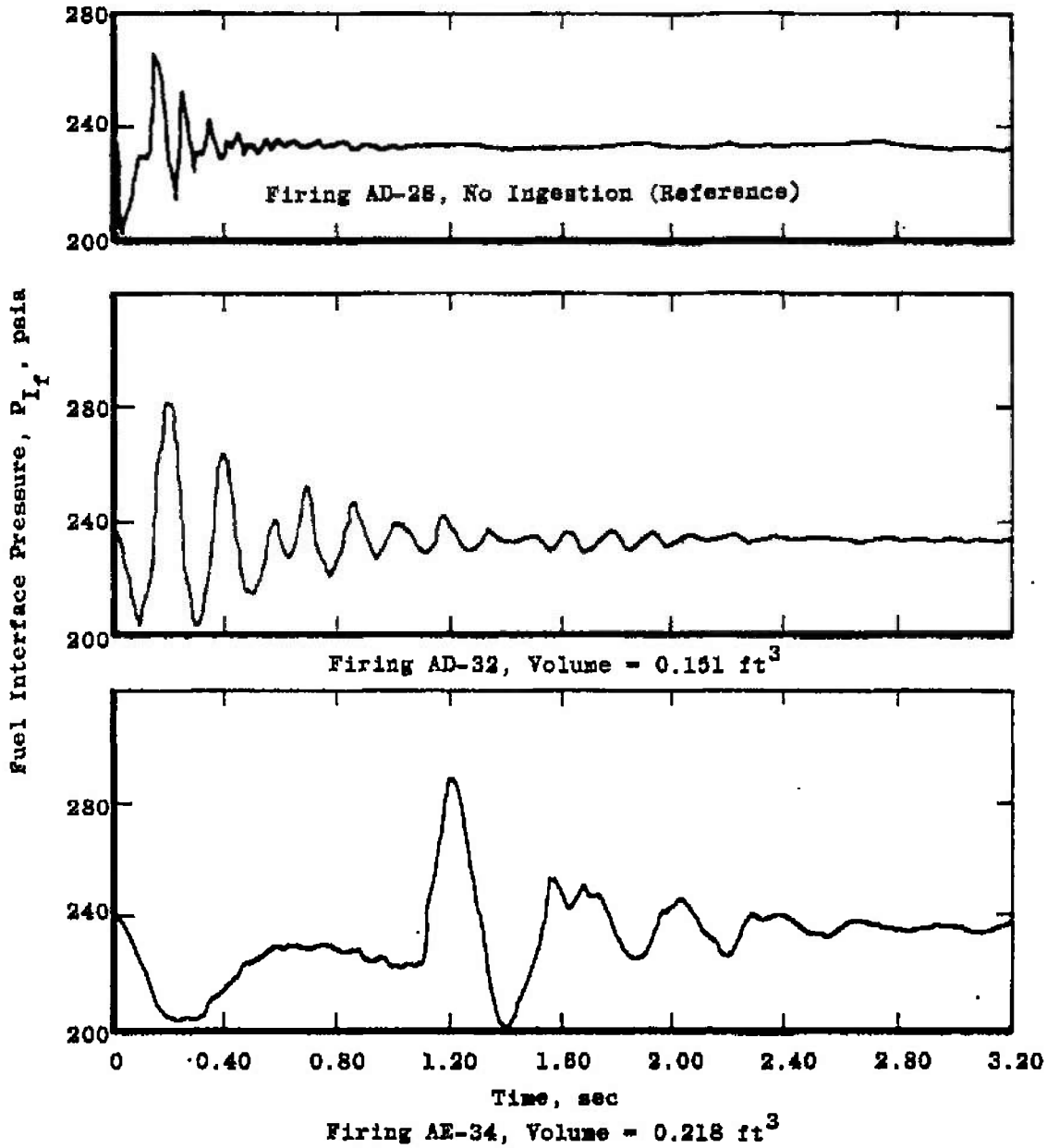

Fig. 15 Concluded

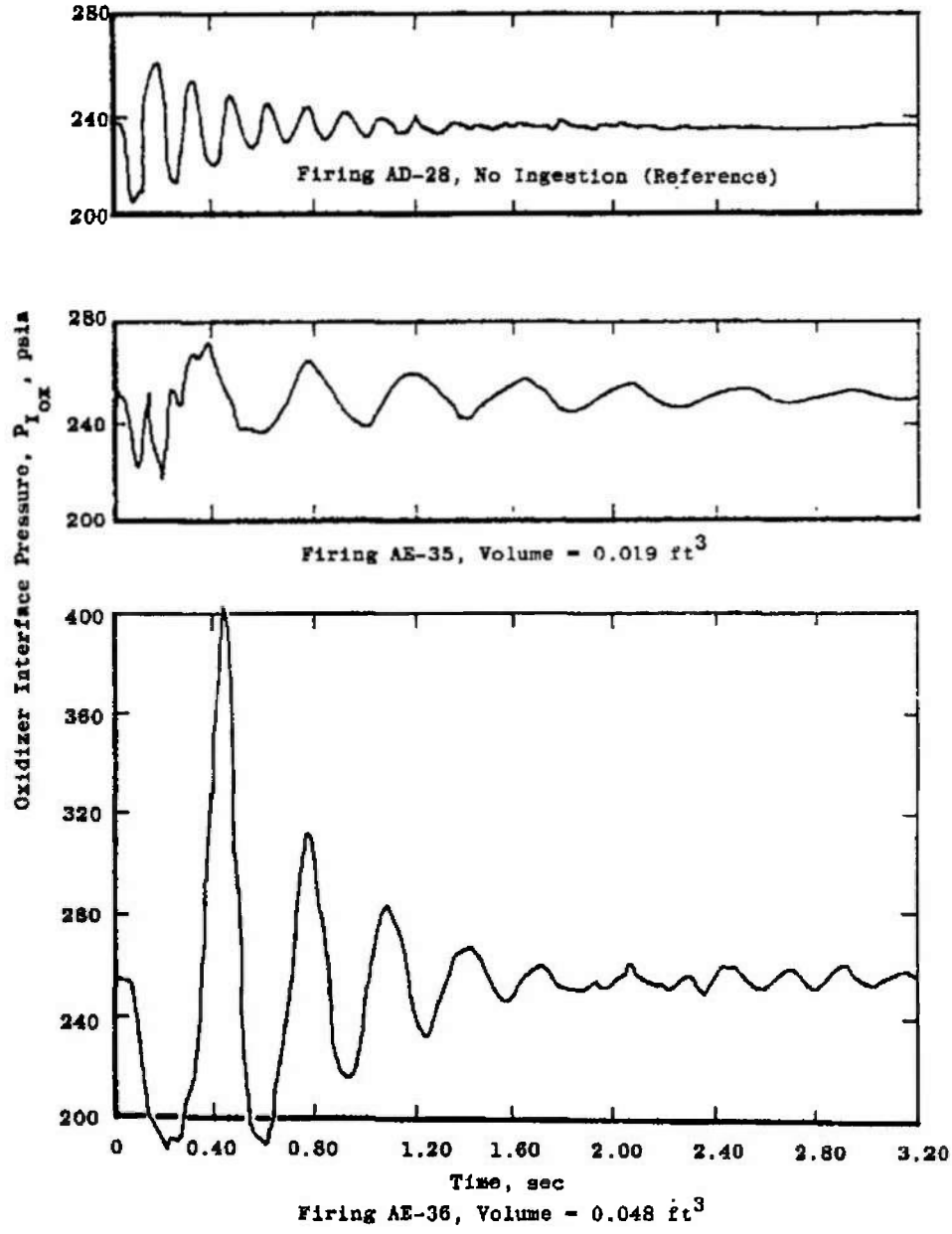

Fig. 16 Oxidizer Interface Pressure Ignition History

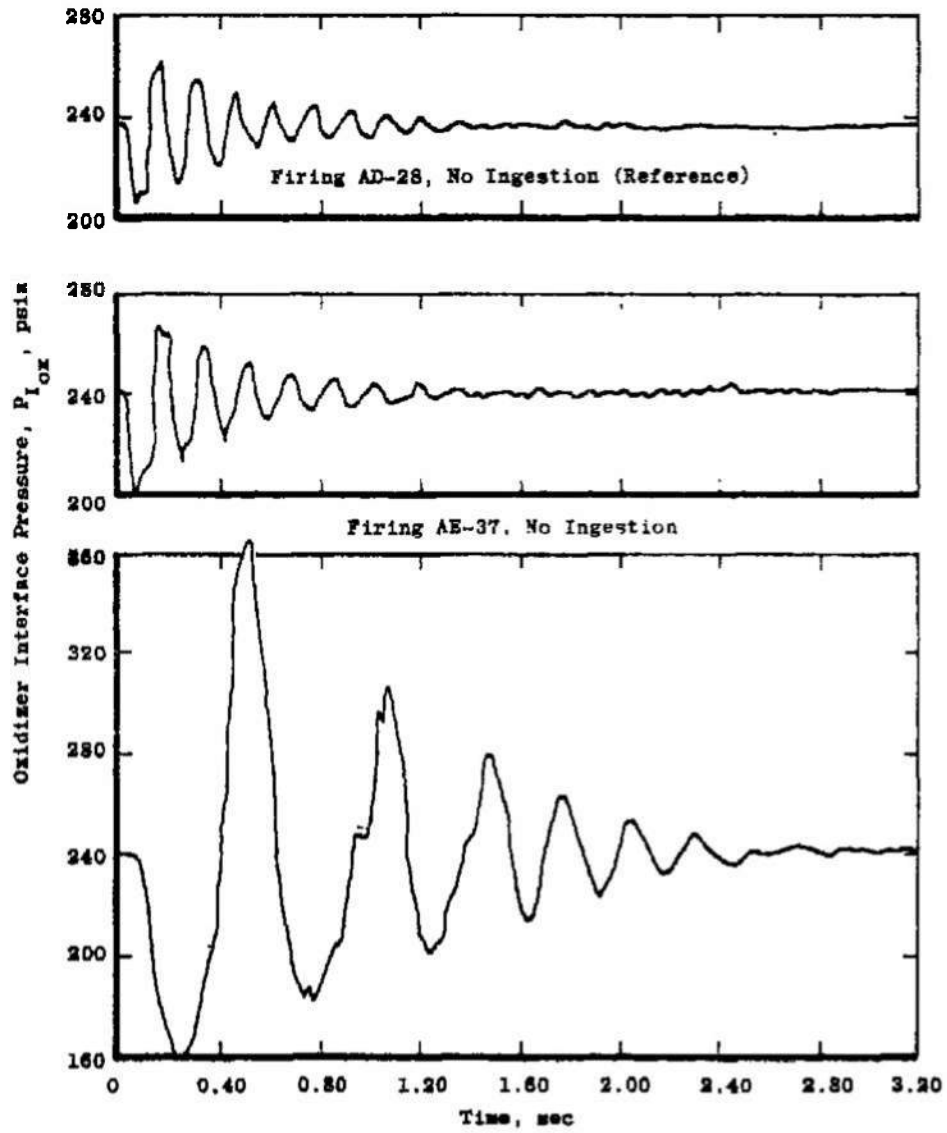

Fig. 16 Continued

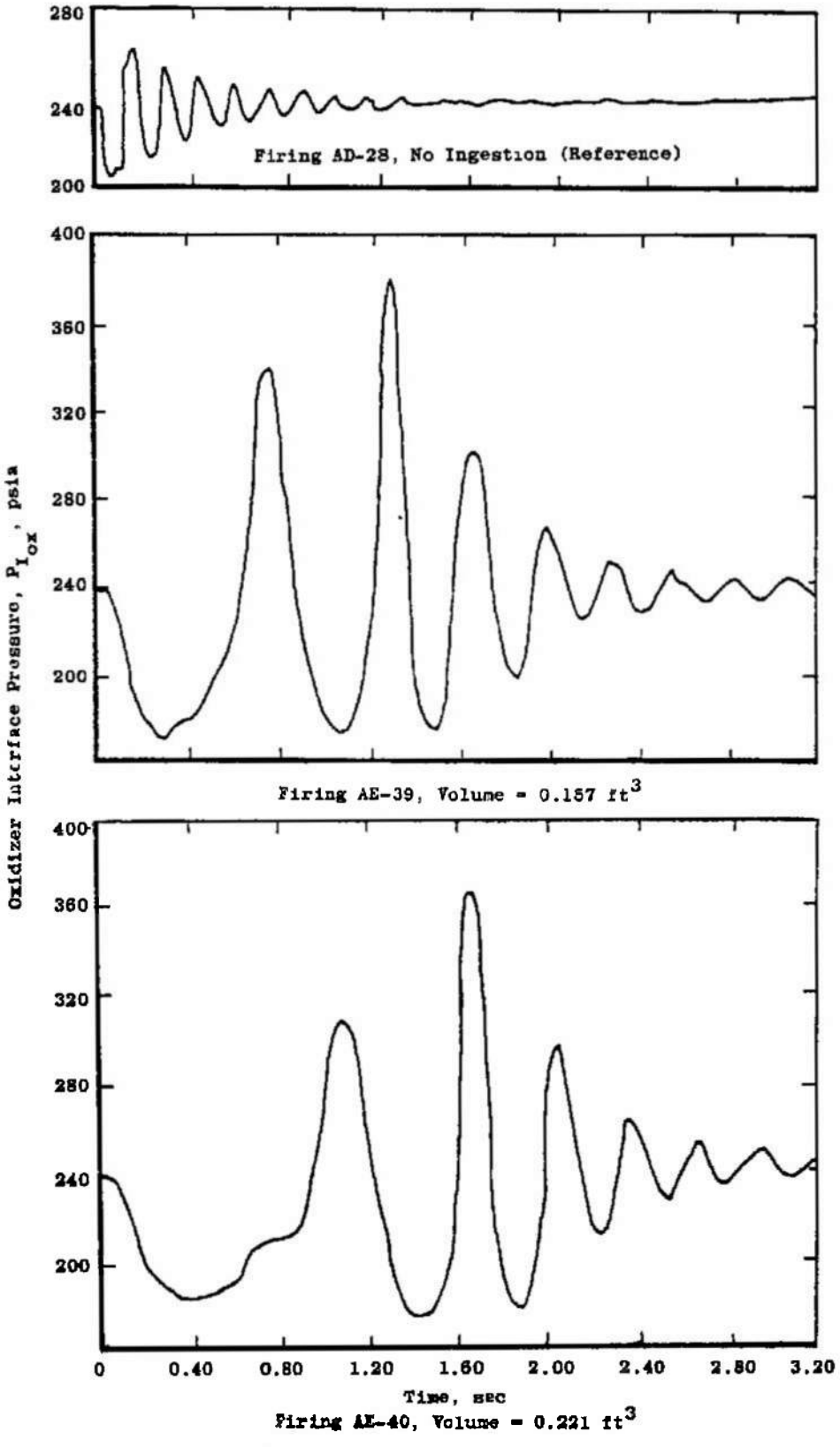

Fig. 16 Concluded

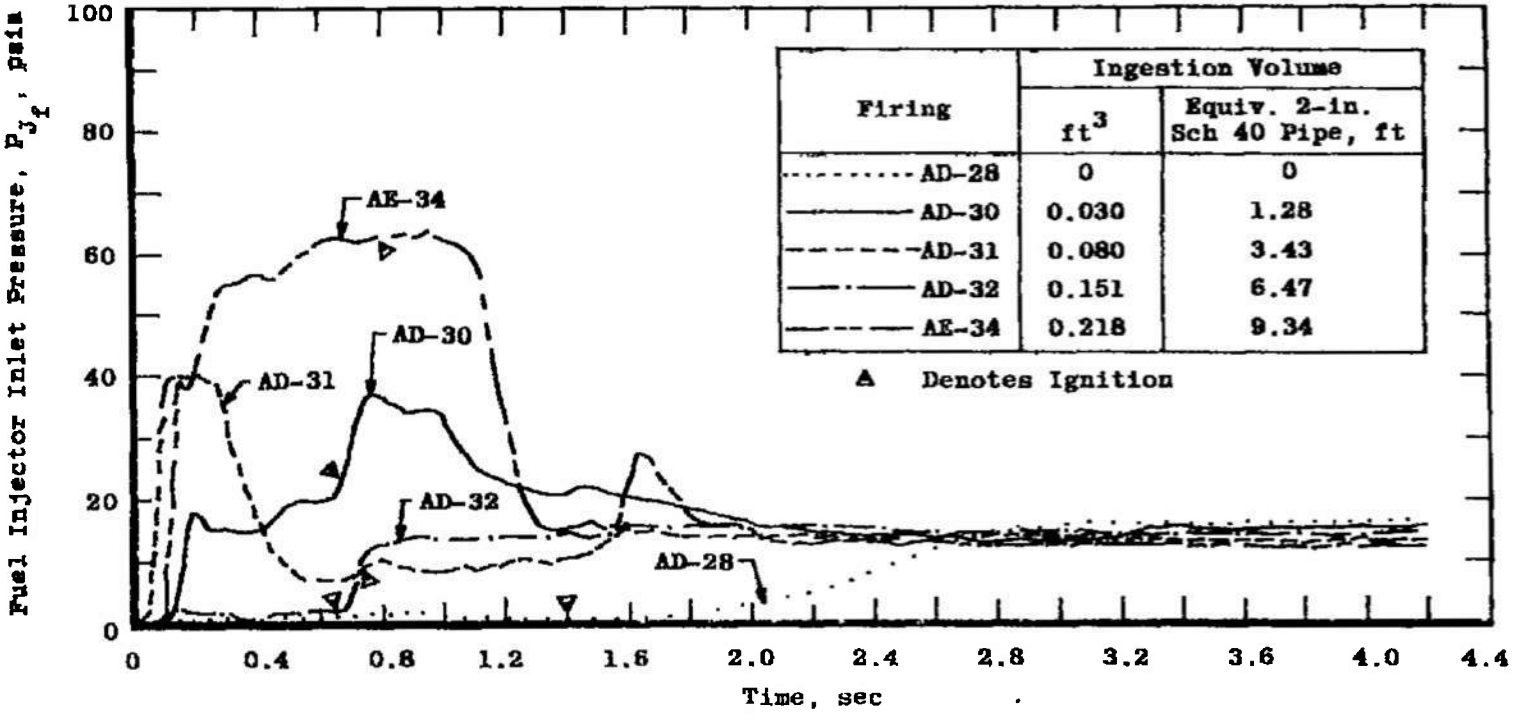

a. Fuel

Fig. 17 Injector Manifold Pressure History

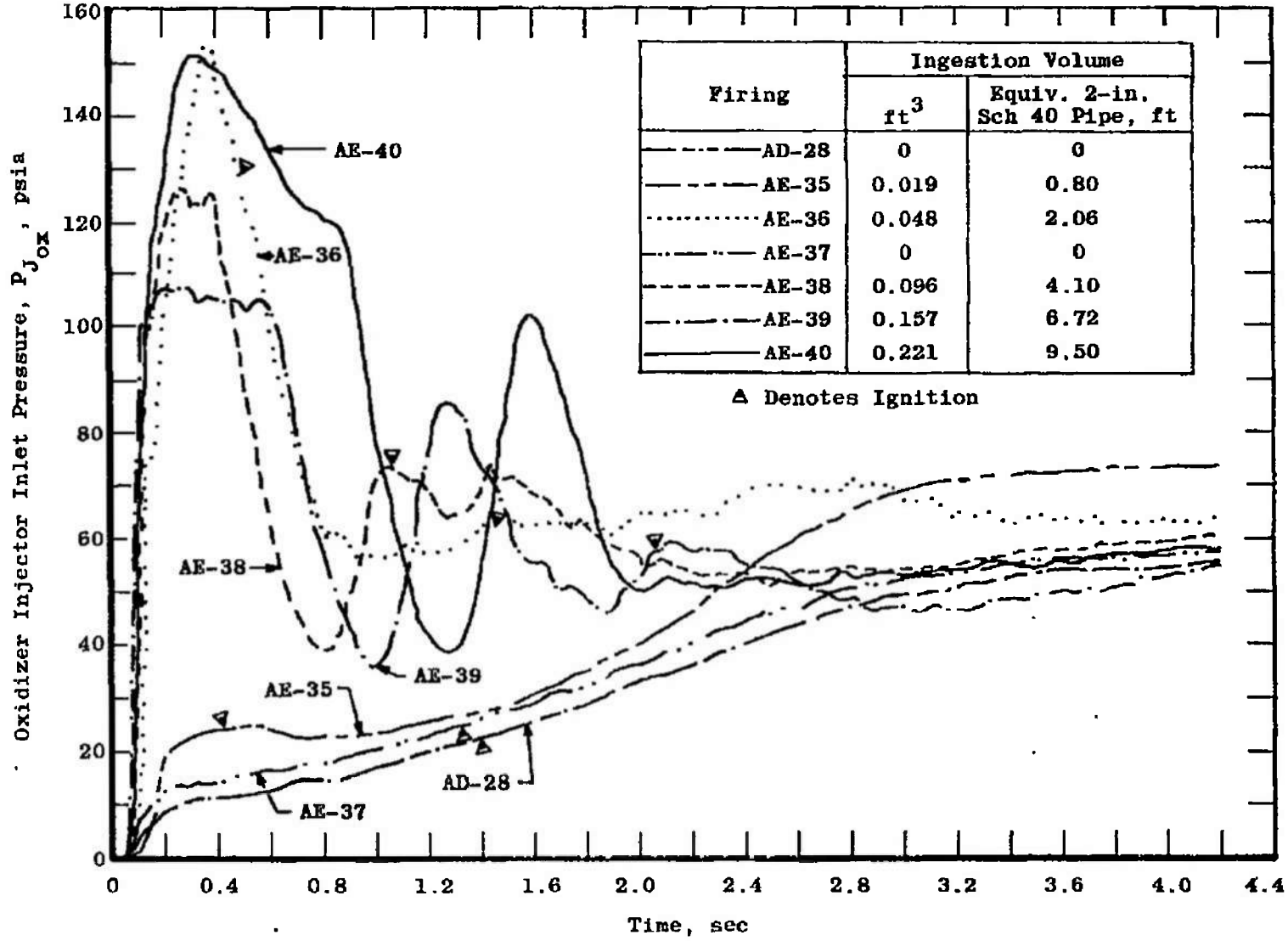

b. Oxidizer

Fig. 17 Concluded

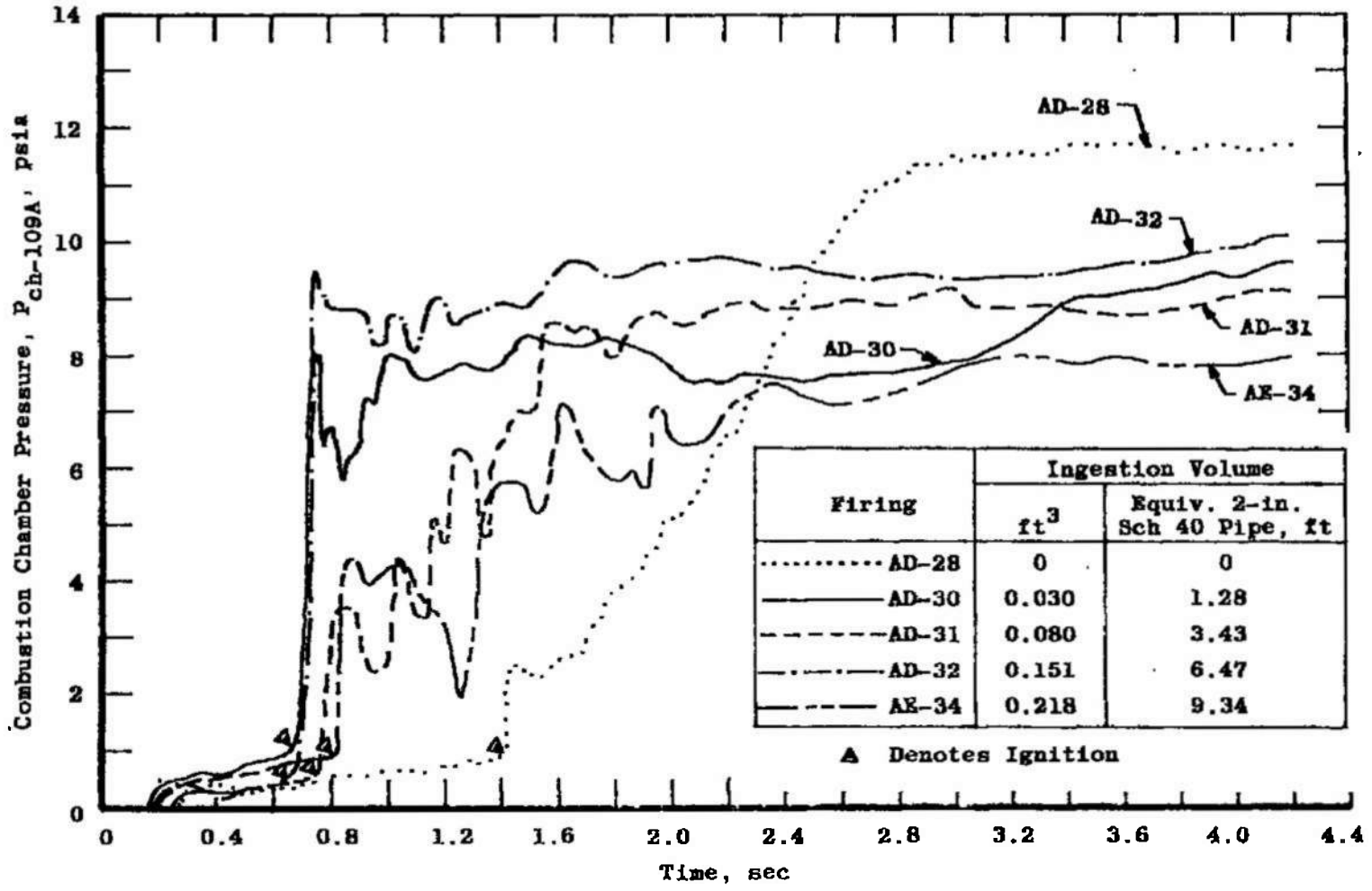

a. Fuel Side Ingestion

Fig. 18 Combustion Chamber Pressure Ignition History

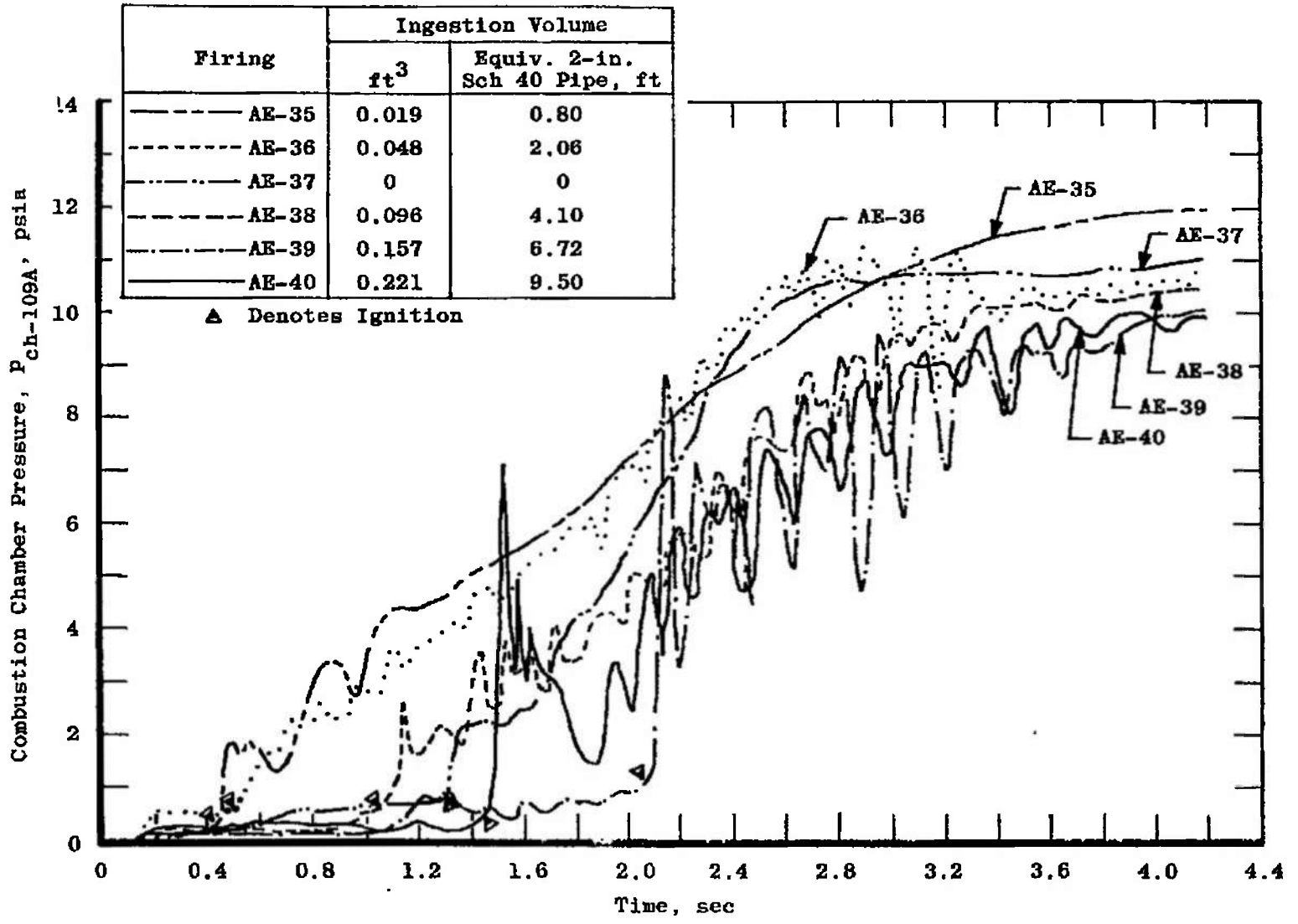

b. Oxidizer Side Ingestion

Fig. 18 Concluded

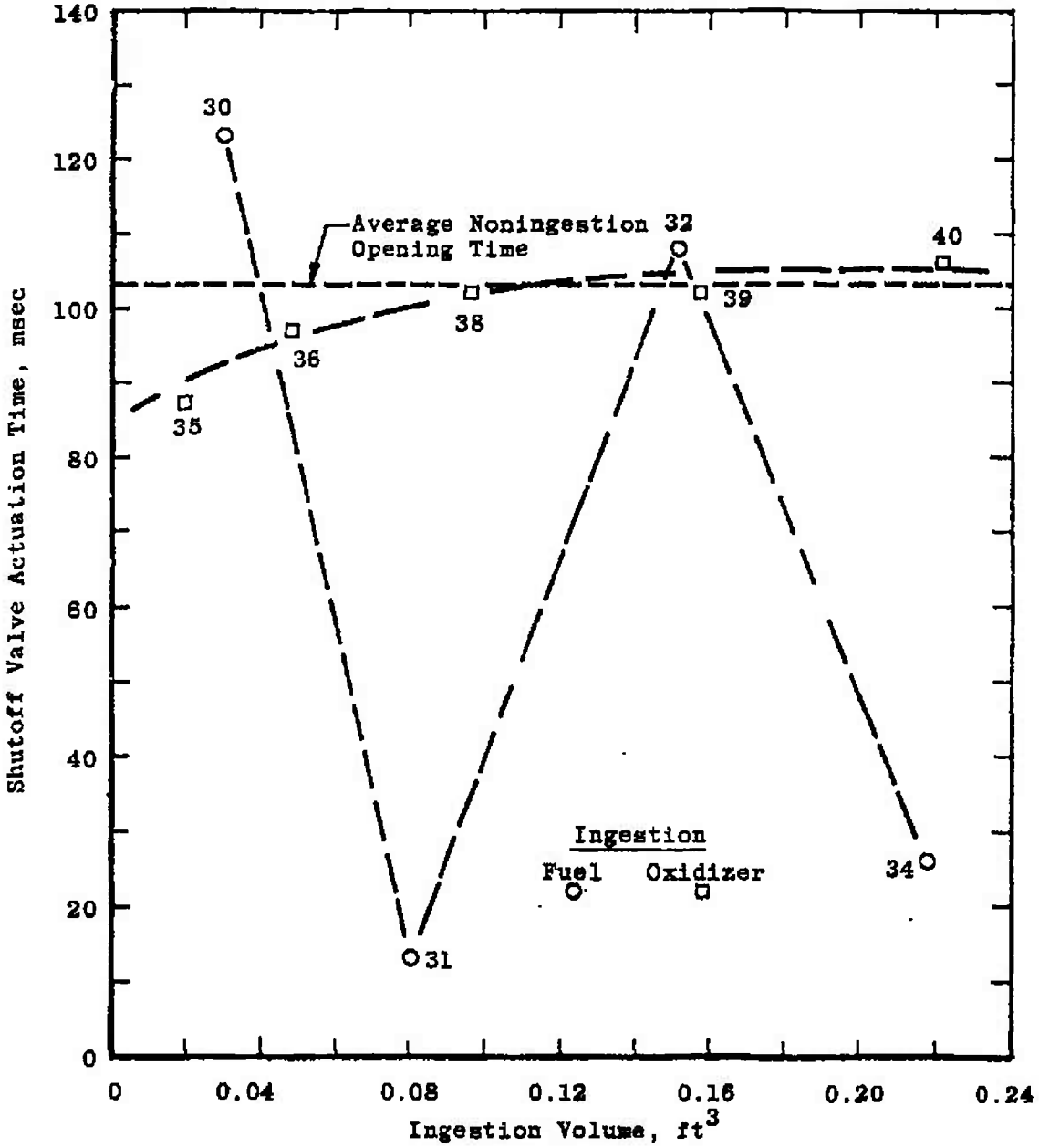

Fig. 19 Shutoff Valve (Set "B") Actuation Time as a Function of Ingestion Volume

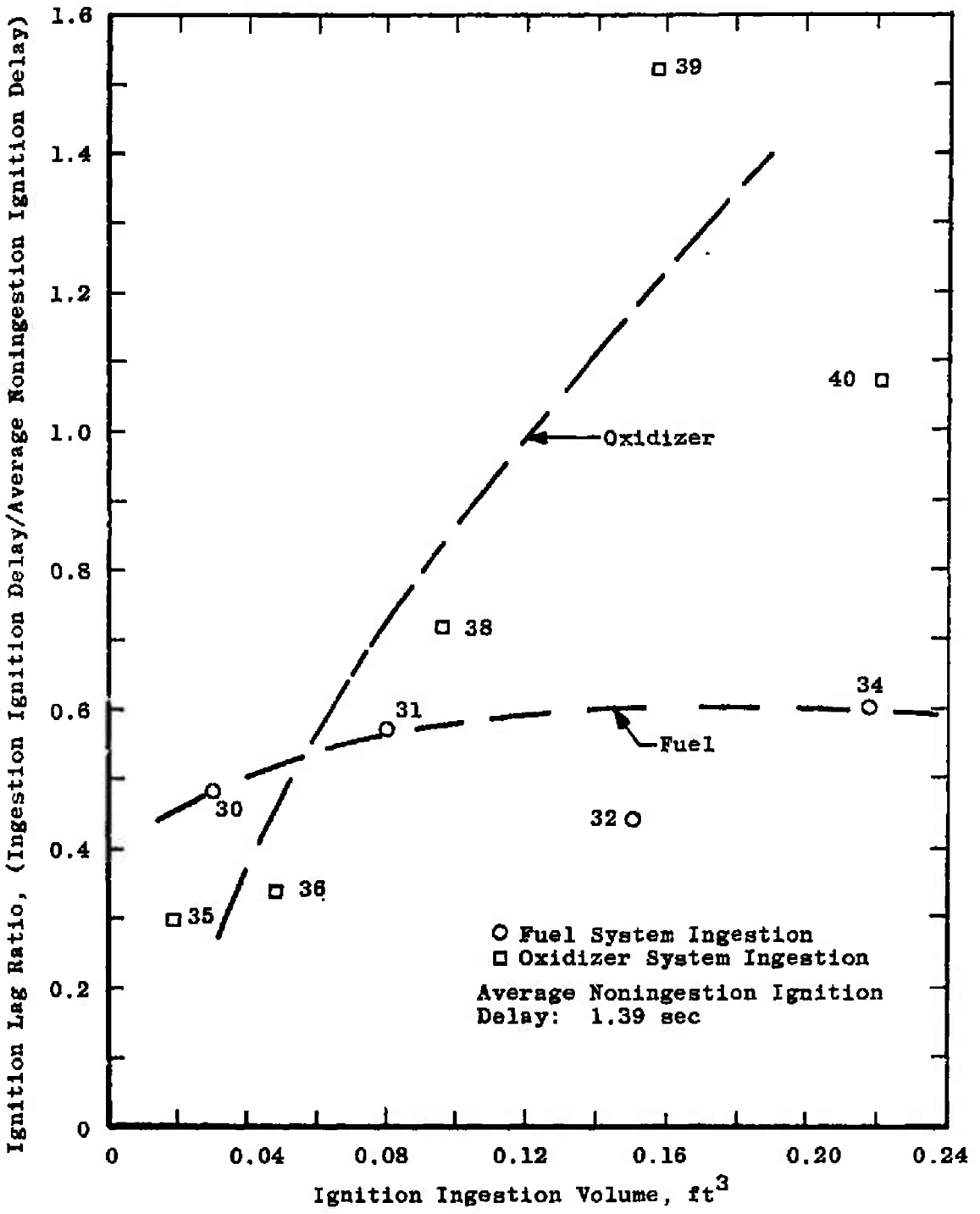

Fig. 20 Ignition Delay as a Function of Ingestion Volume

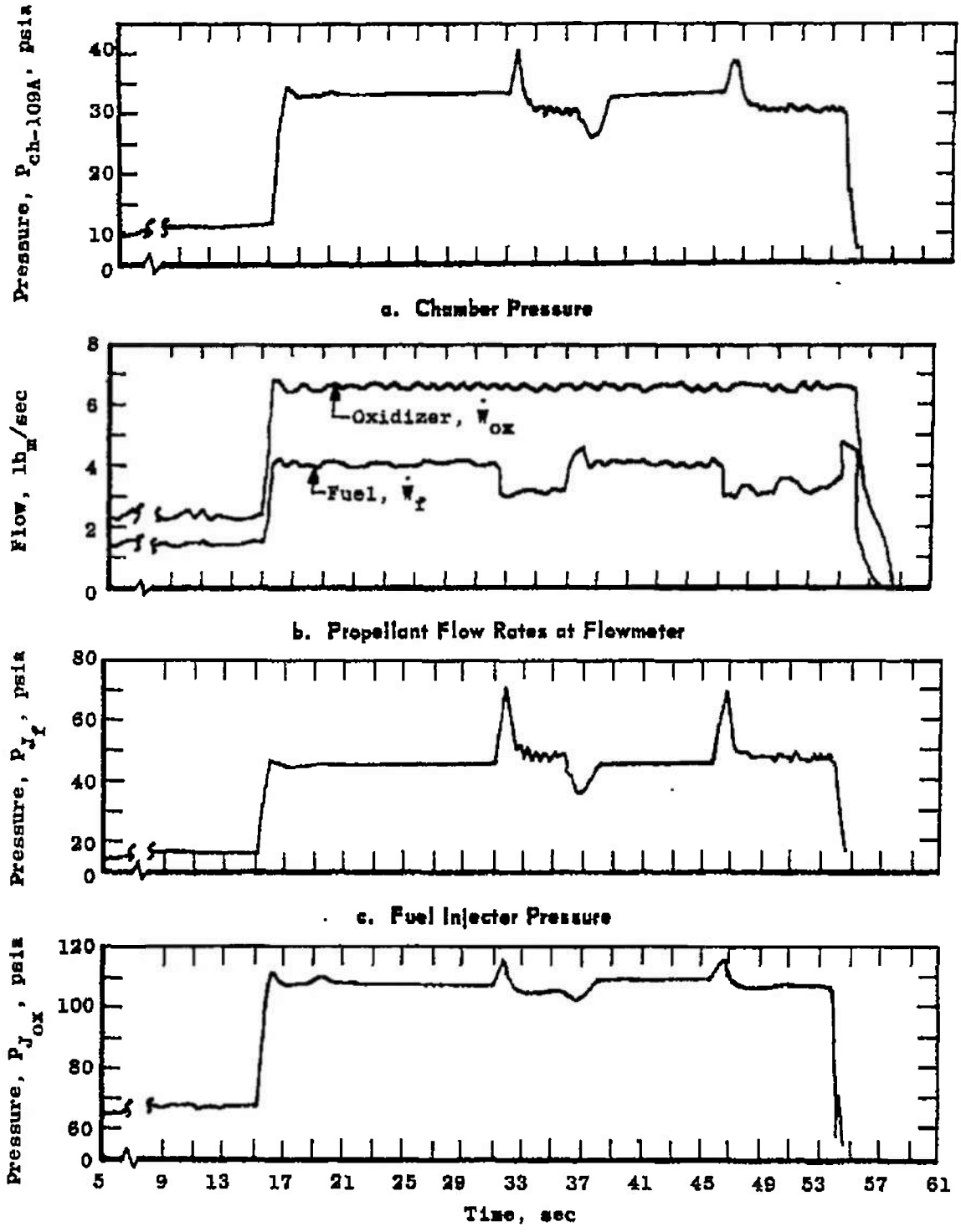

Fig. 21 Typical Fuel System Partial Depletion (Firing AD-31)

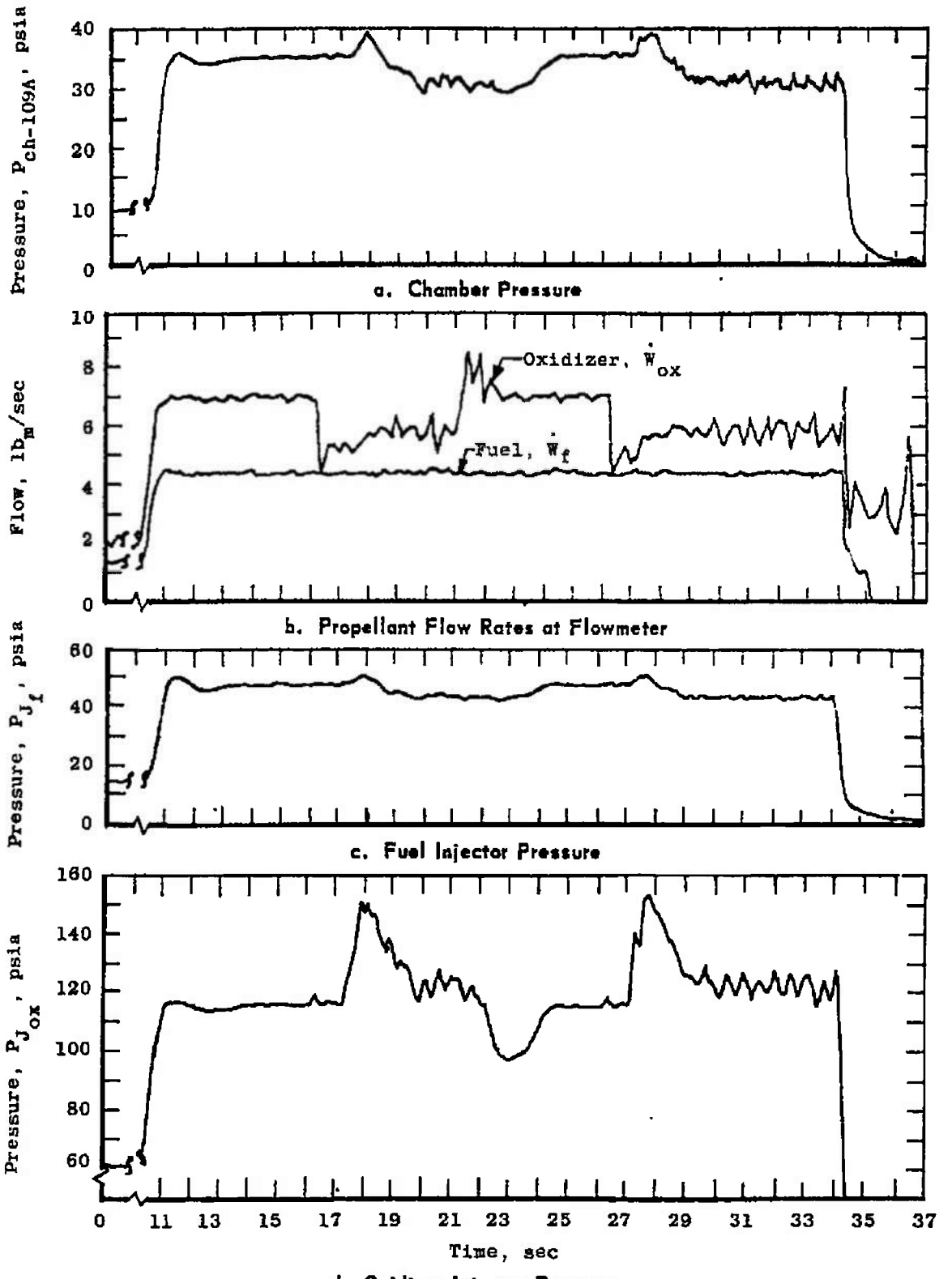

Fig. 22 Typical Oxidizer System Partial Depletion (Firing AE-34)

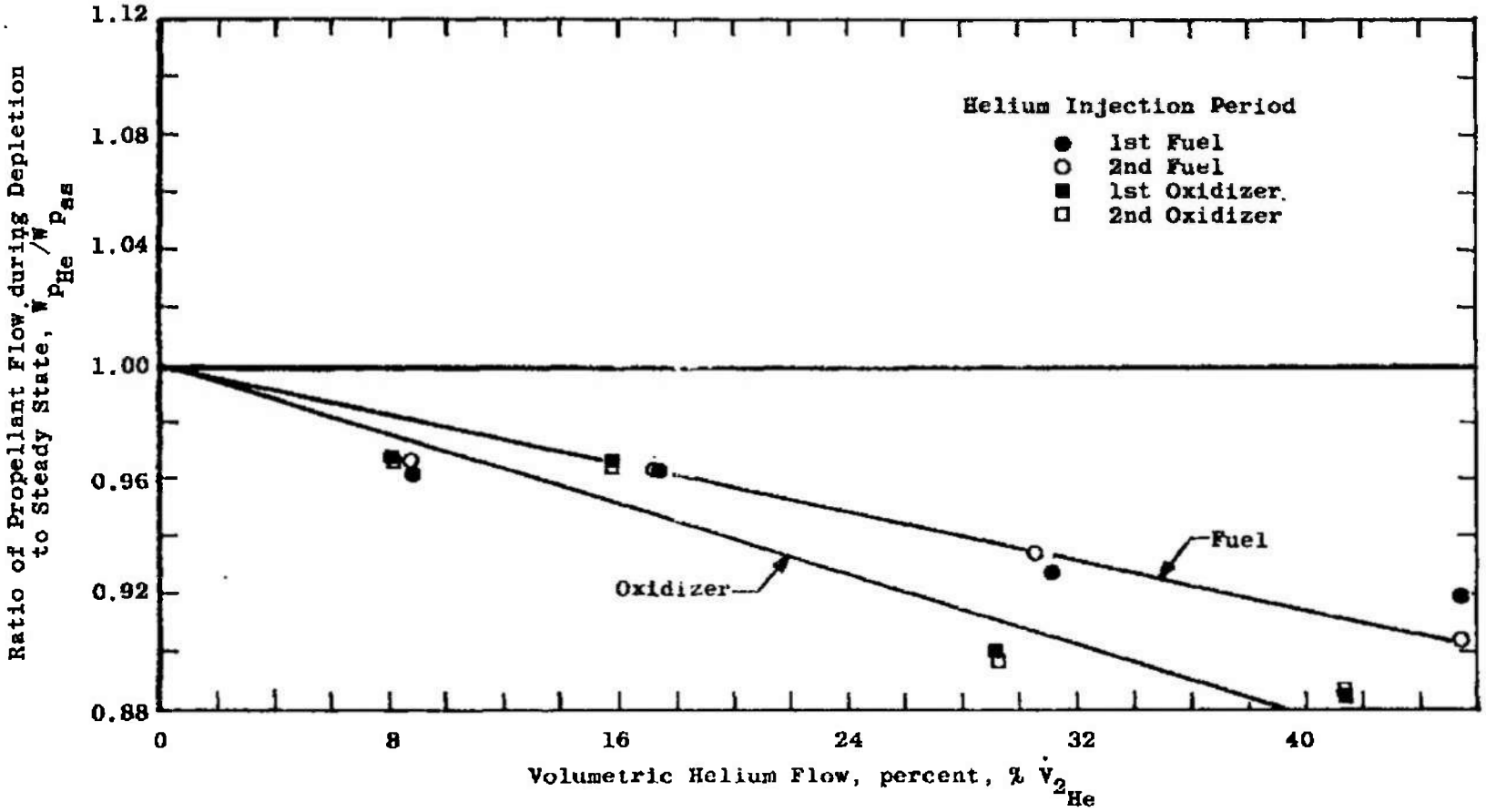

a. Propellant Flow Rates

Fig. 23 Performance Degradation as a Result of Injection

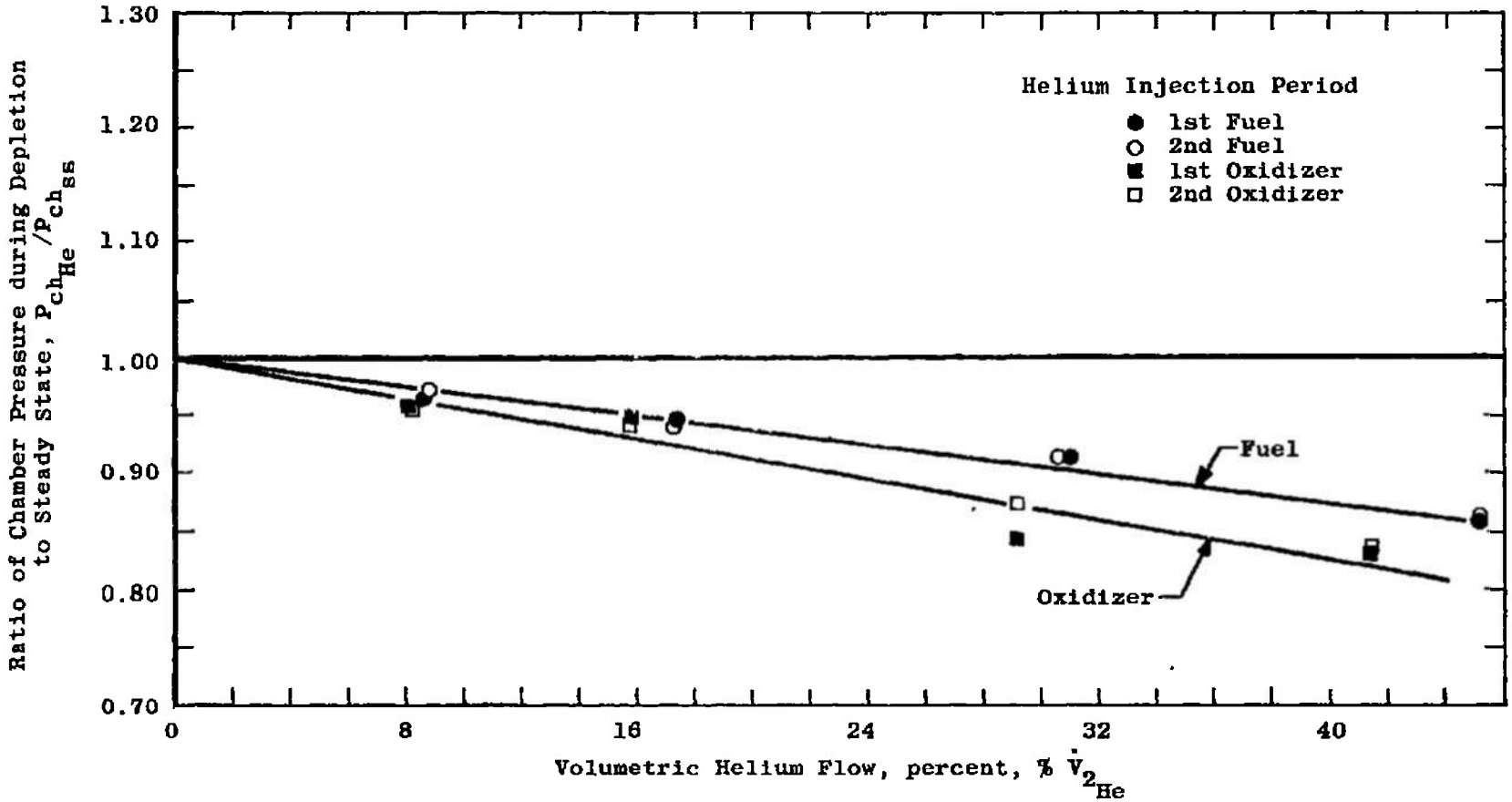

b. Chamber Pressure

Fig. 23 Continued

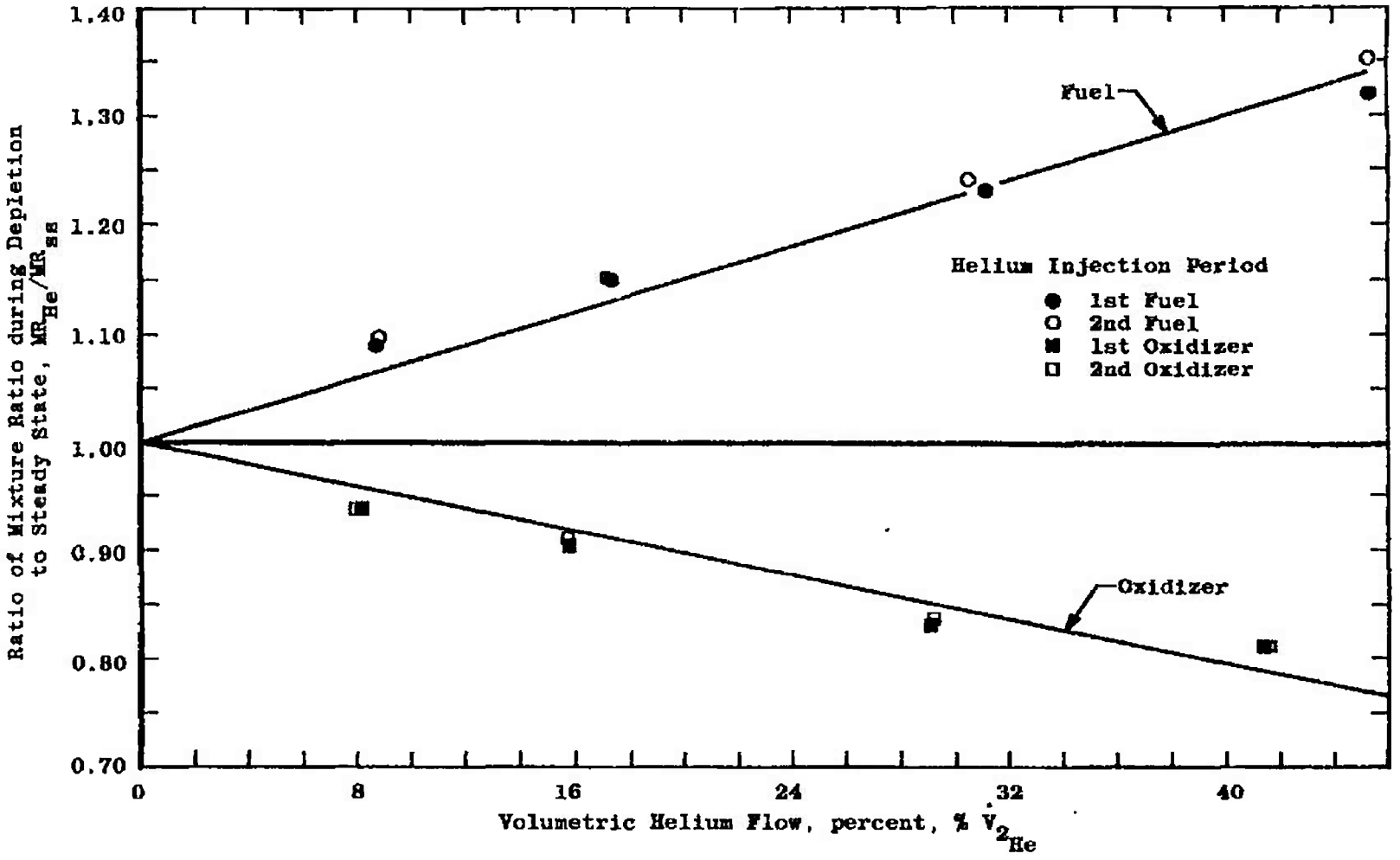

c. Mixture Ratio

Fig. 23 Continued

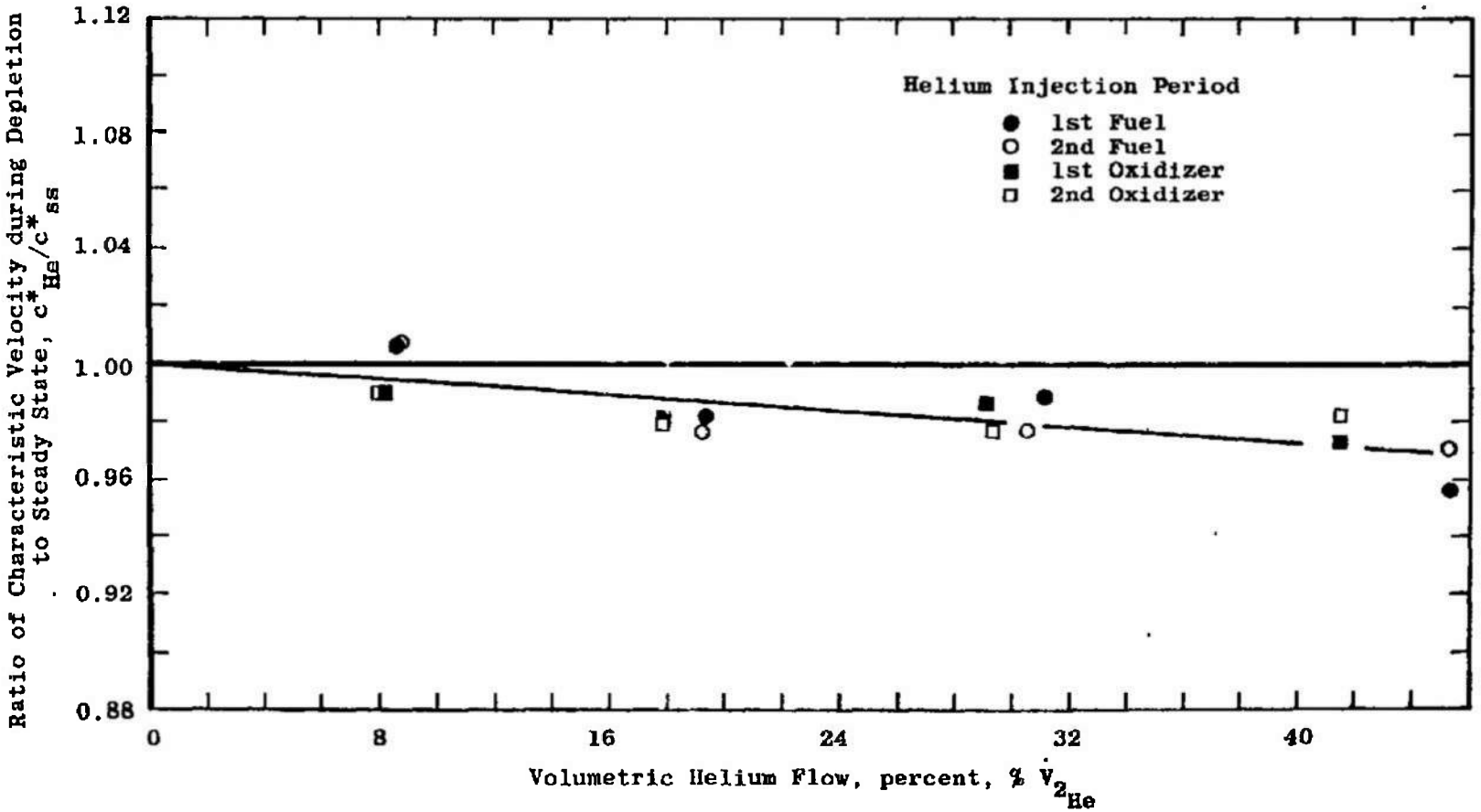

d. Characteristic Velocity

Fig. 23 Continued

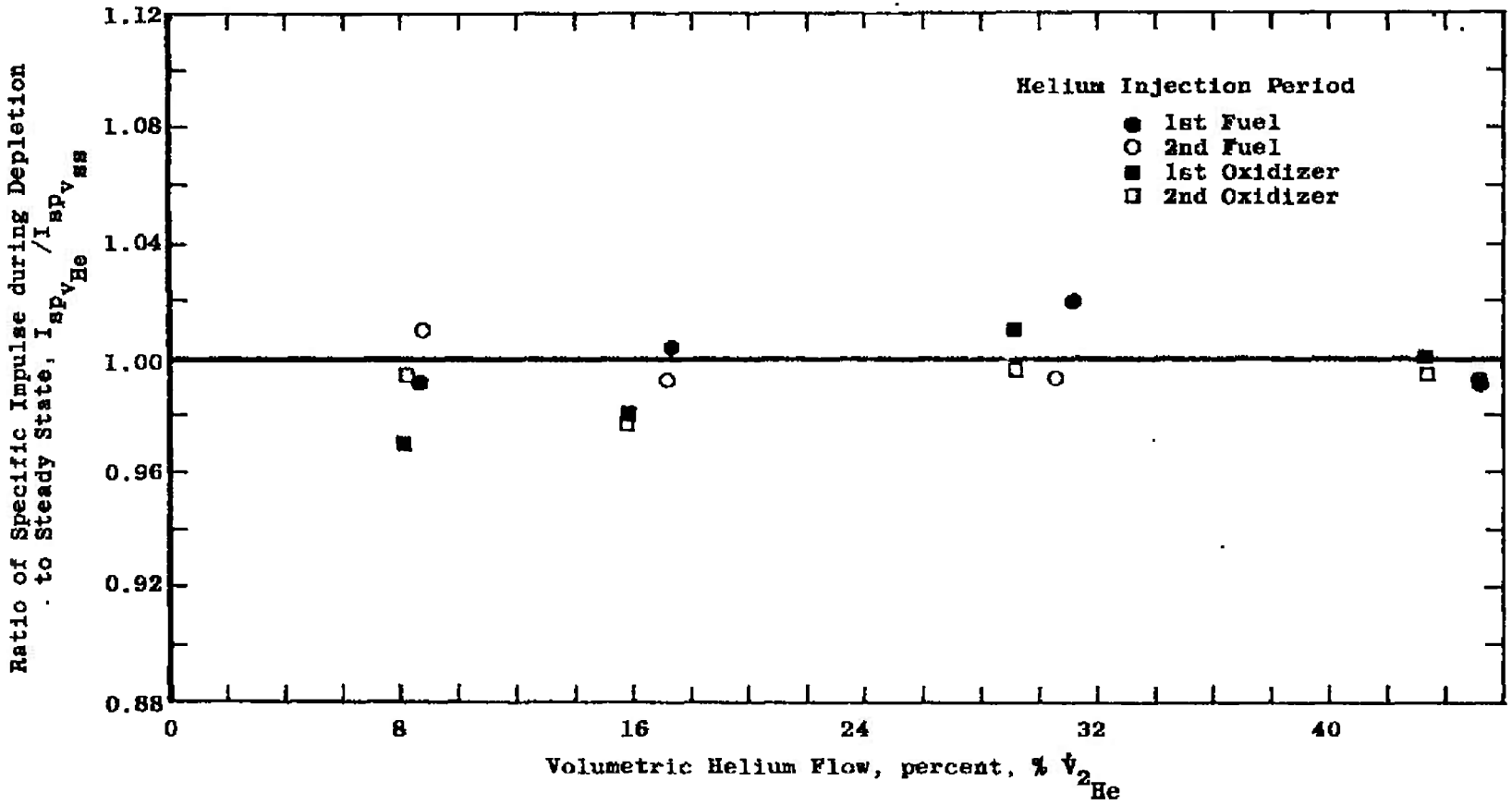

e. Vacuum Specific Impulse

Fig. 23 Concluded

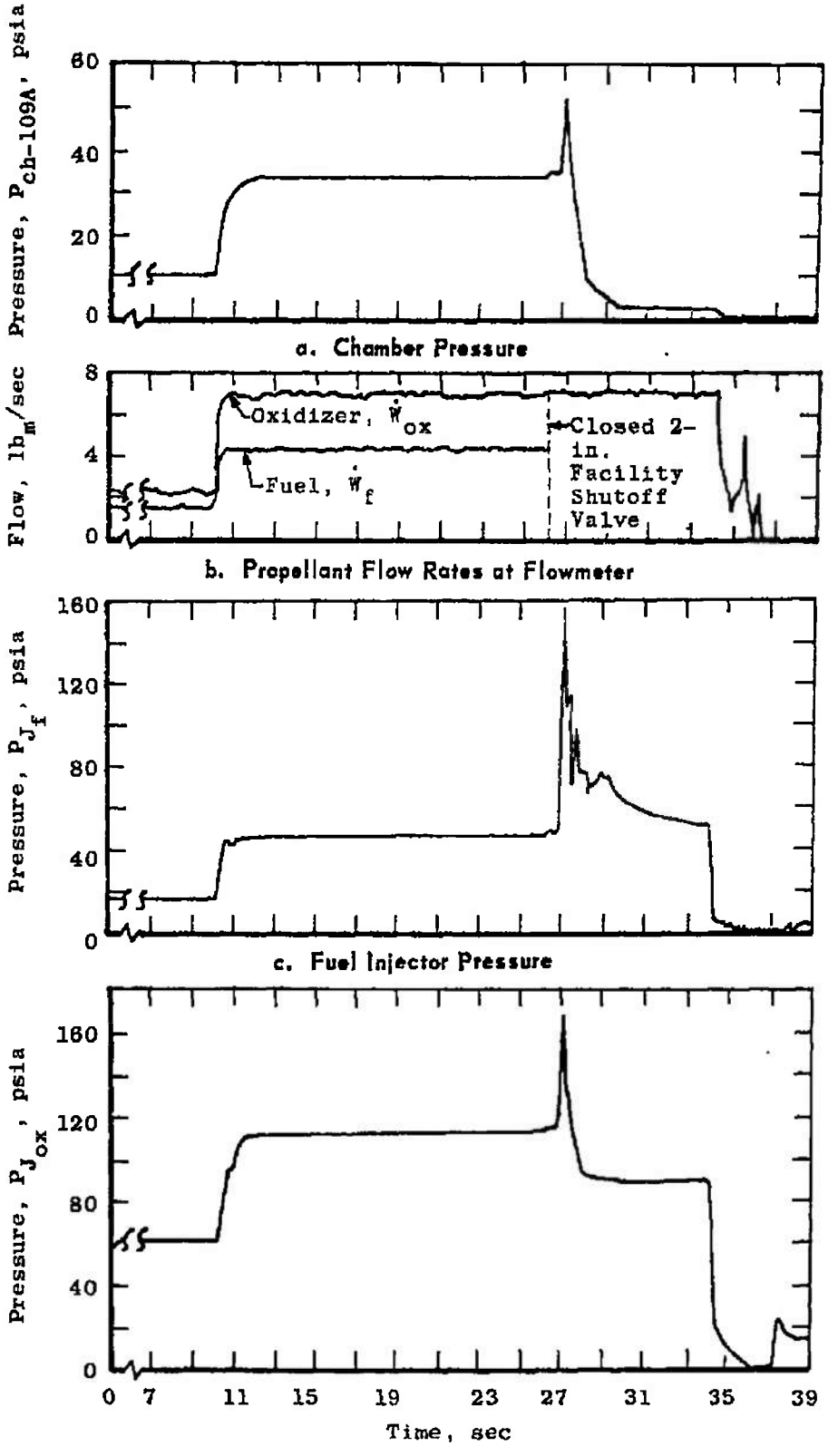

Fig. 24 Fuel System Total Depletion (Firing AE-39)

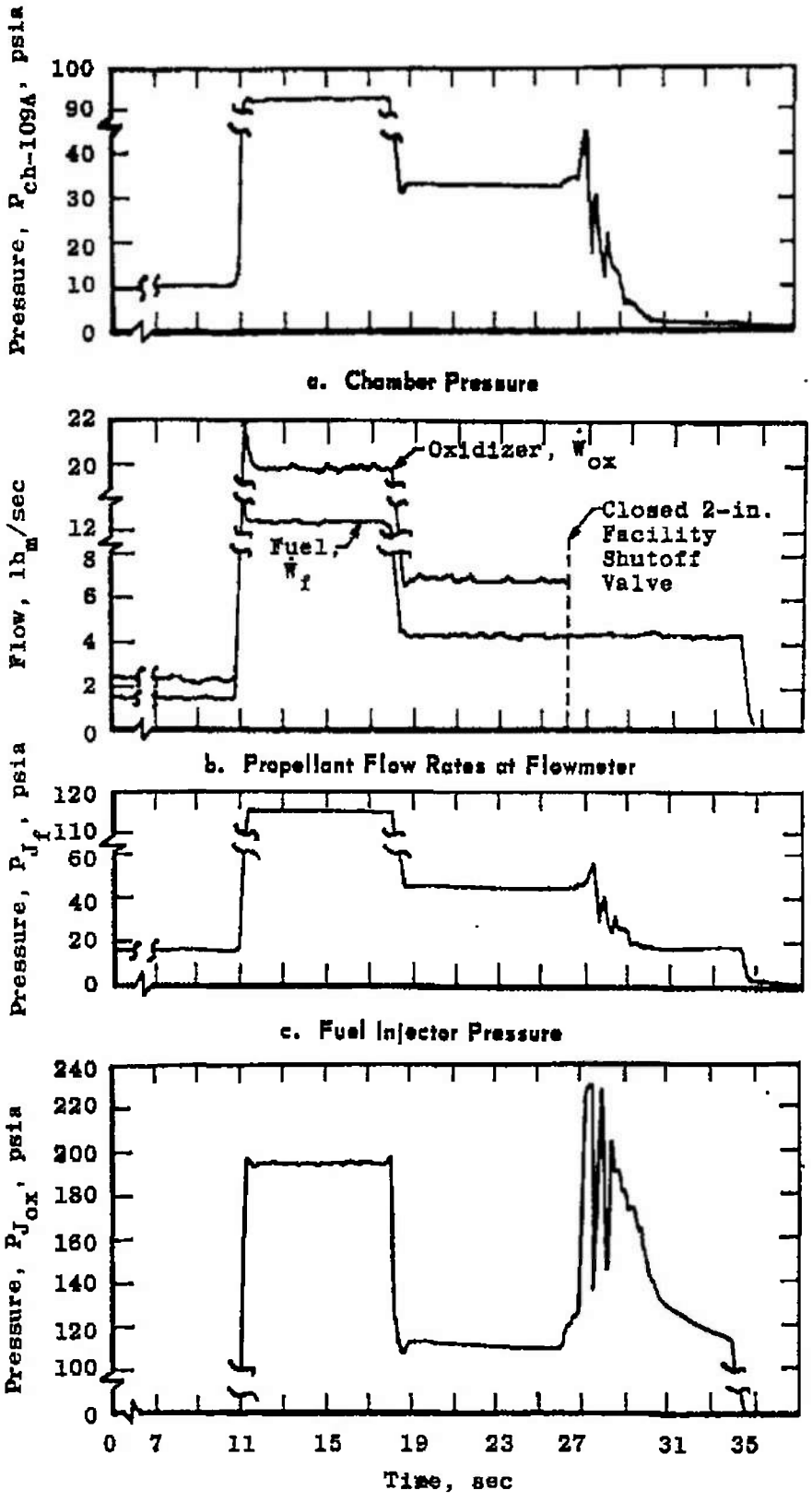

Fig. 25 Oxidizer System Total Depletion (Firing AE-40)

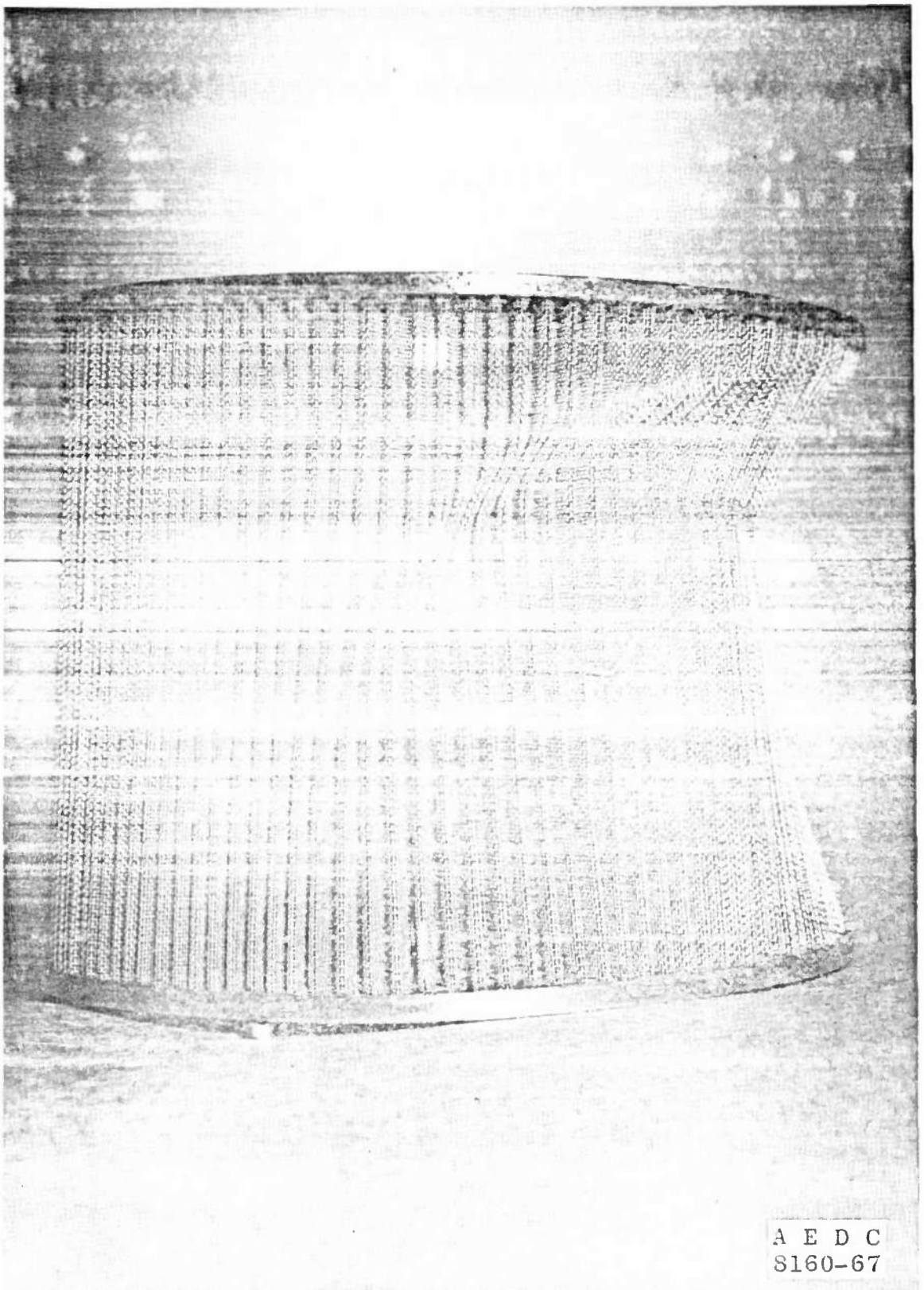

Fig. 26 Photograph of Damaged Oxidizer Strainer

TABLE I

LMDE ENVIRONMENTAL TESTING AT AEDC IN THE J-2A TEST CELL

	PHASE I Project No. RL1433 Cell Occupancy: 3/22/65 – 12/7/65					PHASE II Project No. RL1618 Cell Occupancy: 5/23/66 – 6/23/67				
Test Period	AA	AB	AC	AD	AE	AA	AB	AC	AD	AE
Test Dates	8/13	9/29	9/30	11/30	12/2	7/24–7/25	8/24–8/31	12/8–12/10	4/23–5/1	6/1–6/7
Engine S/N	P1005	P1005	P1005	P1006	P1006	P1009	P1009	P1014	P1014	P1014
No. of Firings	4	3	2	2	1	3	18	4	7	8
Total Burn Time, sec	20	99	641	200	710	22	168	95	213	251
Initial Coast Duration, hr	–	–	–	25	–	74	75	52	–	–
Total Exposure to Space Environment, hr	–	–	–	31	–	143	240	144	147	122
Cell Temperature*	ww	ww	ww	cw	ww	cw	cw	cw	cw	cw
Objectives	Engine and Facility Checkout	Engine and Facility Checkout	Duty Cycle	Duty Cycle	Descent Phase of Duty Cycle	Normal Start Characteristics	Normal Start Characteristics	Normal Start Characteristics	GHe Ingestion and Depletion	GHe Ingestion and Depletion

*ww – warmwall (test cell walls at ambient temperatures)
cw – coldwall (test cell walls at LN_2 temperature, –320°F)

TABLE II
LMDE NOMINAL DESIGN CHARACTERISTICS

Expansion area ratio	47.4:1
Contraction area ratio	2.9:1
Throat area, $in.^2$	54.37
Throat diameter, in.	8.32
Exit area, $in.^2$	2577
Exit diameter, in.	57.28
Chamber inside diameter, max., in.	14.2
Chamber length, injector face to throat, in.	10.7
Nozzle length, throat to exit plane, in.	62.11
Overall length, in.	90
Nozzle contour, percent bell	72.3
Total engine dry weight, lb_m	350
Throttling range, percent of rated	10 to 60

TABLE III

LMDE COMPONENT IDENTIFICATION

(Supplied by TRW Systems, Inc.)

Component	Engine 1014 Serial Number	Part Number
Engine Assembly	1014	SK114050a
Head End Assembly	014	SK114049-1A
Thrust Control Assembly	---	X108580-2
Injector Assembly (Manifold)	XX4	X113673-3
Shutoff Valve Assembly	124	SC104619-24
Prevalve Assembly	130	---
Oxidizer Propellant Line Assembly	103	X108611 2
Fuel Propellant Line Assembly	103	X108604-2
Fuel Flow Control Valve Assembly	117	SK401414-1
Oxidizer Flow Control Valve Assembly	117	SK401413-1
Throttle Actuator Assembly	206	C104622-5
Thrust Chamber Assembly	108	X109400-5
Nozzle Extension Assembly	102	E109404
Gimbal Assembly	119	105947-3C1
Electrical Package Installation (Modified B-2)	---	X223897-1

TABLE IV
ENGINE COMPARTMENT COMPONENT IDENTIFICATION

Component	Part or Drawing Number
HD-4 Rig Assembly	LDW430-6290
Main Frame Assembly	LDW430-6335-1
Heat Shield Support Assembly	
Cross Member	LDW430-1066-1
Support Brace	LDW430-6531-11 LDW430-6531-13
Suspension Brace	LDW430-1064-1 LDW430-1064-3
Blast Deflector	LDW430-1278-1
Heat Shield, Aft	LTM280-20753-3 LTM280-20752-1
Heat Shield, Engine Skirt (Lightweight)	LTN280-20931
Engine Mount Truss Assembly	
Upper Struts	LTM280-20726-13
Lower Struts	LTM280-20815-11
Yoke (-Y Axis)	LTM280M20165-3
Yoke (+Y Axis)	LTM280M20165-1
Gimbal Actuator Stiff Links	LDW300-11700-3

TABLE V
TEST SUMMARY

Firing Number	Date 1967	Clock Time of Firing	Nominal Thrust, percent	Pre-Fire Propellant Temperature at Interface, °F		Pre-Fire Altitude, ft (Ref. 3)	Firing Duration, sec	Helium Ingestion			Propellant Depletion				
								Size			Flow Rate				
				Oxidizer	Fuel			Ft^3	Equivalent Length of Feed Line, ft	System	$\dot{W}_{He}$, lbm/sec x 10^{-3}	$\dot{V}_{He}$, ft^3/sec x 10^{-3}	$\dot{V}_{1_{He}}$, percent	$\dot{V}_{2_{He}}$, percent	System
AD-26	4/23	1918	10/30	80	80	245,000	9.925	---	---	---	---	---	---	---	---
AD-26A	4/25	1552	10/30	82	64	246,000	11.150	---	---	---	---	---	---	---	---
AD-27	4/26	1737	10/30/94/60/50	43	35	320,000	39.935	---	---	---	---	---	---	---	---
AD-28	4/27	0940	10	25	26	313,000	10.176	---	---	---	---	---	---	---	---
AD-30	4/30	0723	10/30	41	74	304,000	54.579	0.030	1.28	Fuel	1.16	6.61	9.7	8.7	Fuel
											1.16	6.61	9.7	8.8	
AD-31	4/30	1921	10/30	40	65	282,000	54.014	0.080	3.43	Fuel	4.60	2.62	38.2	31.2	Fuel
											4.55	2.59	37.8	30.6	
AD-32	5/1	1705	10/30	41	61	306,000	33.974	0.151	6.47	Fuel	1.10	6.26	9.3	8.2	Ox
											1.08	6.15	9.12	8.1	
AE-33	6/1	1510	10/30	84	65	165,000	11.669	---	---	---	---	---	---	---	---
AE-34	6/3	1936	10/30	43	32	313,000	34.111	0.218	9.34	Fuel	4.60	2.82	39.0	29.2	Ox
											4.65	2.85	39.4	29.3	
AE-35	6/4	1815	10/94	35	42	295,000	33.960	0.019	0.80	Ox	7.15	4.07	19.1	17.4	Fuel
											7.15	4.07	19.1	17.3	
AE-36	6/5	1452	10/94	43	42	281,000	34.137	0.048	2.06	Ox	7.13	4.06	19.2	15.8	Ox
											7.13	4.06	19.2	15.8	
AE-37	6/6	0021	10/30	39	38	284,000	34.138	---	---	---	7.96	4.53	86.5	45.3	Fuel
											7.96	4.53	86.5	45.3	
AE-38	6/6	1623	10/30	40	38	268,000	34.091	0.096	4.10	Ox	7.83	4.46	66.4	41.5	Ox
											7.83	4.45	86.4	41.5	
AE-39	6/7	0638	10/30	84	38	286,000	34.050	0.157	6.72	Ox	115	655	1015	100.0	Fuel
AE-40	6/7	2400	10/94/30	40	45	295,000	34.196	0.221	9.50	Ox	225	1340	1930	100.0	Ox

NOTE: (1) Firing AD-29 was deleted.

(2) First and second flow rate entries under Propellant Depletion correspond to first and second injection periods.

(3) Firings AD-26, -26A, and AE-33 were warmwall; all other firings were with test cell liner at LN_2 temperatures.

TABLE VI

PRE-FIRE TEST ARTICLE TEMPERATURES

Firing Number	Thermocouple Identification*									
	TJ-705	TJ-706	TJ-707	TJ-708	TC-725	TC-726	TC-731	TC-732	TC-741	TC-742
	Temperature, °F									
AD-30	50	34	37	48	33	35	15	16	-100	-94
AD-31	63	71	72	65	78	84	99	101	- 45	-38
AD-32	34	33	35	33	35	42	37	39	-105	-93
AD-34	41	36	---	40	36	34	24	24	- 69	-67
AD-35	36	34	---	35	32	31	25	25	- 88	-85
AD-36	34	35	---	33	34	36	38	38	- 83	-81
AD-38	46	50	---	44	55	53	65	65	- 60	-57
AD-39	47	50	---	45	56	53	65	65	- 58	-55
AD-40	46	45	---	42	46	46	48	48	- 69	-66
Space Coast Reference Temperature (Ref. 1)	35	33	34	35	29	32	24	21	- 35	-32

*See Fig. 12 for thermocouple locations.

TABLE VII
ACCELERATION AND PEAK CHAMBER PRESSURE DATA SUMMARY

Firing Number	Throttle Level, percent	A_{J_Y} 561 g-pk	A_{J_Z} 562 g-pk	A_{J_X} 563 g-pk	AT_Z 569 g-pk	A_{G_X} 565 g-pk	A_{G_Z} 566 g-pk	A_{G_Y} 567 g-pk	AT_X 568 g-pk	P_{ch-110} (Kistler), psia	Remarks: Ingestion / Depletion	Remarks: Recorded During
AD-26	10/30	---	150	1020	20	330	420	218	25	72	---	Ignition
AD-26A	10/30	---	---	---	---	135	192	64	---	24	---	Shutdown
AD-27	10/30/94/80/50	---	198	---	61	665	868	260	98	107	---	Shutdown
AD-28	10	---	---	---	---	---	---	---	---	---	---	---
AD-30	10/30	---	---	745	15	544	695	262	42	128	Fuel / Fuel	Ignition
			---	1360	---	306	321	113	---	48		2nd Depletion
AD-31	10/30	---	---	1990	20	440	590	220	45	116	Fuel / Fuel	1st Depletion
				1835	20	460	395	190	45	172		2nd Depletion
AD-32	10/30	---	---	2300	45	738	530	291	67	118	Fuel / Ox	Shutdown
					$A_{J_{X-2}}$							
AE-33	10/30	---	---	---	---	---	---	---	---	---		---
AE-34	10/30	---	---	---	---	100	---	---	---	9	Fuel / Ox	Throttle
AE-35	10/94	185	---	231	100	131	858	---	---	8	Ox / Fuel	Ignition
		4580	173	3820	8070	895	2340	102	88	140		Shutdown
AE-36	10/94	880	205	1320	1290	675	2070	92	100	120	Ox / Ox	1st Depletion
		3850	205	2040	1290	1070	2220	92	100	209		2nd Depletion
AE-37	10/30	810	210	1650	1850	770	2120	108	108	98	--- / Fuel	1st Depletion
		870	200	1900	1600	940	1680	106	100	93		2nd Depletion
AE-38	10/30	490	220	925	680	376	1000	109	100	50	Ox / Ox	1st Depletion
		350	230	850	250	215	690	---	---	35		2nd Depletion
AE-39	10/30	362	389	813	490	420	1690	67	50	30	Ox / Fuel	Ignition
		1350	3540	1540	1710	700	1860	95	100	92		Throttle
		3050	out	2550	2610	1620	3130	110	175	126		Depletion
AE-40	10/94/30	610	out	950	975	530	3140	57	50	64	Ox / Ox	Ignition
		3670	out	2000	1370	930	5700	190	100	180		Throttle
		300	out	400	---	212	713	---	150	20		Depletion

NOTE: Peaks are shown for the portions of each firing during which measurable data were recorded.

TABLE VIII

SHUTOFF VALVE ACTUATION TIME

Firing	FS-1 to Valve Initiation		Opening Time		FS-2 to Valve Initiation		Closing Time	
	SOV-A	SOV-B	SOV-A	SOV-B	SOV-A	SOV-B	SOV-A	SOV-B
AD-26	56	50	122	91	20	26	272	302
AD-26A	11	10	9	7	15	15	235	250
AD-27	57	52	134	108	18	20	232	245
AD-28	47	45	139	107	16	18	247	272
AD-30	52	48	157	123	29	59	297	278
AD-31	35	31	38	13	40	47	79	73
AD-32	52	51	150	108	17	20	147	166
AE-33	52	50	135	101	15	18	220	222
AE-34	53	52	101	26	37	40	121	117
AE-35	71	46	130	87	22	55	297	263
AE-36	50	46	143	97	19	17	297	279
AE-37	52	49	144	99	16	18	286	270
AE-38	50	42	148	102	17	16	256	253
AE-39	48	42	144	102	16	17	251	255
AE-40	52	47	145	106	16	17	248	236

NOTE: AD-29 was deleted

Security Classification

DOCUMENT CONTROL DATA - R & D

(Security classification of title, body of abstract and indexing annotation must be entered when the overall report is classified)

1. ORIGINATING ACTIVITY (Corporate author)	2a. REPORT SECURITY CLASSIFICATION
Arnold Engineering Development Center ARO, Inc., Operating Contractor Arnold Air Force Station, Tennessee	UNCLASSIFIED
	2b. GROUP N/A

3. REPORT TITLE

OPERATING CHARACTERISTICS OF THE APOLLO LM DESCENT ENGINE WITH HELIUM INGESTION AND PROPELLANT DEPLETION IN A SIMULATED SPACE ENVIRONMENT

4. DESCRIPTIVE NOTES (Type of report and inclusive dates)

April 23 to June 7, 1967 - Final Report

5. AUTHOR(S) (First name, middle initial, last name)

K. L. Farrow, J. A. German, and T. M. Gernstein, ARO, Inc.

6. REPORT DATE	7a. TOTAL NO. OF PAGES	7b. NO. OF REFS
November 1967	89	7

8a. CONTRACT OR GRANT NO.	9a. ORIGINATOR'S REPORT NUMBER(S)
AF 40(600)-1200 b. PROJECT NO. 9158	AEDC-TR-67-193
c. System 921E	9b. OTHER REPORT NO(S) (Any other numbers that may be assigned this report) N/A
d.	

10. DISTRIBUTION STATEMENT

This document is subject to special export controls and each transmittal to foreign governments or foreign nationals may be made only with prior approval of NASA Manned Spaceflight Center (EP-2), Houston, Texas.

11. SUPPLEMENTARY NOTES	12. SPONSORING MILITARY ACTIVITY
Available in DDC	National Aeronautics and Space Administration, Manned Spaceflight Center (EP-2), Houston, Texas

13. ABSTRACT

An Apollo Lunar Module Descent Engine (LMDE) was tested under a simulated thermal radiation and pressure space environment in Propulsion Engine Test Cell (J-2A) to investigate (1) engine ignition characteristics at 10-percent throttle, while ingesting various trapped volumes of helium (the flight vehicle propellant tank pressurant), and (2) engine operating and shutdown characteristics while injecting various flow rates of helium into the propellant feed lines. Fifteen firings were conducted during two test periods. The first test period consisted of seven firings; four were checkout and baseline performance tests, and three were helium ingestion propellant depletion tests. Eight firings were conducted during the second test period; seven were helium ingestion propellant depletion tests. Helium volumes equivalent to over 9 ft of propellant feed line were ingested during the starts, and helium flow rates equivalent to more than 40 percent of the total volumetric flow of each propellant were injected into the feed lines during engine operation with insignificant engine damage. Except for the two largest helium volumes in the oxidizer system, ignition delay was decreased by helium ingestion. Chamber pressure was degraded by as much as 17 percent while injecting helium into the feed lines during steady-state operation, but the corresponding degradation of characteristic velocity was only approximately 2 percent.

This document is subject to special export controls and each transmittal to foreign governments or foreign nationals may be made only with prior approval of National Aeronautics and Space Administration, Manned Spaceflight Center (EP-2), Houston, Texas.

DD FORM 1 NOV 68 1473

Security Classification

14. KEY WORDS	LINK A		LINK B		LINK C	
	ROLE	WT	ROLE	WT	ROLE	WT
Apollo						
LM Descent Engine						
helium ingestion						
propellant depletion tests						
performance						
ignition						
operating characteristics